MASTER OF SCIENCE

Cyclic di-GMP signalling and the regulation of virulence, biofilm formation and epiphytic fitness in the phytopathogen Xanthomonas campestris

Hollmann, Birte

Award date:
2016

MSc thesis

To achieve the academic degree Master of Sciences (MSc) by research

Cyclic di-GMP signalling and the regulation of virulence, biofilm formation and epiphytic fitness in the phytopathogen *Xanthomonas campestris*

University of Dundee, Division of Molecular Microbiology

Robert Ryan Lab

Tracy Palmer Lab

Birte Hollmann

Dundee, July 2016

Declaration by candidate

I hereby declare that this thesis is my own work and that it has not been submitted for any other academic award. The experimental work is almost entirely my own work; the collaborative contributions have been indicated clearly and acknowledged. Due references have been provided on all supporting literatures and resources.

Signature: ……..

Date: ……..

Acknowledgements

This work would not have been possible without the support of many people.

Above all, I would like to express my deep gratitude to Tracy for her support and guidance over the last months. She was there at short notice when I needed her and rearranged her scheduling to fit me in. Thanks to her, I was able to finish this work. Thank you Tracy for all your time and advice both on a professional and personal level! I really appreciate that.

I would also like to give special thanks to Nicola and Helge for all their support and advice especially when things were not always going perfectly. I am very thankful that your doors were always open for me.

I want to thank Dr Helge Dorfmueller and Dr Jacob Malone for accepting being my internal and external examiners.

I also have to thank the Wellcome Trust. Without their funding, this project would not have been possible.

A big thank-you to all my colleagues in MMB, especially to Anne and Kushal for all the support and friendship as well as to Connor, Chris, John, Yao and Sarah for all the laughs and deep discussions about sciences and more we had together. I will keep the good moments in mind.

I would also like to thank Jackie and Michele who always make sure that our lab is running smoothly and especially Erin for all her help with organisation and administration issues, you are really great.

Thank you to Robert who gave me the opportunity to do this project and taught me a lot during this time as well as Shi-Qi An who guided me through the beginning of the project.

Finally I would like to thank my friends and family for accompany me on my way and to encourage me in all my decisions. You were always there to help me and I am very thankful for that.

Table of Contents

Abbreviations

ADP	adenosine diphosphate
AMP	adenosine monophosphate
Ara	arabinose
ATP	adenosine triphosphate
c-di-GMP	cyclic di-guanosine monophosphate
cGMP	cyclic guanosine monophosphate
Clp	cyclic-AMP receptor-like protein
CMC	carboxymethylcellulose
cNMP	cyclic nucleotide binding domain
DGC	diguanylate cyclase
DNA	deoxyribonucleic acid
DSF	diffusible signal factor
eDNA	extracellular DNA
EPS	exopolysaccharide
et al.	*latin: et alii, et aliae,* and others
Fle	Flagellar regulatory protein
fwd	forward
g	gram

g	acceleration caused by gravity
gDNA	genomic DNA
GTP	guanosine triphosphate
h	hour/s
HPLC	high performance liquid chromatography
HR	hypersensitive response
hrp	hypersensitive response and pathogenicity
kb	kilo base pair
KEGG	Kyoto Encyclopedia of Genes and Genomes
L	litre
LB	lysogeny broth
Mb	mega bases
mg	milligram
min	minute/s
mL	millilitre
mm	millimetre
MRM	multi reaction monitoring
MS	mass spectrometry
ng	nanogram
nm	nanometre

n x n	number of biological replicates x number of technical replicates
OD	optical density
ORF	open reading frame
PCR	polymerase chain reaction
PDE	phosphodiesterase
pel	*putative exopolysaccharide exporter*
pGpG	5‘-phophoguanylyl-(3‘-5‘)-guanosine
pmol	pico mol
PTI	pattern-triggered immunity
pv.	pathovar
qRT-PCR	quantitative real-time PCR
rev	reverse
rpf	regulation of pathogenicity factor
rpm	rounds per minute
sec	second/s
SMART	Simple Modular Architecture Research Tool
Spc	Spectinomycin
Tet	Tetracycline
TIC	total ion chromatogram

T2SS	Type II secretion system
T3SS	Type III secretion system
UV	ultra-violet
V	volt
Xcc	*Xanthomonas campestris* pv. *campestris*
xps	*Xanthomonas* protein secretion
µL	microlitre
µm	micrometre
µM	micro molar
°C	degree Celsius
%	percent
% (w/v)	weight/volume percent

1 Abstract

The full virulence of *Xanthomonas campestris* pathovar *campestris* (*Xcc*) for its host plant is dependent on many different factors (Chan and Goodwin, 1999). A pivotal role is played by the second messenger cyclic di-GMP. C-di-GMP is essential for successful infection of the host not only by *Xcc* but also by many other pathogens. Roles for c-di-GMP include the regulation of motility, production of virulence determinants and the switch from a motile to a biofilm forming lifestyle for example (Hengge, 2009; Jenal and Malone, 2006; Römling *et al.*, 2005; Wolfe and Visick, 2008). In *Xcc*, 37 genes were found to encode proteins with one of the three domains that are involved in c-di-GMP turnover, named GGDEF, EAL and HD-GYP (Ryan *et al.*, 2007). GGDEF domain proteins play a role in the synthesis of c-di-GMP whereas EAL and HD-GYP domain proteins are part of the c-di-GMP degradation system (Christen *et al.*, 2005; Paul *et al.*, 2004; Ryan, 2013). Some of these proteins have already been well examined but the functionality of most of the enzymes has yet to be determined.

The basis for this study was a mutant library composed of 37 Tn5 or pk18mob insertion strains for these c-di-GMP pathway genes constructed in Nanning, China. These mutations were constructed using a non-directed approach. A data set for two different virulence assays that were performed using these 37 mutants was provided by Dr Robert Ryan and was analysed in this study. These mutants were further characterised based on their motility, EPS production and protease activity. RpfG, the first characterised HD-GYP domain protein, operates as an active phosphodiesterase and is part of a two component system that is involved in the quorum sensing pathway of the signal molecule DSF (diffusible signal factor). The deletion mutant of the corresponding gene was used to verify the functionality of these phenotypic assays. The phenotypic screen revealed differences between each mutant and the wild type. Based on these results and the analysis of the virulence assays, five genes were chosen for the further work: *XC0362, XC1755, XXC2459, XC2793* and *XC3962*. After successful construction of either unmarked deletion mutants or directed insertion mutants for four of the five selected genes, the phenotypic assays were repeated comparing the new strains and the library mutants. Previously observed phenotypes including reduced production of protease or reduced motility was reproducibly observed for the library mutants, but could not be confirmed using the newly constructed strains. Therefore, no confident conclusions could be drawn to date regarding the activity and role of these proteins in c-di-GMP signalling. A domain analysis of the selected proteins was used to gain more information about their role regarding the sensing of environmental signals.

A mass spectrometry analysis was performed to determine differences in the c-di-GMP levels between the wild type strain and a subset of the mutants. So far, only two mutants, *ΔrpfG* and *XC2459::pK18mob*, have been tested, with one replicate each, revealing an increased level of c-di-GMP for both mutants compared to the wild type. This result leads to the suggestion that these genes do play a role in c-di-GMP turnover. Additional replicates are required to confirm this conclusion.

2 Introduction and background

2.1 Brassicaceae and infection by the phytopathogen *Xanthomonas campestris* as an example for a host-pathogen interaction

Brassicaceae encompass different kinds of popular green leafy vegetables such as broccoli, cabbage, cauliflower and the model plant *Arabidopsis thaliana*, which are found all over the world because of their adaptation to different climatic conditions and soil (Department of Agriculture Forestry and Fisheries, South Africa). These crop plants are primarily known for human nutrition and for positive effects to health due to the presence of antioxidants (Jahangir *et al.*, 2009). A common characteristic for Brassicaceae flowers are four petals that are perfectly aligned (Rubatzky and Yamaguchi, 1997). The five countries with the highest cultivation of cabbage are China, India, Russia, South Korea and Japan (Food and Agriculture Organization of the United Nations, 2013). Both annual and biennial species of vegetables belong to the family of Brassicaceae. They mostly grow in temperate zones but also in subarctic climates.

The cultivation of cabbage is subject to variable crop yields. The plants can be attacked by different biological agents including fungi, nematodes and bacteria. Large crop losses result from different types of microbial infections that cause diseases like black rot (*Xanthomonas campestris* pv. *campestris*), downy mildew (*Perenospora parasitica*) and wilt (*Fusarium oxysporum*) (Mcdowell *et al.*, 2000; Ploetz, 2006). A considerable crop loss worldwide is a result of different *Xanthomonas* infections (Alvarez, 2000). Late recognition of black rot, caused by *Xanthomonas campestris* pv. *campestris*, makes this infection one of the most effective cabbage diseases (Alvarez, 2000). The most common hosts of black rot are Brassicaceae, especially *Brassica oleracea*, which includes cabbage, broccoli and cauliflower.

The dispersal of the pathogen happens very quickly and can result in enormous crop loss in warm and humid months (Leyns *et al.*, 1984), making it a particular problem in the developing regions of Africa and Asia (Qian *et al.*, 2005). The most common reason for infection of plants by *Xanthomonas* species are contaminated seeds (Ryan *et al.*, 2011). However, the pathogens can also invade the plants using alternative ways, for example an infection can occur via water droplets that gain access to the vascular system through natural entrances like hydathodes and stomata, or through lesions (Huang, 1986). Additionally, all Xanthomonads can produce cell wall degrading enzymes such as amylases, cellulases and lipases (Thieme *et al.*, 2005). An example image of infected leaves of *Brassica oleracea* var. *capitata* cv. Bartolo by *Xanthomonas* is given in Figure 1.

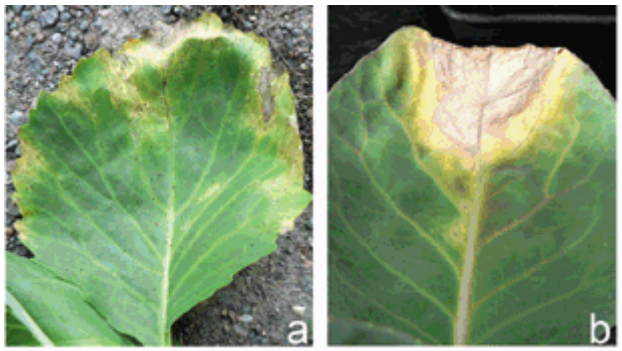

Figure 1: Leaves of *Brassica oleracea* var. *capitata* cv. Bartolo after infection with *Xanthomonas campestris* pv. *campestris* and *Xanthomonas campestris* pv. *aberrans*. A) Infected leaf showing dark spots with typical V-shaped lesions and black veins. **B)** Infected leaf showing typical V-shaped lesions and black veins. (Fargier and Manceau, 2007)

The appearance of black spots with a V-shaped lesion as shown in the images in Figure 1 is a typical symptom of diseases like black rot caused by *Xanthomonas*. An international survey from 2012 placed *Xanthomonas campestris* at position five of a top 10 bacterial plant pathogen list just after *Xanthomonas oryzae* pv. *oryzae* (ranked four) and preceding

Xanthomonas axonopodis pathovars (ranked six) (Mansfield *et al.*, 2012), highlighting the importance of these species.

2.2 Xanthomonads and the pathovar *Xanthomonas campestris*

Xanthomonads belong to the family of Xanthomonadaceae that includes the genera *Xanthomonas* and *Xylella*, which are both known plant pathogens. *Xanthomonas* is a large genus of Gram-negative bacteria that are known to be involved in various plant diseases. Most of the species possess a single circular chromosome with a size between 4.8 and 5.3 Mb. The 27 different species can cause diseases in over 400 different plant hosts, both monocotyledonous and dicotyledonous (Ryan *et al.*, 2011). These hosts include several economically important crops, for example *Xanthomonas oryzae* pv. *oryzicola* that can infect rice or *Xanthomonas citri* pv. *citri* that causes citrus canker. Most of these bacteria are not only restricted to the infection of specific hosts but they also have tissue specificity and can therefore be divided into vascular and mesophyllic pathogens. Vascular pathogens usually enter the plant and invade the xylem elements of the vascular system whereas mesophyllic pathogens invade the intercellular spaces of the mesophyllic parenchyma tissue of plants (Ryan *et al.*, 2011). An overview is given in Figure 2.

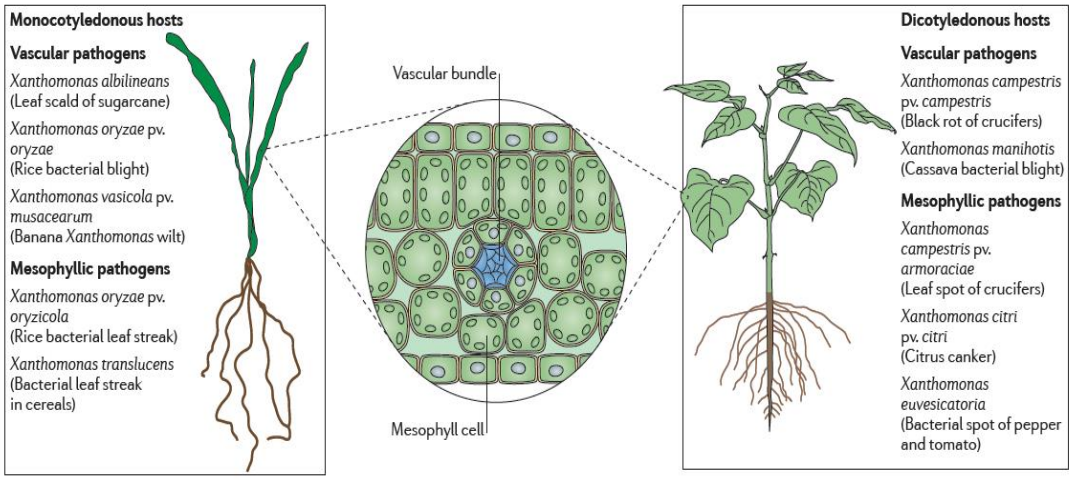

Figure 2: Selection of different *Xanthomonas* species divided into various groups to show host and tissue specificity. The left part shows pathogens that infect monocotyledonous hosts, the right part species infecting dicotyledonous hosts. Additionally, the pathogens are divided into vascular and mesophyllic pathogens. (Ryan *et al.*, 2011)

The species used in this study is *Xanthomonas campestris* pv. *campestris* (*Xcc*), a vascular pathogen that infects dicotyledonous plants and the causative agent of the black rot in crucifers, leading to a high crop loss in agricultural yield worldwide (Qian *et al.*, 2005). The wild type strain *Xcc* 8004 used here has developed spontaneous rifampicin resistance and is derived from strain *Xcc* NCPPB No. 1145 that was isolated from infected cauliflower in Sussex, UK, 1958. The whole genome was sequenced and published in 2005 (Qian *et al.*, 2005). *Xcc* is a Gram-negative rod shaped bacterium with a length of 1.2-3.0 µm and a width of 0.4-1.0 µm (Schaad *et al.*, 2001). The bacterium is an obligate aerobe with an optimal growth temperature of 25°C to 30°C (Averre, 1914) and is used as a model organism to study plant-bacteria interactions (Qian *et al.*, 2005). The membrane-bound xanthomonadin pigments protect the bacterium against photo-oxidative damage and give the bacterium a characteristic yellow colour (Rajagopal *et al.*, 1997). *Xanthomonas* also produces the extracellular polysaccharide xanthan gum that contributes to the mucoid appearance of the bacterium as shown in Figure 3.

Figure 3: Representative picture of *Xanthomonas campestris* pv. *campestris* wild type strain *Xcc* 8004 grown on agar plate. The yellow colour of *Xanthomonas* can be observed due to the membrane-bound xanthomonadin. The plate was incubated at 30°C for 2 days.

Xanthan gum is the major component of the exopolysaccharide (EPS) produced by *Xanthomonas*. The *Xanthomonas* strain B100 is industrially used for the production of xanthan as an additive in different food and cosmetics (Serrania *et al.*, 2008). Additionally, it is utilised as a thickening agent and emulsifier in the pharmaceutical and oil industries (Becker *et al.*, 1998). The bacterium uses xanthan as a natural protection against environmental stress, for example dehydration and toxic substances (Denny, 1995). There is also some suggestion that xanthan may contribute to bacterial pathogenicity and epiphytic survival (Vorhölter *et al.*, 2008). Furthermore, exopolysaccharide is part of biofilms generated by *Xcc* on plant surfaces. For the formation of a biofilm, *Xcc* is using a cell-cell communication system that includes a diffusible signal factor (DSF) (Torres *et al.*, 2007). Xanthan gum is also linked to the evasion of PAMP (pathogen-associated molecular patterns) triggered immunity in plants (Aslam *et al.*, 2008).

2.3 Biofilms and the potential role in host-pathogen interactions

A biofilm is a community of microorganisms that attaches to various surfaces, for example on biomaterials, on contact lenses or in pipes (Elder *et al.*, 1995). The community of microorganisms can consist both of bacteria and fungi, for example *Candida albicans* (Elias and Banin, 2012). After forming a biofilm, the pathogens are located in a distinct extracellular matrix. This extracellular matrix provides an increased tolerance against antibiotics and a protection against the depletion of the biofilm. Among other things, it consists of extracellular polysaccharides, structural proteins, cell debris and nucleic acids (Elder *et al.*, 1995; Høiby *et al.*, 2010). An important role is played by extracellular DNA (eDNA) which provides structural stability but does not carry any genetic information (Mann and Wozniak, 2012). *Xcc* and other biofilm-producing bacteria use biofilms as a mechanism of defence, for example against phagocytes (Jesaitis *et al.*, 2003), osmotic and oxidative stress (Hall-Stoodley and Stoodley, 2009), antibiotics (Hassett *et al.*, 2002) or antibodies (Cerca *et al.*, 2006). Biofilm formation is classified into different phases as shown in Figure 4.

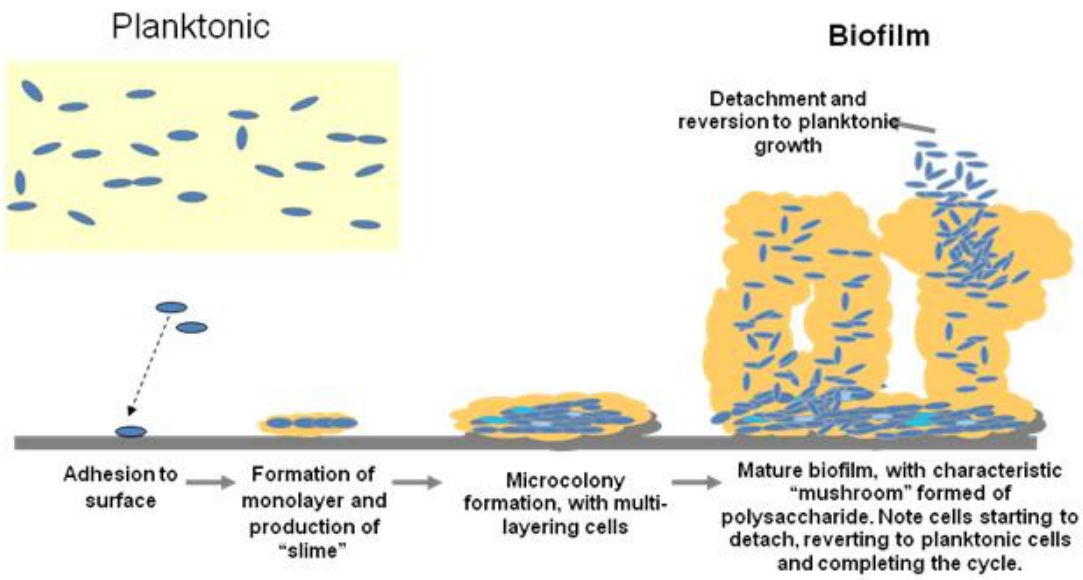

Figure 4: Schematic representation of the formation of a biofilm in four stages. The formation begins with attachment of the planktonic cells followed by the adhesion to the surface. The bacteria then form a monolayer and start to produce an extracellular matrix. Next, a microcolony is formed where multilayers appear. During the final stage, cells start to detach and the biofilm will disperse. (Vasudevan, 2014)

The first stage includes the initial contact of the moving planktonic bacteria with the surface, which is still reversible at this stage. The bacteria will then start to form a monolayer and will produce an extracellular matrix or "slime" for protection. The initial steps are dominated by eDNA, whereas polysaccharides and structural proteins take over later on. In these stages, the formation of microcolonies takes place, which exhibit significant cell-cell communication and growth. The biofilm grows in a three-dimensional manner and the attachment is now irreversible. In the last stage, cells of the mature biofilm start to detach and disperse into the environment as planktonic cells again. These cells can attach to surfaces to start a new round of biofilm formation. It is also possible, that parts of the cell aggregate detach or a movement of the whole biofilm takes place (Sauer *et al.*, 2002; Tolker-Nielsen *et al.*, 2000).

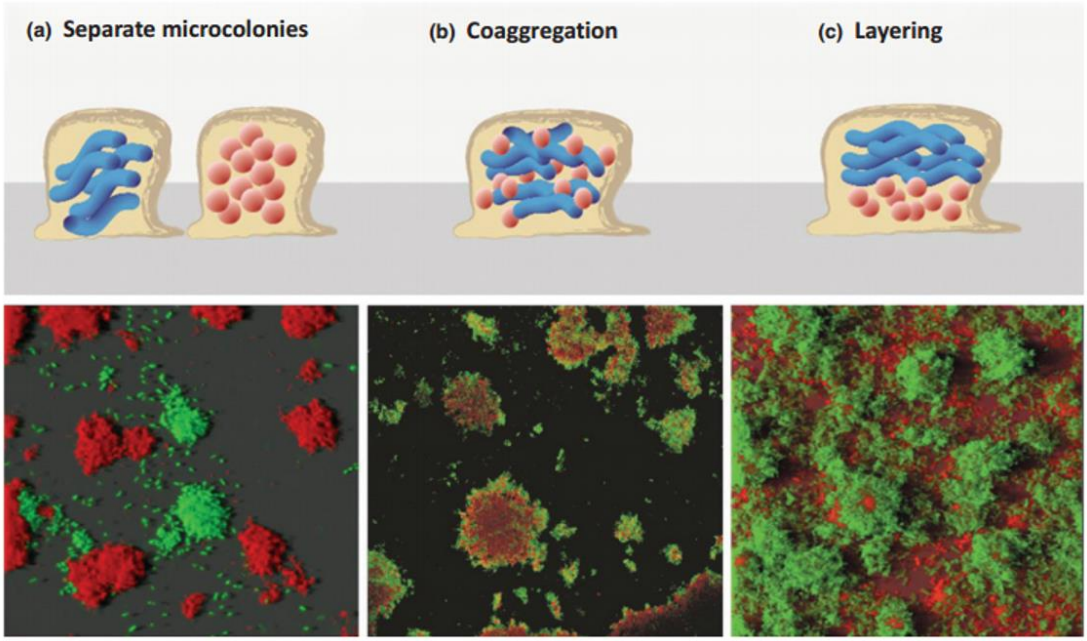

Figure 5: Spatial distribution of a biofilm of different species. The pictures were taken using confocal laser scanning microscopy. a) Separate one-species microcolonies (Nielsen *et al.*, 2000), b) Co-aggregation of the species (Rickard *et al.*, 2006), c) Distribution of the species in layers (Hansen *et al.*, 2007) (Elias and Banin, 2012)

Figure 5 shows three different options for the spatial distribution of a biofilm consisting of different species. In part a, the different species of the biofilm are separated. Part b shows a co-aggregation and part c the distribution in layers. The variable distribution affects the communication of the cells. Here, the spatial proximity of the cells is important for the communication between each other (Elias and Banin, 2012). This cell communication is also named quorum sensing. Quorum sensing relies on a threshold cell number to function.

In addition to the protective function of biofilms for bacteria, they are part of many human pathogenic forms of diseases. *Staphylococcus* and *Pseudomonas* are often involved in diseases associated with biofilm formation (Costerton *et al.*, 1999), but also plant pathogens produce biofilms during infection. In those cases, where a relationship between biofilm formation and virulence in plant infections could be examined, the production of the extracellular matrix and in particular the EPS leads to a blocking of the xylem vessels which

in turn results in a water loss, wilting and tissue necrosis (Fujishige *et al.*, 2006). Because of the increasing amount of biofilms in clinical fields and diseases, the control of biofilms has a high priority. The extracellular matrix is used as diffusion barrier against antibiotics and other bactericidal substances (Fux *et al.*, 2005; Hall-Stoodley and Stoodley, 2009).

One strategy is to prevent the initial attachment of the bacteria at the beginning so that no biofilm can be formed. Therefore, dispersin-B (produced by *Actinobacillus actinomycetemcomitans*) can be used as a biofilm degrading enzyme. It does not lead to an inhibition of biofilm formation but it can disperse parts of the already formed biofilm, allowing the targeted killing of the dispersed cell aggregates by bacteriophages (Itoh *et al.*, 2005; Izano *et al.*, 2008a; Izano *et al.*, 2008b; Kaplan *et al.*, 2004; Lu and Collins, 2007; Venketaraman *et al.*, 2008). The functionality of this enzyme was tested in a sheep that was infected with *S. aureus* and led to significantly reduced bacterial colonisation (Darouiche *et al.*, 2009). Several other approaches are currently under investigation, for example the blocking of communication between cells by quorum sensing signals. The ability of most bacteria to sense and respond to unscheduled changes in their environment is crucial for the organism's survival and ability to cause disease.

2.4 Pathogenicity and virulence factors in *Xanthomonas*

The pathogenesis of plant associated bacteria involves many different steps, starting with the invasion of the plants through different routes, where the bacteria can then establish themselves and start to multiply (Chan and Goodwin, 1999). Diseases caused by *Xanthomonas* species often occur because of contaminated seeds, pruning and misting of seedbeds by rainwater, by the formation of aerosols that can carry bacteria from adjacent infected fields, by contaminated soil and possibly by insects (Ryan *et al.*, 2011). Some bacteria can grow epiphytically on the surface of the leaves, where they initially secrete

compounds which can increase host nutrient loss or avoid or suppress unfavourable conditions in the host (Chan and Goodwin, 1999; Ryan *et al.*, 2011). Virulence determinants are encoded by bacterial genes and might be secreted, for example cell-wall degrading enzymes and toxins, or can be part of the cell surface in case of extracellular polysaccharides, lipopolysaccharides or outer membrane proteins. Some of these factors can directly induce effects in the plant hosts, others in turn can help to promote bacterial survival.

The production of virulence determinants is highly controlled and is only activated when required. That means that pathogens that can grow epiphytically or saprophytically (in soil and water) must be able to differentiate between external environments to coordinate the expression of virulence factors and behaviours associated with virulence for energy conservation, appropriate disease development, evasion of host defence and eventual dispersal (Barber *et al.*, 1997; Mole *et al.*, 2007). To effect this, bacteria have developed a controlled global virulence regulation network (Mole *et al.*, 2007). Upon contact with the host, external signals can lead to the activation of various two-component signalling pathways in *Xanthomonas*, for example the RpfC/RpfG system, the RavS/RavR system or the CorS/CorR system, which are known to have a role in the virulence of *Xanthomonas* (He *et al.*, 2009; Potnis *et al.*, 2015; Qian *et al.*, 2008a; Qian *et al.*, 2008b).

Another response regulator system is the HrpG-HrpX system that has been well studied in *Xanthomonas euvesicatoria* and is known to control the activation of the Type II and Type III secretion systems (T2SS and T3SS) (Bonas *et al.*, 1991; Koebnik *et al.*, 2006; Noël *et al.*, 2002; Potnis *et al.*, 2015). Both protein secretion systems are essential for virulence in *Xanthomonas* species (Chan and Goodwin, 1999). Some of the enzymes secreted by the T2SS include plant cell-wall degrading enzymes, for example xylanase, cellulase, endoglucanase, polygalacturonase and protease (Dow and Daniels, 2000; Dow *et al.*, 1987). The T2SS is

encoded by the *xps* (*Xanthomonas* protein secretion) gene cluster, consisting of 11 genes (*xpsD* to *xpsN*) (Dums *et al.*, 1991; Lee *et al.*, 2000). Proteins secreted by the T3SS are called Type III effector proteins and are translocated directly into the host plant cells, where they may interfere with metabolic and signalling pathways of the host and suppress plant host defence (Mudgett, 2005). The T3SS is encoded by the *hrp* (hypersensitive response and pathogenicity) cluster and is already synthesised during the early stage of plant infection to establish cell-cell contact. Mutants lacking the T3SS have issues in multiplying and colonisation (Mudgett, 2005) thus the *hrp* genes are essential for bacterial growth *in planta* (Noël *et al.*, 2001).

Expression of the *hrp* cluster depends on HrpG, the two-component response regulator and HrpX, an AraC-type (arabinose C-type) transcriptional activator controlling the expression of a genome wide regulon (Noël *et al.*, 2001). The gene cluster is not expressed in complex media but is activated in *hrp* inducing minimal media and on plant surfaces (Schulte and Bonas, 1992; Wengelnik and Bonas, 1996). The actual roles of most of the T3SS effectors remain uncharacterised, however much is known about how plants have evolved resistance to combat T3SS effectors (Mudgett, 2005). These plant defence reactions often are referred to as the hypersensitive response (HR) and lead to a rapid localised plant cell death in resistant plant tissues.

Another pathogenesis associated gene cluster consists of the *gum* genes, which are present in most of the *Xanthomonas* species similar to the *hrp* genes (Lu *et al.*, 2008). The *gum* cluster comprises up to twelve genes (*gumB* to *gumM*) encoding synthases for the extracellular polysaccharide xanthan (Chou *et al.*, 1997; Qian *et al.*, 2005). Xanthan is a polymer of repeating pentasaccharide units consisting of a cellulose backbone and trisaccharide side chains of two mannose and one glucuronate residue that are attached to every second

glucose moiety of the main chain (Jansson *et al.*, 1975). The biosynthesis of this exopolysaccharide occurs in two stages (Dow and Daniels, 2000). As previously mentioned, xanthan is important for full bacterial pathogenicity, epiphytic survival and biofilm formation as part of the extracellular matrix. Once the bacteria have made their way inside the plant through natural routes in rainwater and guttation (a process in which water in liquid form is given off by plants) or via wounds, the cells start to multiply in the cellular spaces and spread throughout the leaf system until the spaces become filled with bacteria and bacterial extracellular polysaccharide (Chan and Goodwin, 1999). In this respect, xanthan may cause wilting of host plants by obstructing the water flow in xylem vessels (Denny, 1995). Because of its negative charge, xanthan can suppress the plant cell-wall defence by binding of extracellular calcium ions, which interferes with signal transduction linked to callose synthetase activation (Aslam *et al.*, 2008; Yun *et al.*, 2006). The importance of the production of EPS for the pathogenicity of *Xanthomonas* was demonstrated using EPS deficient mutants (Dharmapuri and Sonti, 1999; Katzen *et al.*, 1998).

Mutations in secretion pathway genes as well as genome sequence information identified many other genes encoding virulence associated proteins in different *Xanthomonas* species (Chan and Goodwin, 1999; Ryan *et al.*, 2011). Examples include the *thiG* gene from *Xanthomonas oryzae* pv. *oryzae* that is required for the full virulence by preventing cell aggregation (Yu *et al.*, 2015) or *purC* that is required for purine synthesis and whose interruption causes complete loss of virulence in *Xcc* (Qian *et al.*, 2005; Yuan *et al.*, 2013). Furthermore, the flagellum of plant-associated bacteria plays an important role during plant infection. It can act as a virulence factor as well as a potent immunogen. The host plant can recognise the main building block of the flagellum, flagellin, by its plant pattern recognition receptors (Pfeilmeier *et al.*, 2016).

In addition to the pathogenicity clusters *xps*, *hrp* and *gum* already discussed, a fourth pathogenesis-associated gene cluster was found in all *Xanthomonas* species named the regulation of pathogenicity (*rpf)* cluster, that involves the second messenger cyclic di-GMP (bis-(3'-5')-cyclic di-guanosine monophosphate). Recent studies have revealed that c-di-GMP is a major contributor to virulence gene regulation in Gram-negative bacteria and will be discussed in more detailed in the following section.

2.5 The signal molecule cyclic di-guanosine monophosphate (c-di-GMP) as a regulator of virulence and biofilm formation

Cyclic di-GMP is a ubiquitous second messenger in bacteria that was first described as an allosteric activator of cellulose synthase in *Gluconacetobacter xylinus* (Ross *et al.*, 1987). It was seen that the purified cellulose synthase showed less activity than the cellular enzyme, indicating that a co-factor is needed for full activity (Delmer, 1999). Shortly after its discovery, c-di-GMP-dependent enzymes were found in *Agrobacterium tumefaciens* suggesting a broader distribution within the phyla (Amikam and Benziman, 1989). Enzymes regulating c-di-GMP synthesis were later found in all bacterial phyla indicating a universal and highly conserved second messenger (Jenal and Malone, 2006; Römling *et al.*, 2013; Ross *et al.*, 1987). It is now established that this nucleotide regulates a range of functions in diverse bacteria including the virulence of bacterial pathogens of animals and humans (Hengge, 2009; Römling *et al.*, 2005; Wolfe and Visick, 2008). C-di-GMP can have repressing as well as activating functions as shown in Figure 6.

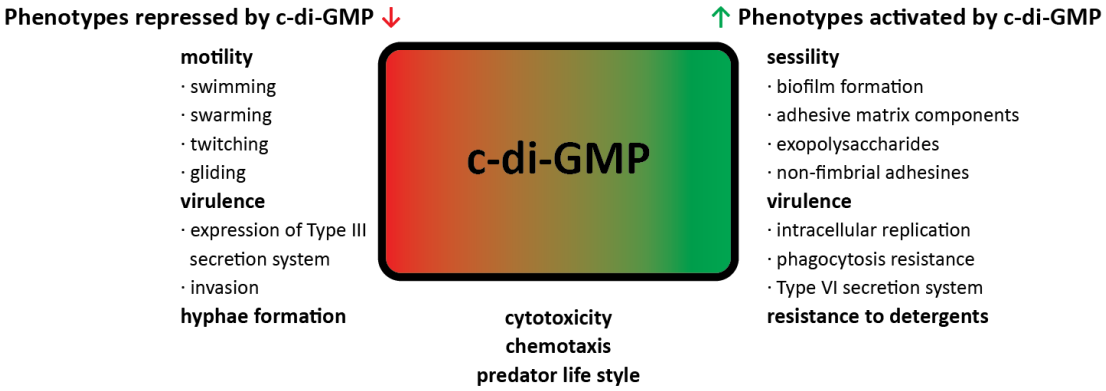

Figure 6: Regulated phenotypes by c-di-GMP. On the left, repression by c-di-GMP is represented, on the right activation by c-di-GMP is shown. (Adapted from (Römling *et al.*, 2013))

The left part of Figure 6 represents some functions that are repressed by c-di-GMP, for example motility of the cells by swimming or swarming and the expression of the Type III secretion system that plays a role during the infection of cells. On the right, functions that are activated by the second messenger can be found. Among other things, an increased resistance to detergents and biofilm formation can occur (Römling *et al.*, 2013).

A lot of c-di-GMP dependent signal metabolic pathways control the ability of bacteria to interact with their environment and other bacteria. Often, c-di-GMP plays an essential role in the change from the motile to sessile phase of bacteria that is central for biofilm formation (Jenal and Malone, 2006). It is also involved in the switchover from a virulent stage to a non-virulent stage (Römling *et al.*, 2013). Furthermore, the second messenger plays a role in the evasion of the plant defence response, called pattern-triggered immunity (PTI). It is reported that high levels of c-di-GMP in several *Pseudomonas* species inhibit flagellin synthesis and help to evade flagellin-specific plant pattern recognition receptors (Pfeilmeier *et al.*, 2016).

C-di-GMP networks consist of mechanisms to produce signals and to respond to changing c-di-GMP levels. Therefore, bacteria are using several effector systems. These effectors or

receptors are binding proteins, in which the second messenger c-di-GMP controls the change of structure and the output function of the effectors (Hengge, 2009). One example is the effector system of FleQ, a transcription regulator of the gene *pelA* in *Pseudomonas aeruginosa* (Hickman and Harwood, 2008; Ryan *et al.*, 2012). The structural polysaccharide Pel is primary involved in the biofilm formation and is part of the extracellular matrix. The maintenance of the biofilm is dependent on the function of Pel to initiate and establish cell-cell communication (Colvin *et al.*, 2012).

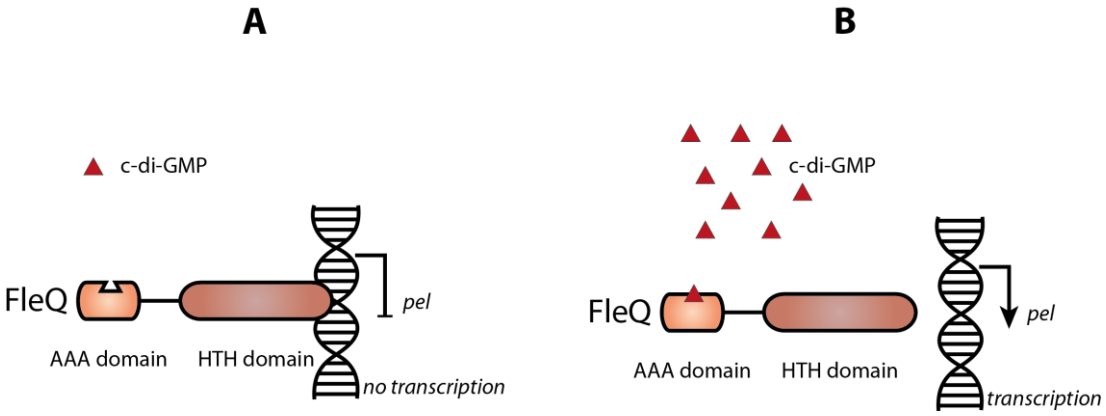

Figure 7: Schematic representation of FleQ and its c-di-GMP dependent regulation of the *pel* gene expression in *Pseudomonas aeruginosa*. A) At low c-di-GMP levels, FleQ binds to the *pelA* promoter leading to repression of transcription. **B)** Once the c-di-GMP level increases, c-di-GMP binds FleQ and the transcription regulator dissociates from the DNA leading to activation of the *pelA* promoter. (Adapted from (Ryan *et al.*, 2012))

Figure 7 shows the schematic representation of the FleQ effector system. The helix-turn-helix domain of the transcription regulator FleQ binds to the *pelA* promoter as long as the c-di-GMP level in the cells is low. This binding leads to repression of transcription of the *pel* gene. In wild type cells, the protein FleN and ATP/ADP can bind to FleQ to reduce the repression of the *pelA* promoter by FleQ. Once the c-di-GMP level reaches a certain threshold, the second messenger binds to the N-terminal AAA domain of FleQ leading to dissociation from the DNA and therefore to activation of *pelA* expression (Ryan *et al.*, 2012).

However, c-di-GMP effectors are not only represented by transcription factors but also by riboswitches, proteins involved in RNA processing and PilZ domain proteins, for example (Ryan *et al.*, 2012). The synthesis and degradation of c-di-GMP involves two different kind of proteins, diguanylate cyclases and phosphodiesterases, which are described in the following section.

2.5.1 Synthesis and degradation of the second messenger c-di-GMP

After the discovery of the bacterial second messenger, various genes were identified that are involved in its synthesis and degradation. These genes code for proteins that often comprise one of the three characteristic amino acid motifs: GGDEF, EAL or HD-GYP (Jenal and Malone, 2006; Römling *et al.*, 2013; Ryan *et al.*, 2006; Tal *et al.*, 1998). Proteins carrying a GGDEF domain are often involved in the formation of c-di-GMP and are called diguanylate cyclases (DGC) whereas proteins with an EAL or HD-GYP domain are mostly involved in c-di-GMP hydrolysis and named phosphodiesterases (PDE) (Ryan *et al.*, 2012). The functional analysis of many of these proteins in different bacteria showed the regulation of various functions like biofilm formation, motility and virulence factor induction (Ryan, 2013; Wolfe and Visick, 2008). An overview of c-di-GMP regulation is given in Figure 8.

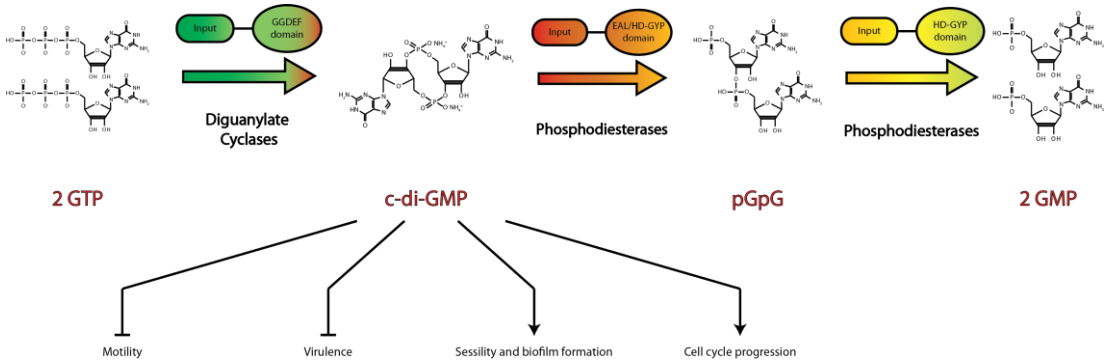

Figure 8: Cyclic di-GMP synthesis and degradation. GGDEF domain proteins (diguanylate cyclases) catalyse the synthesis of c-di-GMP from two molecules of GTP. EAL or HD-GYP domain proteins (phosphodiesterases) catalyse the degradation to pGpG and following to two molecules of GMP. (Adapted from (Christen *et al.*, 2005; Ryan, 2013))

C-di-GMP is synthesised from two molecules of guanosine triphosphate (GTP) with the help of DGCs and degraded by PDEs in a first step to pGpG and in a second step to two molecules of GMP (Christen *et al.*, 2005; Paul *et al.*, 2004; Ryan, 2013). Many of these proteins contain additional signalling domains such as PAS, GAF or REC suggesting that they might be responsive to the environment to modulate their activities (Ryan, 2013; Ryan *et al.*, 2007). However, not all bacteria possess proteins with all three conserved domains, for example *Thermotoga maritima* and *Treponema pallidum* both encode proteins with GGDEF and HD-GYP domains but not EAL domain proteins (Galperin *et al.*, 2001). Furthermore, there are proteins that consist of more than one of the conserved domains.

In *Xcc* strain 8004, 37 proteins with a GGDEF, EAL and/or HD-GYP domain were identified, of which 21 contain a GGDEF domain, 5 an EAL domain, 8 both a GGDEF and EAL domain and 3 an HD-GYP domain (Ryan *et al.*, 2007). Some of the proteins contain domains where amino acids are substituted, suggesting that their roles might not directly be involved in c-di-GMP turnover. A mutant library for these 37 genes was constructed and tested for virulence to plants and virulence factor production, where 13 mutants displayed a reduction in virulence, supporting the suggestion that c-di-GMP is involved in the virulence of *Xcc* (Ryan *et al.*, 2007).

One of these genes encodes the protein RpfG, the first characterised enzyme in *Xcc* containing an HD-GYP domain and demonstrated to be involved in the degradation of c-di-GMP (Galperin *et al.*, 1999; Galperin *et al.*, 2001; Ryan *et al.*, 2006).

2.5.2 The HD-GYP domain protein RpfG

The HD-GYP domain protein RpfG is part of the regulation of pathogenicity (Rpf) system in *Xcc*, that regulates most of the known pathogenicity genes in this species as well as biofilm formation and the synthesis of extracellular enzymes and the exopolysaccharide xanthan (Barber *et al.*, 1997; Dow *et al.*, 2003; Slater *et al.*, 2000; Von Bodman *et al.*, 2003). The *rpf* gene cluster consists of nine genes (*rpfA-rpfI*) in most of the *Xanthomonas* species (Slater *et al.*, 2000). The genes *rpfADEI* and their encoded proteins do not have any important regulatory roles in *Xcc* identified to date (Dow *et al.*, 2003). RpfF and RpfB are involved in the synthesis of the diffusible signal factor (DSF) that is part of a cell-cell signalling system in *Xanthomonas*. RpfC and RpfG belong to a two-component system that is part of the DSF signalling pathway (Barber *et al.*, 1997; Slater *et al.*, 2000). *RpfB* and *rpfF* are transcribed as an operon (*rpfBF*) as are *rpfG*, *rpfH* and *rpfC* (*rpfGHC*). These two operons are close to each other and are transcribed convergently (Slater *et al.*, 2000). Although *rpfH* is transcribed as part of the *rpfGHC* operon, the function of the protein remains unclear. An example of regulation by the *rpf* cluster is through the transcription factor system Clp (cyclic-AMP receptor-like protein) that also interacts with the DSF signalling system. Both are represented in Figure 9.

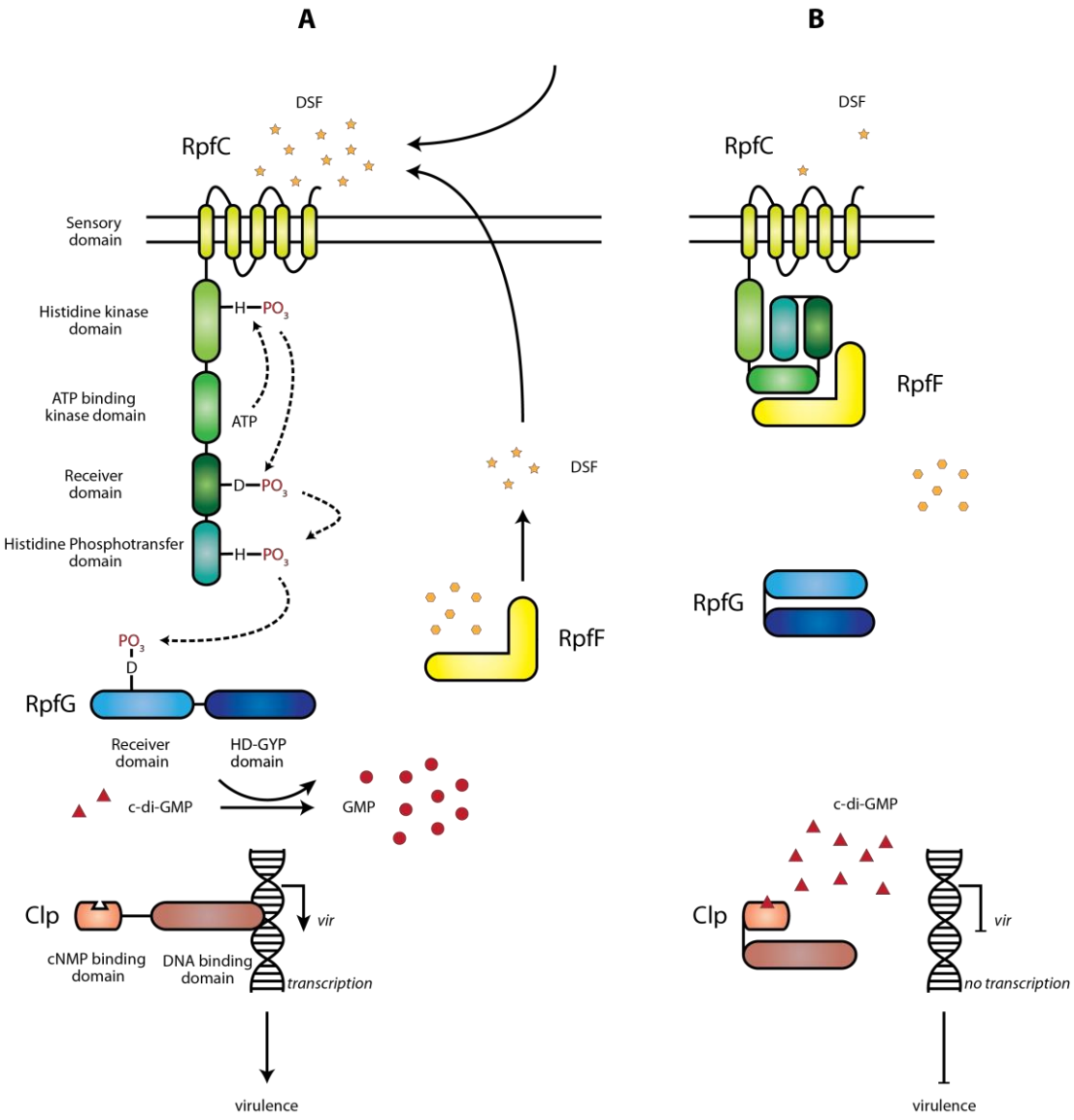

Figure 9: Schematic representation of the DSF signalling pathway involving the RpfCG two-component system and Clp regulation. A) High cell density leads to a production of the cell-cell signal molecule DSF that is sensed by the two-component system RpfCG. The function of the regulator RpfG as a PDE is activated and c-di-GMP is degraded. Thus, the transcription factor Clp is no longer repressed and binds to DNA to activate transcription. **B)** At low cell density, no DSF is produced thus the c-di-GMP level increases. Clp is bound and repressed by c-di-GMP, and the transcription of *vir* genes is no longer activated. (Adapted from (Ryan and Dow, 2011; Tao *et al.*, 2010))

The Rpf two-component system in *Xcc* comprises of the sensor kinase RpfC and the response regulator RpfG. RpfC possesses an N-terminal sensory domain located in the cell membrane, a histidine kinase domain, an ATP binding kinase domain, a CheY-like receiver domain (REC)

and a C-terminal histidine-phosphotransfer domain. The response regulator RpfG consists of a receiver domain and an HD-GYP domain. At a low cell density, RpfF binds to the receiver domain of RpfC so that no DSF is generated. Thus RpfG is inactive and the c-di-GMP level increases. At high levels of c-di-GMP, the molecule binds to the cNMP binding domain of the transcription regulator Clp and thus prevents the binding of Clp to promoter DNA to activate the Clp dependent virulence regulon, represented by *vir*, including genes encoding flagella, extracellular enzymes and Hrp, the master regulator of *Xcc hrp* regulon (He *et al.*, 2009; He *et al.*, 2007). In contrast, if the cell density rises, extracellular DSF is sensed by the sensory domain of RpfC leading to auto phosphorylation of the histidine kinase followed by a phosphorelay. Thereby, RpfF is released and initiates DSF synthesis. Once the receiver domain of RpfG is phosphorylated, a conformational change takes place and the HD-GYP domain becomes activated. After activation, RpfG functions as a PDE degrading c-di-GMP to GMP. Thus Clp becomes released and the DNA binding domain can bind to promoter DNA to initiate the transcription of *vir* (Ryan and Dow, 2010; Tao *et al.*, 2010). During the examination of several mutants for the *rpf* cluster, it could be observed that no DSF was produced in *rpfF* mutants whereas the level of c-di-GMP in both *rpfF* and *rpfG* mutants was higher compared to wild type cells (Barber *et al.*, 1997; Slater *et al.*, 2000). Additionally, the *rpfF* mutant produced less extracellular enzymes and exopolysaccharide than the wild type. The phenotype for *rpfF* could be restored by adding extracellular DSF, however the *rpfG* mutant did not respond to exogenous DSF consistent with the proposed role of RpfG in the DSF signalling system (Barber *et al.*, 1997; Slater *et al.*, 2000).

3 Aims and objectives

Recent domain analysis of the phytopathogen *Xanthomonas campestris* pv. *campestris* genome already revealed 37 genes encoding proteins with one of the three conserved domains involved in cyclic di-GMP synthesis and degradation. The major aim of the work described here is to extend the understanding of the role that c-di-GMP signalling plays in pathogens with respect to virulence and biofilm formation. Therefore, the first objective was to test the hypothesis that c-di-GMP signalling proteins have a role in biofilm formation, virulence and epiphytic colonization of *Xanthomonas campestris*. The effects of loss of different c-di-GMP signalling proteins on virulence were assessed by analysing a pre-existing dataset derived from leaf clipping and leaf spraying assays using a panel of 37 c-di-GMP signalling mutants. Furthermore, the effects of the mutations on the synthesis of specific virulence determinants were examined. These include motility assays, protease assays, EPS assays, endoglucanase assays and cell aggregation assays. A small number of genes was selected for further complementation studies with cloned wild type genes expressed *in trans* and a repetition of the phenotypic assays. The actual c-di-GMP levels in the different strains were determined using a mass spectrometry approach to identify alterations. Additionally, a more detailed domain analysis gave further information about the predicted functions of the proteins identifying additional protein domains involved in environmental signal sensing.

4 Materials and methods

4.1 Material

The bacterial strains and plasmids as well as the media and solutions that were used during the experiments are listed below.

4.1.1 Bacterial strains

The strains that were used for this work are listed in Table 1. Lysogeny broth (LB) was used as standard growth media (liquid or solid as agar plate) for all *E. coli* strains and NYG media was used for growth of *X. campestris*. Antibiotics, if necessary, were added at the required concentration (Table 3) after autoclaving of the media. *E. coli* strains were incubated at 37°C, *X. campestris* at 30°C. All liquid cultures were shaken at 200 rpm or incubated on a roller. Overnight cultures were prepared in 5 mL or 10 mL liquid media and inoculated with a single bacterial colony. The growth period was between 16-20 hours. Strains were stocked as glycerol cultures which were made by using 1 mL overnight culture with 1 mL sterile 50% glycerol and stored at -80°C.

Table 1: Bacterial strains used in this work.

Strain	Genotype/Notes	Source
Escherichia coli DH5α	*sup*E44, *lac*U169(Φ80*lac*ZΔM15) *rec*A1 *end*A1 *hsd*R17 *thi*-1 *gyr*A96 *rel*A1	(Hanahan, 1985)
Escherichia coli TOP10	F– *mcr*A *Δ*(*mrr-hsd*RMS-*mcr*BC) Φ80*lac*ZΔM15 *Δlac*X74 *rec*A1 *ara*D139 *Δ*(*ara leu*) 7697 *gal*U *gal*K *rps*L (StrR) *end*A1 *nup*G	(Thermofisher Scientific)
Xanthomonas campestris pv. *campestris* 8004	Wild type (has developed spontaneous rifampicin resistance)	(Turner *et al.*, 1984)
Xanthomonas campestris pv. *campestris ΔrpfG*	Mutant derived from WT 8004 with deletion of gene *rpfG*	(Ryan *et al.*, 2006)
Xanthomonas campestris pv. *campestris* mutant library	Mutant library derived from WT 8004	(Ryan *et al.*, 2007)

4.1.2 Plasmids

The plasmids used in this study are listed in Table 2.

Table 2: Plasmids used in this work.

Name	Resistance	Reference
pCR®2.1-TOPO®	Kanamycin	ThermoFisher Scientific (Invitrogen™)
pk18mob	Kanamycin	(Schäfer *et al.*, 1994)
pk18mob*sacB*	Kanamycin	(Schäfer *et al.*, 1994)
pLAFR3	Tetracycline	(Staskawicz *et al.*, 1987)
pRK2073	Spectinomycin	(Leong *et al.*, 1982)

4.1.3 Antibiotics

The antibiotics and the concentration at which they were used are given in Table 3.

Table 3: Antibiotics used in this study

Name	Used concentration ($\mu g * mL^{-1}$)	
Kanamycin (Kan)	*E. coli* strains:	25
	Xcc strains:	25
Spectinomycin (Spc)	*E. coli* strains:	50
Rifampicin (Rif)	*Xcc* strains:	50
Tetracycline (Tet)	*E. coli* strains:	15
	Xcc strains:	5

4.1.4 Kits and Enzymes

The kits and enzymes used during this work are listed in Table 4, with name and manufacturer.

Table 4: Kits and enzymes utilised in this study.

Name	Manufacturer
*Eco*RI-HF® with CutSmart® Buffer	NEB
*Bam*HI-HF® with CutSmart® Buffer	NEB
GoTaq® Green Master Mix	Promega
*Hind*III-HF® with CutSmart® Buffer	NEB
*Sma*I with CutSmart® Buffer	NEB
TOPO® TA Cloning® Kit for Subcloning	ThermoFisher Scientific (Invitrogen™)
T4 DNA Ligase with ligation buffer	Sigma-Aldrich
QIAquick® PCR Purification Kit	QIAGEN
QIAprep® Spin Miniprep Kit	QIAGEN

4.1.5 Media and Solutions

The media and solutions used in this work are listed in Table 5.

Table 5: Media and solutions used in this work.

Name	Manufacturer / Components (per L)
5x Loading Buffer Blue	Bioline
0.5% Eiken Agar for motility assay	8 g Difico nutrient broth 5 g Eiken Agar 5 g Glucose
1.5% d.w. Agar	15 g Agar
50 x TAE-buffer	242 g*L^{-1} Tris 57.1 mL*L^{-1} Acetic acid 100 mL*L^{-1} EDTA

Agarose gel mix	0.8% - 2% Agarose in TAE buffer 1 x GelRed™ (Biotium)
Extraction buffer for c-di-GMP isolation	40 mL Acetonitrile (≥99.9%) 40 mL MeOH (≥99.9%) 20 mL HiPerSolv H_2O
L-media for cell aggregation assay	10 g Difco Bacteriological Tryptone 5 g Yeast Extract 5 g NaCl 1 g Glucose
LB broth	10 g Tryptone 5 g Yeast Extract 5 g NaCl
LB agar	LB broth 15 g Agar
Lysis Buffer for gDNA extraction	851.33 mL H_2O 40 mL 1 M Tris Acetate pH 7.8 6.67 mL 3 M NaAc pH 5.2 2 mL 0.5 M EDTA 100 mL 10% SDS w/v
NYG broth	5 g Oxoid Bacteriological Peptone 3 g Difco Yeast Extract 20 mL Glycerol
NYG agar	NYG broth 10 g Agar
Solution A for competent cells	10 ml 1 M $MnCl_2$ 50 ml 1 M $CaCl_2$ 20 ml 500 mM MES pH 6.3

4.1.6 Consumables

Specialised consumables used in this work are listed in Table 6.

Table 6: Specialised consumables used in this work.

Name	Manufacturer
HyperSep™ Aminopropyl Cartridges	ThermoFisher Scientific
Mass-spec grade Eppendorf 1.5 mL	Eppendorf
96 Well Cell Culture Plate, F-bottom	Greiner Bio-one

4.1.7 Oligonucleotide Primers

The sequences of the primers used in this study are given in Table 7. All primer sequences were synthesised by Sigma-Aldrich and labelled with 'fwd' for forward directed primer and 'rev' for reverse directed primer.

Table 7: Oligonucleotide primers used in this work.

Name	Description	Sequence 5' – 3'
C_XC_0362/F	Complementation of gene 0362 + His-tag	GGATCCATGCTCAGAACCATCGACTC
C_XC_0362/R		AAGCTTTTAGTGGTGGTGGTGGTGGTGCG GCAGCCAGAGTTTCTCAA
C_XC_1755/F	Complementation of gene 1755 + His-tag	GGATCCATGCCAGCCCGTCCCCTGCT
C_XC_1755/R		AAGCTTTCAGTGGTGGTGGTGGTGGTGAC GCTCCCGATCCCAGGCGT
C_XC_2459/F	Complementation of gene 2459 + His-tag	GGATCCATGCATTCCACGCCCGCCCC
C_XC_2459/R		AAGCTTTCAGTGGTGGTGGTGGTGGTGGA GGCGCGCGGCTTCCAGTT

C_XC_2793/F	Complementation of gene 2793 + His-tag	GGATCCGTGTTGACCAGAAAAGCAAA
C_XC_2793/R		AAGCTTTCAGTGGTGGTGGTGGTGGTGCAC GCTGCCCGGCGTCACCG
C_XC_3962/F	Complementation of gene 3962 + His-tag	GGATCCGTGAAGCGGCACCGCATCAT
C_XC_3962/R		AAGCTTTCAGTGGTGGTGGTGGTGGTGGC CAGTCCGCCGCAGCGCAT
C_XC_3962/F2	Complementation of gene 3962 + His tag (longer forward primer)	GGATCCGTGAAGCGGCACCGCATCATCAGC GTCACCGTGCTGCTTGC
C_XC_3962/R2		AAGCTTTCAGTGGTGGTGGTGGTGGTGGC CAGTCCGCCGCAGCGCAT
C_XC_3962/F3	Complementation of gene 3962 (without His tag)	GGATCCGTGAAGCGGCACCGCATCAT
C_XC_3962/R3		AAGCTTTCAGCCAGTCCGCCGCAGCGCAT
D_XC_0362L/F	Deletion of gene 0362, Left part (upstream)	CCCGGGTGGCTCACTGCCGGCGCAC
D_XC_0362L/R		GCCGGCGCTGGTCTGCAAGT
D_XC_0362R/F	Deletion of gene 0362, Right part (downstream)	GGCCTCTCGCACGTTTGACG
D_XC_0362R/R		CCCGGGTCCCGGAATAGTTATGCAC
D_XC_1755L/F	Deletion of gene 1755, Left part (upstream)	CCCGGGGCCGAGACCGCCGCCGCGCA
D_XC_1755L/R		GCGGAATCCTTGCGAACCGG
D_XC_1755R/F	Deletion of gene 1755, Right part (downstream)	GAGATGGGAATCGGGAGTTG
D_XC_1755R/R		CCCGGGGGCCGGGATCAGCACCGCCA
D_XC_3962L/F	Deletion of gene 3962, Left part (upstream)	CCCGGGGGCGACGCCGGTGTCGCCCA
D_XC_3962L/R		TTCAGATCCTGACATGGGTG
D_XC_3962R/F	Deletion of gene 3962, Right part (downstream)	GCGTCGGATCGCTGATCTGC
D_XC_3962R/R		CCCGGGAGGGCGGTTGCGTTGGAGTG

NK_XC_2459/F	Insertion of gene 2459 with pk18mob	GGATCCTCCTGGTGATTCCCGATGCC
NK_XC_2459/R		AAGCTTGCCGATACAAGGCGGTGCCG
NK_XC_2793/F	Insertion of gene 2793 with pk18mob	GGATCCGGCTTGAGGTGTTGGTGCAG
NK_XC_2793/R		AAGCTTTGCGGCAGTTCTGCAGCAGG
pKmob18Con	Validation of pK18mob mutant insertions	GCCGATTCATTAATGCAGCTGGCAC
pKmob18F		CCCGCGCGTTGGCCGATTCATTAATG
pKmob18R		GCCAGTGCCAAGCTTGCATGCCTG
pL3validation (Tet)F	Validation of plasmid pLAFR3 (tet-cassette)	TTTCCTGACGGGCTGTTTCC
pL3validation (Tet)R		CCACCTGCCTGGACAACATT
XC_2228_FL/Fw	Amplification of gene 2228 To validate insertion	ATGTGGAGCCCTGTGATCCCG
XC_2228_FL/Rv		CTATTCCCGGCCGTTCCGCAAC

4.1.8 Equipment

The equipment used in this work is listed in Table 8.

Table 8: Equipment used in this work.

Name	Product	Company
EnSpire Multimode Plate Reader	Plate Reader	Perkin Elmer
Eppendorf Concentrator plus	Concentrator	Eppendorf
Eppendorf Thermomixer comfort	ThermoMixer	Eppendorf
Fisherbrand Magnetic Stirrer FB15045	Magnetic stirrer	Fisher Brand
GENESYS™ 10S UV-Vis Spectrophotometer	UV-Spectrometer	Thermo Scientific™

Microcentrifuge, Micro Star 12	Centrifuge for microtubes	VWR
Molecular Imager® Gel Doc™ XR+ System	Image equipment for DNA and protein gels	Bio-Rad
MultiSUB Gelkammern	Gel chambers	Cleaver Scientific
Multitron Standard	Shaker	Infors HT
New Brunswick™ Innova® 2100 benchtop open air shaker	Open air shaker	Eppendorf
PHMT-PSC24 Thermoshaker	Thermoshaker	Grant Instruments
PowerPac™Basic Power Supply System	Power supply system	Bio-Rad
Refrigerated SIGMA 3-16K Centrifuge	Centrifuge for falcons and overnight container	Sigma
Scales Talent TE2101	Balance	Sartorius
Spectrafuge™ Mini Laboratory Centrifuge	PCR-tube centrifuge	Labnet International
TC-7 tissue / microbial culture roller drum	Roller	Eppendorf
Thermocycler, peqSTAR	PCR-Cycler	VWR Peqlab
Vortex-Genie 2	Vortex	Scientific Industries

4.1.9 Bioinformatics tools and software

Software and tools that were used for this work are listed in Table 9.

Table 9: Bioinformatics tools and software used in this work.

Name (Version)	Reference/Company
Adobe Illustrator CS5 (Version 15.1.0)	Adobe Systems Incorporated
blastn	(Altschul *et al.*, 1990)
CLC Main Workbench (Version 7.6.2)	QIAGEN Aarhus A/S (www.clcbio.com, https://www.qiagenbioinformatics.com/)
EndNote X7.5	Thomson Reuters
Enspire Manager Software 4.1	Perkin Elmer
Image Lab™ Software (v5.1)	ImageLab, Bio-Rad
ImageJ (1.49j)	(Schneider *et al.*, 2012)
KEGG	(Kanehisa and Goto, 2000; Kanehisa *et al.*, 2016)
MARS Data Analysis Software (Version 3.01 R2)	BMG LABTECH
SMART	(Letunic *et al.*, 2015; Schultz *et al.*, 1998)

4.2 Methods

4.2.1 General methods for molecular biology

4.2.1.1 Agarose gel electrophoresis

DNA molecules were separated in 0.8% - 2% agarose gels at 100 V by gel electrophoresis. GelRed™ (Bioline) was added to the gels for the detection of DNA via ultra violet (UV) light. For PCR samples, the loading buffer was already included in the GoTaq® Green Master Mix

(Promega) and the samples could be loaded directly to the gel. Restriction digestion samples were prepared by adding 5x Loading Buffer Blue (Bioline) before loading the gel. The HyperLadder™ 1 kb Plus (Bioline) was used for size determination. Gel bands were visualised using the UV-trans illuminator (Bioline).

4.2.1.2 DNA extraction

Plasmid DNA was extracted from 10 mL LB overnight cultures of *E. coli* following the manufacturer's instructions (QIAprep® Spin Miniprep Kit by Qiagen).

For the extraction of genomic DNA from *Xcc*, 1.4 mL of overnight culture were harvested by centrifugation at maximum speed for 2 min. After removing the supernatant, the pellet was suspended in 400 µL lysis buffer and incubated for 2-4 minutes. Afterwards, 200 µL 5M NaCl was added and mixed by inverting, followed by incubation at -20°C for 20 min and centrifugation at 4°C for 15 min at maximum speed. The supernatant was transferred into a fresh tube (~400 µL) and 800 µL (double the volume) 100% EtOH was added. The remaining liquid was centrifuged again for 15 min at 4°C and maximum speed and the supernatant was carefully removed and discarded. The pellet was resuspended in 30 µL water and stored at -20°C.

4.2.1.3 Polymerase chain reaction (PCR)

PCR reactions were carried out according the manufacturer's instructions (GoTag® Green Master Mix Usage Information by Promega). The composition of a 20 µL reaction using GoTag® (Promega) and the standard programme are listed in Table 10. Sequences for primers can be found in Table 7.

Table 10: Components of GoTaq® PCR reaction and adjustment of the programme.

Component	Volume (µL)	PCR programme	
GoTaq® Green Master Mix	10	1) Initial denaturation	95°C, 5 min
Forward primer (10 µM)	0,5	2) Denaturation	95°C, 30 sec
Reverse primer (10 µM)	0,5	3) Annealing	56°C, 30 sec
DNA template (≤ 250 ng)	1	4) Elongation	72°C, 1 min*kb^{-1}
H_2O	8	*Repeat step 2) - 4) 30 times*	
	20	5) Finale Elongation	72°C, 7 min
		6) Store	10°C, ∞

For colony PCR, a single colony was picked from a plate and resuspended in 20 µL water. The cells were lysed at 95°C for 10 min (*E. coli*) or 20 min (*Xcc*) and then used as DNA template as described above.

4.2.1.4 Restriction digestion of DNA

Plasmid restriction was carried out by following the restriction enzyme manufacturer's instructions (New England Biolabs). The composition of a 20 µL reaction is given in Table 11.

Table 11: Restriction digestion using NEB restriction endonucleases. The components and the corresponding volumes are listed.

Component	Volume (µL)
Enzyme	1
CutSmart® Buffer (10X, NEB)	2
DNA template	16
H_2O	Fill up to 20
	20

4.2.1.5 T4 ligation

Ligation of DNA fragments was undertaken using T4 ligase (ThermoFisher Scientific). The composition of the ligation reaction is given in Table 12.

Table 12: T4 ligation reaction. The components and the corresponding volumes are listed.

Component	Volume (µL)
DNA part 1	4
DNA part 2	4
T4 ligase	1
T4 Buffer	1
	10

After adding all components, the reaction was stored at room temperature for ~16 h before being used for transformation.

4.2.1.6 Preparation of *E. coli* competent cells

To inoculate 25 mL LB containing 15 mM $MgCl_2$ in a 250 mL flask, 500 µL of an overnight culture of *E. coli* strain DH5α was used. The bacteria were grown to an OD_{600} of 0.4-0.6 and then chilled on ice for at least 40 min. The cells were then transferred to Falcon tubes and pelleted at 4°C for 10 min and 3 000 *g*. The pellets were suspended in 10 mL ice cold sterile solution A (see Table 5) and kept on ice for at least 20 min. Another spin down followed at 4°C for 10 min and 3 000 *g* and the pellets were suspended in 1.5 mL solution A + 15% glycerol. Afterwards, the cells were divided into 100 µL aliquots and stored at -80°C for further use.

4.2.1.7 Transformation of *E. coli* DH5α via heat shock

For the transformation of *E. coli* DH5α via heat shock, 10 µL ligation mix were added to 100 µL of competent DH5α and incubated on ice for 15-20 min. The cells were heat shocked at 42°C for 45 sec, incubated on ice for 2-3 min and suspended in 500 µL LB medium. After incubation at 37°C for 60 min and 200 rpm, the cells were pelleted, the supernatant decanted, the pellet resuspended in 50 µl of LB and plated on selective media.

4.2.1.8 TOPO cloning and transformation

TOPO cloning was performed according to the manufacturer's instructions (TOPO® TA Cloning® Kit, ThermoFisher Scientific). The composition of the cloning reaction is given in Table 13.

Table 13: TOPO cloning reaction. The components and the corresponding volumes are listed.

Component	Volume (µL)
PCR product (cut from gel)	4
Salt solution	1
TOPO vector	1
	6

The entire reaction was introduced into one vial of Top10 chemo competent cells provided with the kit and transformed according to the instructions.

4.2.1.9 Plasmid transfer to *Xanthomonas* by triparental mating (conjugation)

Overnight cultures prepared from single colonies were set up for the recipient (*Xcc*), the helper strain (*E. coli* DH5α 2073) and the plasmid-carrying strain (*E. coli* DH5α) in 10 mL NYGA (*Xcc*) or LB medium (*E. coli*), respectively. To gain the most efficient result, the *Xanthomonas*

culture was inoculated 2 h earlier than the *E. coli* cultures. For the conjugation, 2 x 800 µL of the recipient was spun down and the supernatant was discarded. The cells were washed twice in 800 µL 0.9% NaCl before adding 800 µL of the helper strain. After pelleting and discarding the supernatant, 1 mL of the plasmid-carrying strain was added and the mixture was pelleted. The whole mixture was suspended in 800 µL NYGB medium and spun down again. In a final step, the pellet was slowly collected with a pipette tip, stirring the pellet carefully, and the cells were placed on an NYGA plate. The spot was dried for 30 min and then incubated at 30°C for 24 hours. After the incubation, the spot was scraped off the plate using a pipette tip and suspended in 200 µL NYGB. For plating, 100 µL of the suspension were used for one selective plate.

4.2.1.10 Strain construction

In this section the construction of strains used in this work is described. Sequencing of products was carried out by the MRC PPU DNA Sequencing and Services, University of Dundee.

4.2.1.10.1 Complementation

For the complementation of mutant strains, primers were designed covering the whole coding sequencing of the targeted gene including an additional C-terminal His-tag for protein identification and purification. Recognition sequences for *Bam*HI (GGATCC) and *Hind*III (AAGCTT), respectively, were added at the 5' ends of each primer. Wild type *Xcc* 8004 genomic DNA was used as template for amplification of the gene of interest and TOPO cloning was used to clone the purified sequence into the TOPO vector and to transform the reaction mix into *E. coli* TOP10. Clones were verified by DNA sequencing. After restriction digestion of the isolated plasmid using *Bam*HI and *Hind*III, the DNA fragment was isolated by

agarose gel electrophoresis and cloned into similarly digested pLAFR3 (Tetracycline resistance) using T4 ligase. The final plasmid could then be transformed into *Xcc* by triparental mating. A schematic representation can be found in the appendix (see Appendix Figure 1).

4.2.1.10.2 Deletion mutants

For the construction of deletion mutants, two primer sets for each target gene were made. One primer set was set upstream of the target coding sequence containing a *Sma*I restriction sequence (CCCGGG) at the 5' end of the forward primer. The other set was placed downstream and had a *Sma*I restriction sequence at the 5' end of the reverse primer. Both DNA parts were amplified using wild type *Xcc* genomic DNA as template, gel purified and cloned into *E. coli* TOP10 using the TOPO cloning kit. After clones were verified by sequencing, the cloned DNA was released by digestion with *Eco*RI, and both parts of the deletion were ligated together using T4 ligase and then amplified by PCR. The purified fragment was again cloned with the TOPO cloning kit and DNA sequenced for verification. After the release of the cloned insert using *Sma*I, it was ligated into the suicide vector pk18*mobsacB* (Kanamycin resistance) before introduction into wild type *Xcc* 8004 by triparental mating.

Integration of the suicide vector into the genome via a single cross over was verified by PCR. For induction of a second homologous recombination step to drive plasmid excision from the genome, a single colony was placed on an NYGA plate without antibiotics. An overnight culture in 10 mL NYGB was inoculated from a single colony. This was sub-cultured the following morning at 1:100 dilution, incubated during the day and 200 µL of this was subsequently used to inoculate 10 mL of fresh NYGB. Following incubation for 16 hours, a dilution series was prepared and four NYGA plates were plated using 100 µL of the 10^{-6}

dilution for each plate. The plates were incubated at 30°C for three to four days until single colonies could be picked and transferred to NYGA plates containing 15% sucrose. Sucrose induces the second homologous recombination because the presence of the *sacB* gene encoded on the vector causes sucrose toxicity. This excision step could be verified after two days of incubation by PCR. A schematic representation can be found in the appendix (see Appendix Figure 2).

4.2.1.10.3 Insertion mutants

For the construction of insertion mutants, primers were designed to amplify part of the target gene (~500 bp). Restriction sites for *Bam*HI (GGATCC) and *Hind*III (AAGCTT), respectively, were included at the 5' ends of each primer. Wild type *Xcc* 8004 genomic DNA was used as template for the amplification of the gene and TOPO cloning was used to clone the PCR product into the TOPO vector. After sequence verification, the insert was released by digestion with *Bam*HI and *Hind*III, gel purified and cloned into the suicide vector pk18*mob* (Kanamycin resistance) using T4 ligase. The resultant plasmid was introduced into wild type *Xcc* 8004 by triparental mating. The insertion of the plasmid and thereby the disruption of the coding sequence of the target gene took place by homologous recombination. A schematic representation can be found in the appendix (see Appendix Figure 3).

4.2.2 Phenotypic assays

The phenotypic assays used in this work are described in the following section. Images of plates were taken using a compact camera. For a repetition of the phenotypic assays, the Molecular Imager® Gel Doc™ XR+ System (Bioline) was used to make images and ImageJ was used to analyse the areas of interest.

4.2.2.1 Motility assay

For the motility assay, 0.5% Eiken agar plates were used (see 4.1.5). Single colonies following overnight growth on NYGA plates were picked with a pipette tip and inoculated onto a 0.5% Eiken agar plate. The plates were incubated at 30°C for 48 hours before the motility could be determined (see Figure 10).

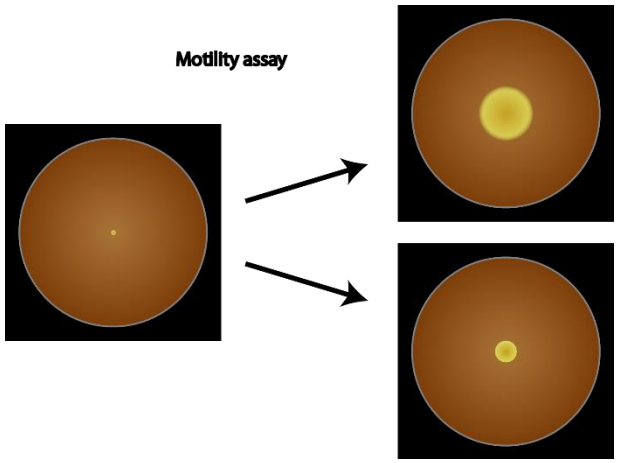

Figure 10: Motility assay. The motility of strains could be determined after 48 hours incubation using 0.5% Eiken agar plates.

4.2.2.1 Protease assay

Plates were prepared by adding 15 mL 20% skimmed milk to 300 mL of molten NYG agar. Overnight cultures of *Xcc* strains of interest were grown in NYGB and adjusted to on OD_{600} of 1. For the determination of protease production and secretion, 3 µL of cells were placed onto the 1% skimmed milk plates, dried for 20 min and incubated at 30°C for 24-48 hours before the diameter of clearance could be determined (see Figure 11).

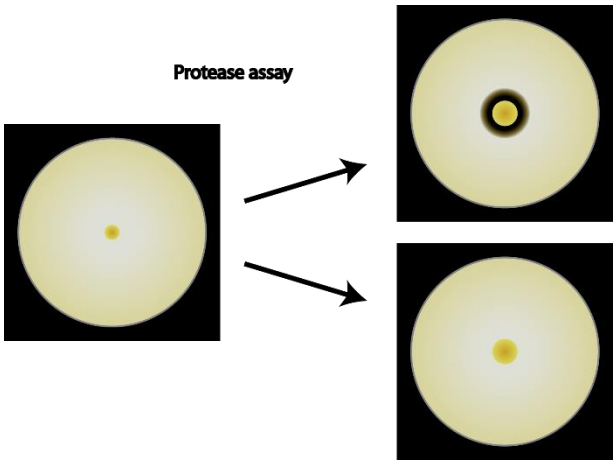

Figure 11: Protease assay. The diameter of clearance could be determined after 24-48 hours incubation using 1% skimmed milk plates.

4.2.2.2 Exopolysaccharide (EPS) assay

Plates were prepared by adding 15 mL 40% glucose to 300 mL of molten NYG agar. Overnight cultures of *Xcc* strains of interest were grown in NYGB and adjusted to on OD_{600} of 1. For the determination of EPS production, 3 µL of the cells were placed on the 2% glucose plates, dried for 20 min and incubated upright at 30°C for 48-72 hours (see Figure 12).

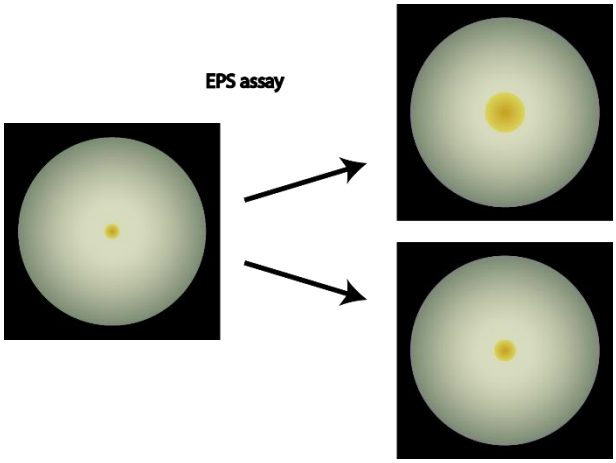

Figure 12: Exopolysaccharide assay. After 48-72 hours of incubation, the production of EPS can be evaluated using 2% glucose plates.

4.2.2.3 Endoglucanase assay

CMC (carboxymethylcellulose) plates were prepared by adding 10 mL 2.5% CMC and 10 mL KPO_4 (1M, pH6.0) to 200 mL of molten 1.5% d.w. agar. Once they were dried, the plates were further processed by making holes in the agar using a pipette tip. Overnight cultures of *Xcc* strains of interest were grown in NYGA and adjusted to an OD_{600} of 1. The cells were spun down and the supernatant (containing secreted proteins) was transferred to a new tube. The holes were filled with 50 µL of supernatant without dilution, at 1:20 dilution or at 1:50 dilution and the plates were incubated upright at 37°C for 24 hours. All plates were stained with 15 mL of Congo Red (0.1%) for 30 min before decanting and repeated washing with water. The plates were covered with 5M NaCl for 10 min. After decanting the NaCl solution, the diameter of clearance could be determined (see Figure 13).

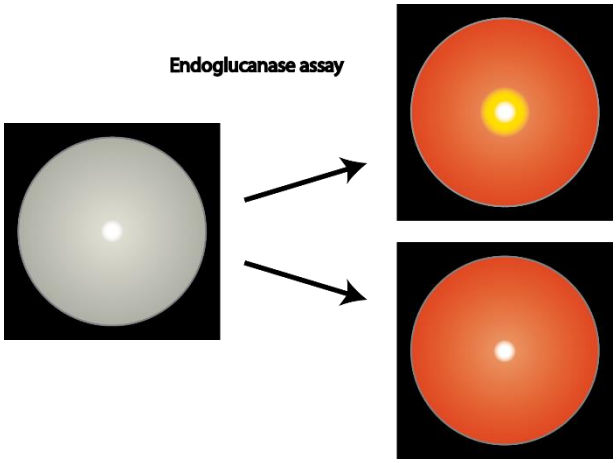

Figure 13: Endoglucanase assay. After 24 hours of incubation, the diameter of clearance can be determined using CMC plates.

4.2.2.4 Cell aggregation assay

For the cell aggregation assay in 250 mL shaking flasks, L-media was used. Overnight cultures were grown in NYGB and adjusted to an OD_{600} of 1. Each 250 mL flask contained 50 mL of L-media and was inoculated with 25 µL cells. The flasks were then incubated at 30°C and 200 rpm for 16 hours, before the biofilm formation (clumping of cells) was determined (see Figure 14).

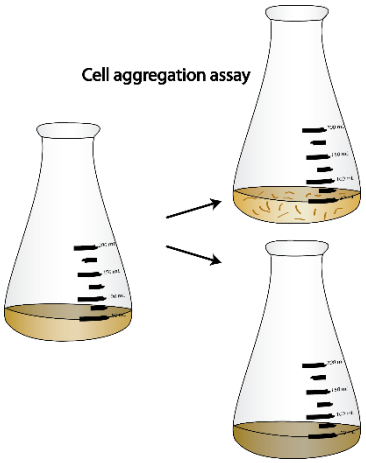

Figure 14: Biofilm assay. After 16 hours of incubation, clumping of bacteria can occur as seen in the right upper flask

4.2.3 Growth measurement

Overnight cultures of *Xcc* strains of interest grown in NYGB and adjusted to OD_{600} of 0.05 were used to measure growth in 96 well plates (F-bottom, Greiner Bio-one). Each well was filled with 200 µL of the diluted culture, 7 wells were used for each strain. The last column was filled with NYGB as negative control. The plate was incubated in a plate reader (EnSpire Multimode Plate Reader, Perkin Elmer) at 28°C with a condensation prevention set up (2°C warmer at the top). Shaking was performed at 200 rpm for 5 sec before each measurement and a read was taken every 15 min for 24 h.

4.2.4 C-di-GMP extraction and detection

For the extraction of c-di-GMP, all reagents used were at least molecular grade and HiPerSolv H_2O (VWR) was used at all times. The solutions were always freshly made on the day.

For the growth of bacteria, agar plates had to be dried before use. After ~6 h, the plates were spread with a lawn of bacteria and incubated at 30°C for 2-3 days. Mass-spec grade Eppendorf tubes (1.5 mL) were weighed and cells were harvested from the plates. The tubes containing the cells were weighed again before suspending the cells in 1 mL ice cold extraction buffer. The samples were then snap frozen in liquid nitrogen for 15 sec and sealed in parafilm before being heated to 95°C for 10 min. After cooling the tubes, they were vortexed for 90 sec and further homogenised using a pipette tip. The samples were spun down at 17 000 *g* for 5 min at 4°C before the supernatant was taken and stored in mass-spec grade Eppendorf tubes on ice at 4°C. The remaining cells were washed with 1 mL extraction buffer and incubated on ice for 15 min. The recent steps (vortexing, homogenising, spinning down and storing supernatant) were repeated twice. All three supernatants were dried at 60°C using a speed vac (programme V-AL). The supernatants from one sample were combined when the volume allowed it (after ~20 min). The dried samples were suspended in 1 mL HiPerSolv H_2O and vortexed for 1 min to collect all dried material from the sides of the tube. The samples can be frozen and stored at -80°C at this step.

HyperSep™ Aminopropyl Cartridges were equilibrated by washing with three times 1 mL 80% methanol and twice with 1 mL HiPerSolv H_2O. The sample was loaded onto the column and allowed to flow through the column slowly to ensure maximum c-di-GMP binding. Afterwards, the columns were washed once with 1 mL HiPerSolv H_2O, and twice with 1 mL of 2% acetic acid in 80% methanol. The columns were finally washed with 1 mL 80% methanol before eluting the bound c-di-GMP with 500 µL 4% ammonium hydroxide in 80% methanol.

The eluent was flushed through the column three times to remove as much bound c-di-GMP as possible. The samples were then dried using a speed vac (programme V-AQ) at 60°C. The dried samples were suspended in 50 µL HiPerSolv H_2O and 0.5 µL internal standard (c-di-AMP, 1 µM) was added (0.5 pmol). The samples were stored at -20°C or -80°C.

For the further analysis, the samples were given to the FingerPrints Proteomics facility, School of Life Sciences, University of Dundee, where 2.5 µL aliquots of the samples were used to detect and measure the c-di-GMP via multi reaction monitoring coupled with mass spectrometry (MRM-MS). With the help of the resulting chromatograms and the area calculated by the programme, the level of c-di-GMP could be determined, taking the internal standard with known concentration and the total weight of used cells into account.

5 Results

5.1 Analysis of two different virulence assays of *Xanthomonas campestris* using Chinese radish as a host plant

The starting point for the work described in this thesis was a prior study of 37 insertion mutants of *Xanthomonas campestris* pv. *campestris* (*Xcc*) each carrying either a Tn5 transposon insertion or a pk18mob insertion in a gene predicted to be involved in the c-di-GMP signalling pathway. These strains were constructed in Nanning, China and are described in Ryan *et al.*, 2007. According to Dr Robert Ryan, the pk18mob insertion mutants were constructed using a conserved sequence in *Xcc* for random and unspecific insertion, which were subsequently verified by PCR. An overview of these strains is given in Table 14.

Table 14: Overview about the 37 *Xcc* strains given with gene name and specification of insertion. The information was provided by Dr Robert Ryan.

Gene	Insertion	Gene	Insertion
XC0249	pK18mob insertion	*XC2226*	pK18mob insertion
XC0362	Tn5 insertion	*XC2228*	pK18mob insertion
XC0420	Tn5 insertion	*XC2274*	pK18mob insertion
XC0613	Tn5 insertion	*XC2275*	pK18mob insertion
XC0637	Tn5 insertion	*XC2276*	Tn5 insertion
XC0641	pK18mob insertion	*XC2324*	Tn5 insertion
XC0675	pK18mob insertion	*XC2335*	pK18mob insertion
XC0831	pK18mob insertion	*XC2459*	Tn5 insertion
XC1036	Tn5 insertion	*XC2715*	pK18mob insertion
XC1383	Tn5 insertion	*XC2793*	pK18mob insertion
XC1411	Tn5 insertion	*XC2795*	pK18mob insertion

XC1476	Tn5 insertion	*XC2866*	pK18mob insertion
XC1582	Tn5 insertion	*XC2946*	pK18mob insertion
XC1755	Tn5 insertion	*XC3163*	pK18mob insertion
XC1766	Tn5 insertion	*XC3800*	pK18mob insertion
XC1803	Tn5 insertion	*XC3829*	pK18mob insertion
XC1824	Tn5 insertion	*XC3962*	pK18mob insertion
XC1841	Tn5 insertion	*XC4313*	pK18mob insertion
XC2161	pK18mob insertion		

The Ryan group together with collaborators in Nanning performed two different virulence assays using these mutant strains of *Xcc* with Chinese radish (*Raphanus sativus*) as the host. The results of these two assays are summarised in Figure 15, and the data is partially taken from ((Ryan *et al.*, 2007); leaf-clipping assays) and some of it is unpublished (spray assays, subset of leaf-clipping assays).

The results of the two virulence assays show that 15 strains in the leaf clipping assay (*ΔrpfG, XC0249, XC0420, XC0637, XC0641, XC0675, XC0831, XC1036, XC1411, XC1476, XC1582, XC1755, XC1841, XC2324* and *XC2335*) and 26 strains in the spray assay (*ΔrpfG, XC0249, XC0362, XC0420, XC0637, XC0641, XC0675, XC1036, XC1411, XC1476, XC1582, XC1766, XC1824, XC1841, XC2226, XC2228, XC2324, XC2335, XC2459, XC2715, XC2793, XC2795, XC2866, XC2946, XC3163* and *XC3962*) have a marked reduction in virulence compared to the wild type *Xcc* 8004. In addition, four mutants showed a significantly increased percentage of infected leaves (*XC0613, XC1755, XC2161, and XC2275*) for the spray method.

Comparing both data sets, 12 of the strains, marked in red (*XC0362, XC1766, XC1824, XC2228, XC2459, XC2715, XC2793, XC2795, XC2866, XC2946, XC3163* and *XC3962*) did not show a significant difference in virulence compared to the wild type for the leaf clipping assay

but had reduced virulence as scored by the spray method. The mutant strain highlighted in green (*XC1755*) showed a reduced virulence for the clipping assay but an increased infection rate for the spray assay.

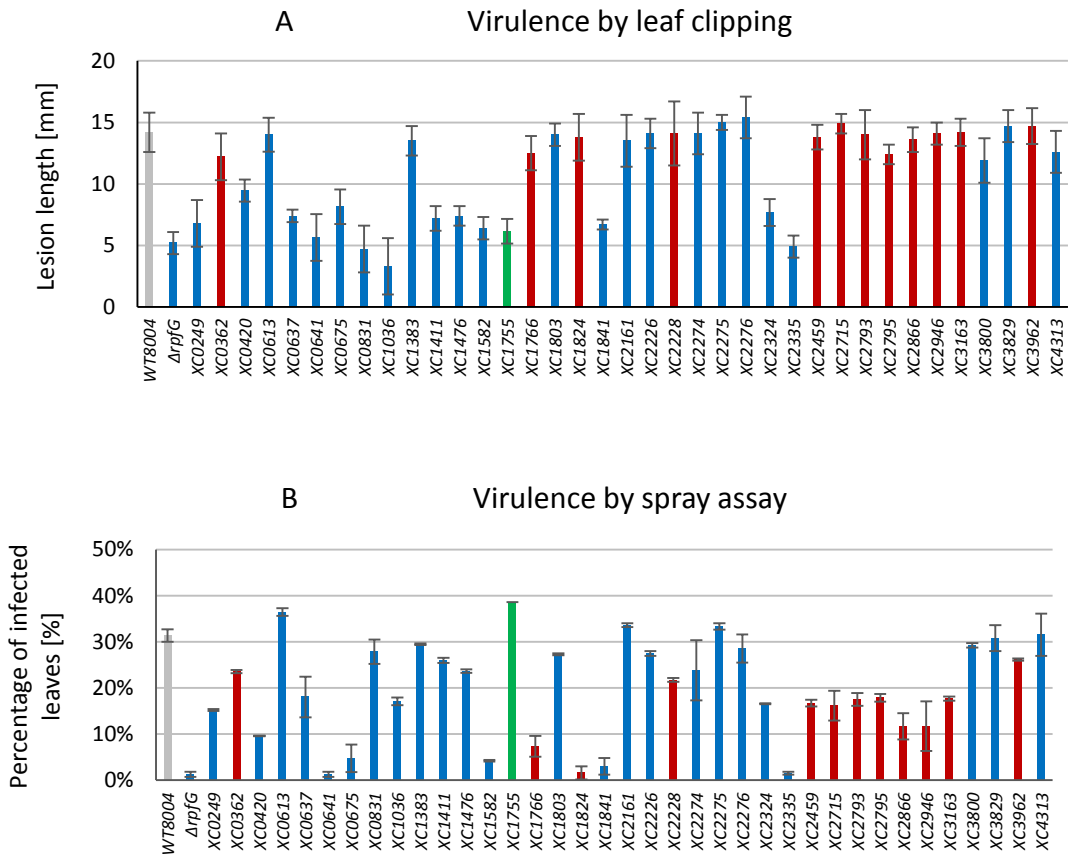

Figure 15: Results for virulence assays of 37 *Xcc* strains using leaf clipping and spray model, respectively. Approximately 100 to 120 leaves of Chinese radish (*Raphanus sativus*) were used as hosts for both assays. Mutants marked in red and green showed differences in the virulence between both methods, wild type is highlighted in grey. **A)** Virulence by clipping. The lesion length in mm was measured two weeks after infection. **B)** Virulence by spray assay. The percentage of infected leaves was calculated ten days after infection. Data provided by Dr Robert Ryan.

5.2 Phenotypic analysis of 37 *Xcc* mutant strains

To study these mutant strains further, additional phenotypic screening assays were performed on each of these 37 *Xcc* strains to assess for effects on motility, cell aggregation, protease, EPS and endoglucanase production, using the methodology described in Section 4.2.2. Firstly, these assays were undertaken on the well-characterised *rpfG* mutant strain, which has previously been reported to display a clear phenotype in some of these assays (Ryan *et al.*, 2006), and the results are presented in Figure 16.

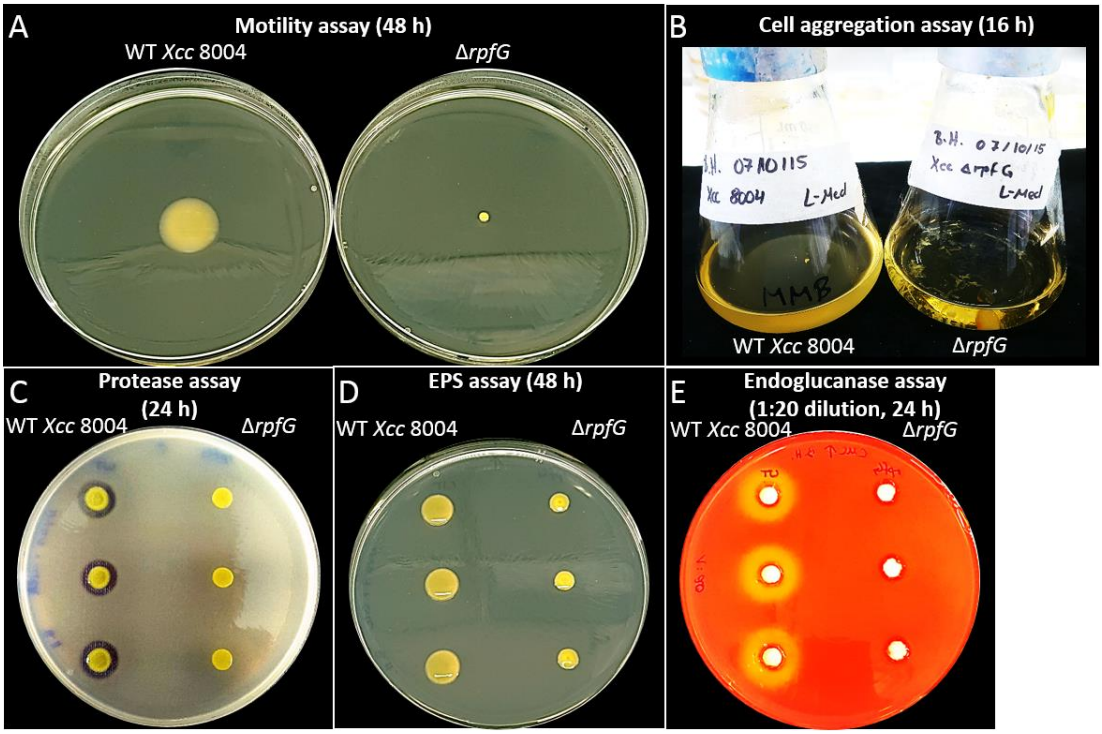

Figure 16: Representative images of phenotypic analysis of the *Xcc* deletion mutant Δ*rpfG* compared to the wild type *Xcc* 8004 using 5 different assays. A) Motility assay after 48 h. A single colony was spotted to the middle of an Eiken agar plate and incubated at 30°C. **B)** Cell aggregation assay after 16 h. 50 mL L-media were inoculated with 25 µL of cells (OD_{600} of 1.0) and incubated at 30°C, 200 rpm. **C)** Protease assay after 24 h. For each spot, 3 µL of cells (OD_{600} of 1.0) were coated on a 1% skimmed milk agar plate and incubated at 30°C. **D)** EPS assay after 48 h. For each spot, 3 µL of cells (OD_{600} of 1.0) were coated on a 2% glucose agar plate and incubated at 30°C. **E)** Endoglucanase assay after 24 h. 50 µL of the supernatant of cells (OD_{600} of 1.0, 1:20 dilution) for each spot were coated on a 0.125% CMC agar plate and incubated at 37°C. Each of these experiments was performed three times, and a representative set of data is shown.

As shown in Figure 16 A, the motility of the *ΔrpfG* mutant was highly reduced. In B, aggregation of cells can be seen for the deletion mutant in the right flask, whereas the wild type did not show any clumping after 16 h under the condition tested (left flask). Pictures C, D and E show a strong reduction in the production or secretion of extracellular protease, EPS and endoglucanase for the mutant (each on the right side) compared to the wild type *Xcc* 8004. Thus the assays showed as expected clear differences between the wild type and the *ΔrpfG* mutant resulting in a loss of virulence phenotypes.

Next, the same phenotypic assays were used to screen the 37 *Xcc* insertion mutants for differences in motility, EPS and protease production. A representative set of data for each mutant strain is presented in Appendix Figure 4, and a summary of the phenotypes including the results of the phenotypic assays and a prediction for the function of the encoded protein is given in Table 15.

Table 15: Overview about the phenotypes of 37 mutant strains compared to the wild type *Xcc* 8004. Motility, EPS and protease production was tested as described above. "–" indicates a reduction, "+" an increase in comparison to the wild type, whereas '0' signifies no difference between the mutant and the wild type. Strong phenotypes are highlighted in dark green, medium phenotypes in middle green and slight differences in light green. Mutant *XC2228* (marked in grey) did not grow. A domain analysis was performed using the online tool SMART (Letunic *et al.*, 2015; Schultz *et al.*, 1998).

Mutant	SMART	Motility	EPS	Protease
XC0249	Diguanylate cyclase with GGDEF	0	- -	- - -
XC0362	Putative uncharacterized protein with HD-GYP	- -	0	--
XC0420	Putative uncharacterized protein with GGEEF	-	+	-
XC0613	Putative uncharacterized protein with GGEEF	0	0	- -
XC0637	Histidine kinase/response regulator hybrid protein with AGDEF	0	0	- - -
XC0641	Diguanylate Cyclase with GGEEF	- - -	+	-
XC0675	Response regulator with GGDEF	+ +	0	-

Mutant	SMART	Motility	EPS	Protease
XC0831	Putative uncharacterized protein with GGEEF	+ +	+	0
XC1036	Putative uncharacterized protein with GGDEF	0	0	0
XC1383	Response regulator with GGEEF	-	0	- - -
XC1411	Response regulator with EAL	0	+	- - -
XC1476	Putative uncharacterized protein with GGDEF and EVL	0	0	- -
XC1582	Probable signalling protein with GSDEF and EAL	- - -	0	-
XC1755	Two-component system regulatory protein with HD-GYP	+ + +	+	-
XC1766	Transcriptional regulator with GGEEF	-	0	-
XC1803	Putative uncharacterized protein with GAAHF	0	-	0
XC1824	Putative uncharacterized protein with GEHSF and EAL	+	+	-
XC1841	GGDEF family protein with GGDEF and EAA	0	0	-
XC2161	Putative uncharacterized protein with EAL	0	+	0
XC2226	Putative uncharacterized protein with SDDEF and EAL	0	0	0
XC2228	C-di-GMP phosphodiesterase A with EAL			
XC2274	GGDEF family protein with GGEEL	- -	- -	- - -
XC2275	GGDEF family protein with GGEEL	+	+	- -
XC2276	GGDEF family protein with GADEF and EAL	- - -	0	-
XC2324	C-di-GMP phosphodiesterase A with AGDEF and EAL	- - -	+	-
XC2335	Cyclic di-GMP phosphodiesterase response regulator RpfG with HD-GYP	+	+ +	0
XC2459	Signaling protein with EAL	-	0	- -
XC2715	Putative uncharacterized protein with GGEEF	+	0	-

Mutant	SMART	Motility	EPS	Protease
XC2793	Sensor histidine kinase with GGEEL	0	0	- - -
XC2795	Putative uncharacterized protein with GGEEF	0	0	0
XC2866	Putative uncharacterized protein with GGEEF	0	0	- - -
XC2946	Sensor histidine kinase with GGEEF	+	+	-
XC3163	EAL domain protein with EAL	- - -	0	- -
XC3800	Response regulator with GGEEL	+	0	0
XC3829	Diguanylate cyclase domain protein with GGEEF	+	+	-
XC3962	Putative uncharacterized protein with EAL	0	0	- - -
XC4313	Putative uncharacterized protein with GGDEF	+ + +	0	- -

Analysing Table 15 shows that nearly every strain has differences in at least one of the assays compared to the wild type. Strains *XC0362, XC0420, XC0641, XC1383, XC1582, XC1766, XC2274, XC2276, XC2324, XC2459* and *XC3163* showed a reduction in motility whereas *XC0675, XC0831, XC1755, XC1824, XC2275, XC2335, XC2715, XC2946, XC3800, XC3829* and *XC4313* showed a motility increase relative to the wild type. The production of EPS was reduced for strains *XC0249, XC0362, XC1803* and *XC2274* but increased for *XC0420. XC0641, XC0831, XC1411, XC1755, XC1824, XC2161, XC2275, XC2324, XC2335, XC2946* and *XC3829*. For the protease assay, all mutants showed a reduced production apart from *XC0831, XC1036, XC1803, XC2161, XC2226, XC2335, XC2795* and *XC3800*.

Each of the mutants studied here has an insertion in a gene coding for a protein containing one or more of the three domains involved in c-di-GMP signalling (GGDEF, EAL or HD-GYP). However, there is no clear pattern between the distribution of the different domains and the phenotypes at this stage.

As mutant strain *XC2228* did not grow on plates or in liquid media, gDNA for the mutant was extracted to check if the pk18mob insertion in gene *XC2228* was still present. PCR was performed using gene specific primers covering the whole open reading frame of the gene with either *XC2228* gDNA or wild type gDNA as template (Figure 17).

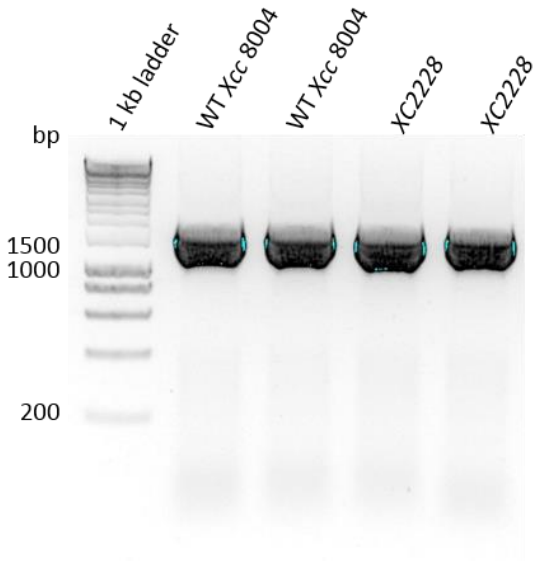

Figure 17: Agarose gel analysis of PCR on WT *Xcc* 8004 and *XC2228* gDNA using gene specific primers. The first two bands show replicates for the wild type, the last two for the mutant. A 1.2% agarose gel was run and the HyperLadder™ 1 kb Plus (Bioline) was used for the size determination.

The sizes of the DNA bands for the PCR of gene *XC2228* were around 1700 bp for both the wild type and the mutant, which is the expected size of gene *XC2228*. This indicates that the pk18mob insertion is not present in the mutant strain and therefore the Kanamycin resistance was also lost.

For further work, five mutants were chosen based on differences in the virulence assays and the phenotypic screening compared to the wild type: *XC0362, XC1755, XC2459, XC2793* and *XC3962*. These five mutants were selected because they showed a reduced virulence for the spray assay but not for the clipping assay, apart from mutant *XC1755* that showed increased virulence in the spray assay. Furthermore, all five strains revealed differences in one or more

of the phenotypic assays. In the following section the phenotypes described in Table 15 of these mutants with respect to motility, EPS and protease production are presented in further detail.

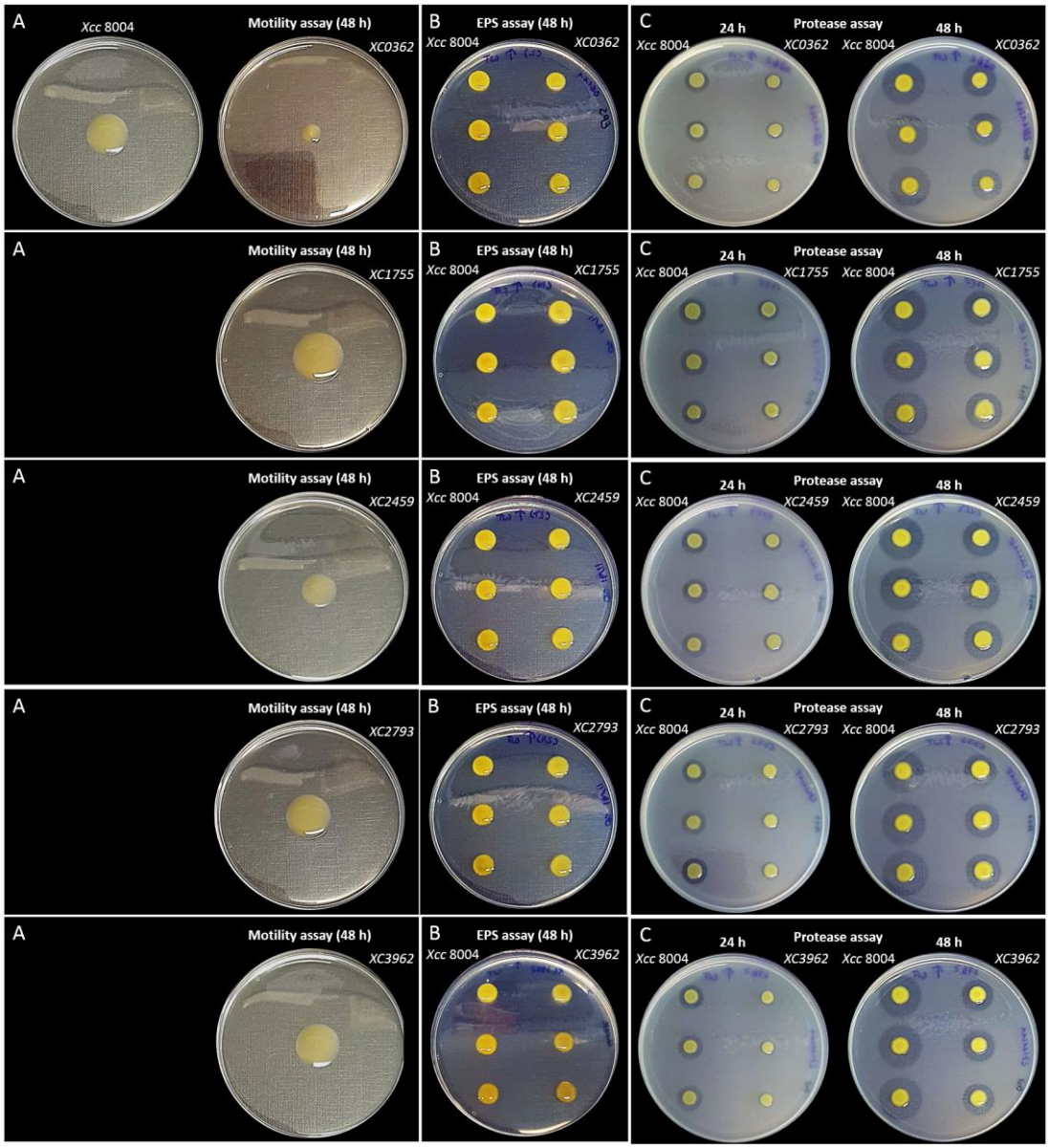

Figure 18: Representative images of phenotypic analysis of mutants *XC0362, XC1755, XC2459, XC2793,* and *XC3962* (top down) using motility, EPS and protease assay compared to the WT *Xcc* 8004 and already described in Table 15. A) Motility assay after 48 h. A single colony was spotted to the middle of an Eiken agar plate and incubated at 30°C. **B)** EPS assay after 48 h. For each spot, 3 µL of cells (OD_{600} of 1.0) were coated on a 2% glucose agar plate and incubated at 30°C. **C)** Protease assay after 24 h and 48 h. For each spot, 3 µL of cells (OD_{600} of 1.0) were coated on a 1% skimmed milk agar plate and incubated at 30°C.

As shown in Figure 18, *XC0362* has reduced motility, whereas the EPS production after 48 h seems to be comparable to the wild type. The production of protease after 24 h and 48 h was reduced relative to wild type. Mutant *XC1755* shows an increase in motility and EPS production but a reduction in protease production. *XC2459* seems to have a slight reduction in motility and protease production but no change in the EPS production. The last two mutants, *XC2793* and *XC3962*, have no difference in motility or EPS production but a reduced production of protease. Additionally, as seen in Figure 15, *XC0362, XC2459, XC2793,* and *XC3962* showed a reduced virulence for the spraying assay but not for the clipping assay, whereas *XC1755* had increased virulence in the clipping assay compared to the wild type.

5.3 Domain analysis of the five predicted c-di-GMP signalling proteins

A domain analysis of the five proteins encoded by the genes disrupted in strains *XC0362, XC1755, XC2459, XC2793* and *XC3962*, undertaken using the online tool SMART (Letunic *et al.*, 2015; Schultz *et al.*, 1998) is shown in Figure 19. According to SMART, all five proteins contain additional protein domains aside from the three protein domains GGDEF, EAL and HD-GYP, which are involved in the c-di-GMP signalling. XC0362 is predicted to have a Pfam DUF3391 domain whereas XC1755 might have a Rec domain. Both proteins contain an HD-GYP domain. The EAL domain protein XC2459 and the GGDEF domain protein XC2793 both also contain a GAF domain, but XC2793 additionally has a Pfam CHASE3 domain with two transmembrane regions. Protein XC3962, another EAL domain protein, also contains one transmembrane region and a Pfam CSS-motif.

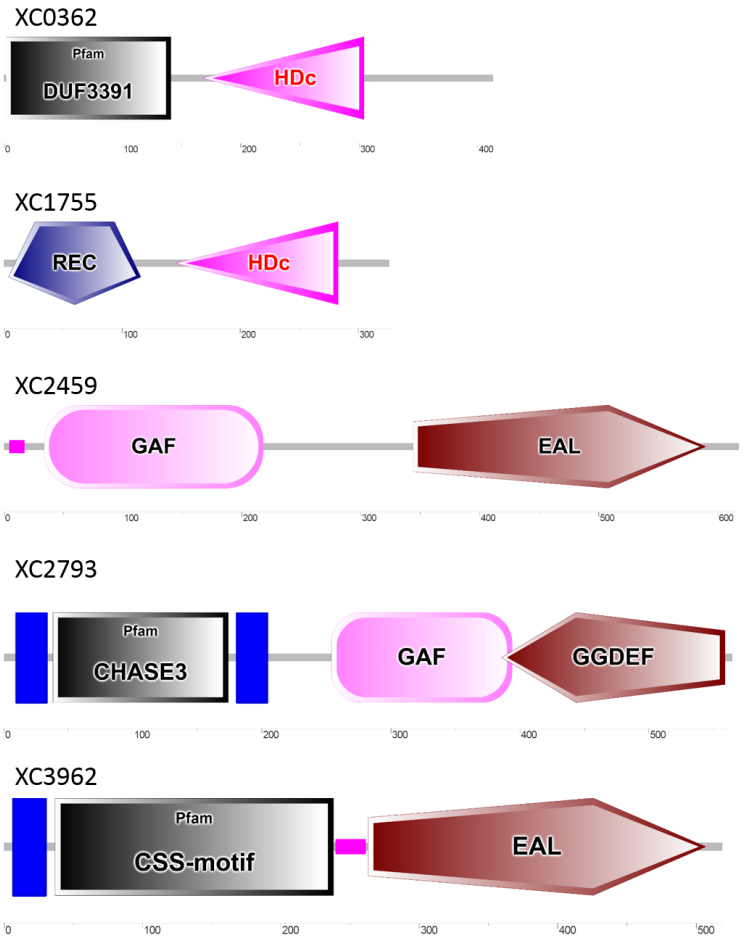

Figure 19: Domain analysis of the proteins XC0362, XC1755, XC2459, XC2793 and XC3962. The prediction was performed using the online tool SMART (Letunic *et al.*, 2015; Schultz *et al.*, 1998).

5.4 Construction of unmarked deletion strains or directed insertion strains

After selecting five genes of interest for further work (see Section 5.2), the first aim was to ensure that the following modifications were unlikely to have polar effects on downstream genes. Therefore, the genomic neighbourhoods of the four genes *XC0362, XC2459, XC2793*

and *XC3962* were observed using the online tool KEGG (Kanehisa and Goto, 2000; Kanehisa *et al.*, 2016) and are demonstrated in Figure 24 - Figure 27.

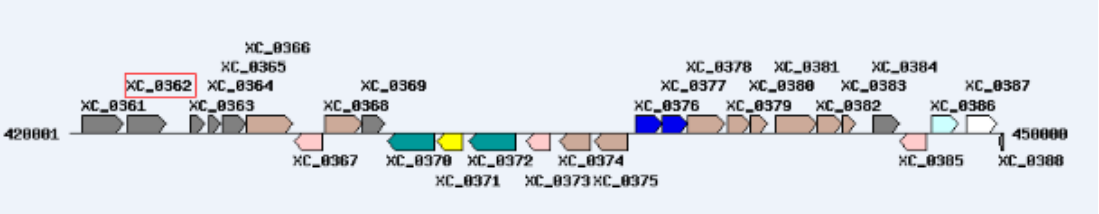

Figure 20: Genome neighbourhood of *XC0362*. The image was taken and cut from KEGG (Kanehisa and Goto, 2000; Kanehisa *et al.*, 2016).

Gene *XC0362* is separated from the downstream gene *XC0363* by a predicted non-coding region of 753 bp, suggesting that they are not transcribed in an operon and therefore the deletion of *XC0362* should not have polar effects.

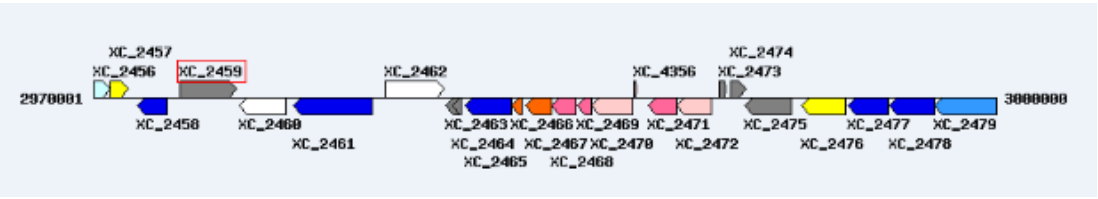

Figure 21: Genome neighbourhood of *XC2459*. The image was taken and cut from KEGG (Kanehisa and Goto, 2000; Kanehisa *et al.*, 2016).

Genes *XC2459* and *XC2460* are separated by 81 bp, where gene *XC2460* is located on the antisense strand, suggesting that there should be no polar effect resulting from the insertion in gene *XC2459*.

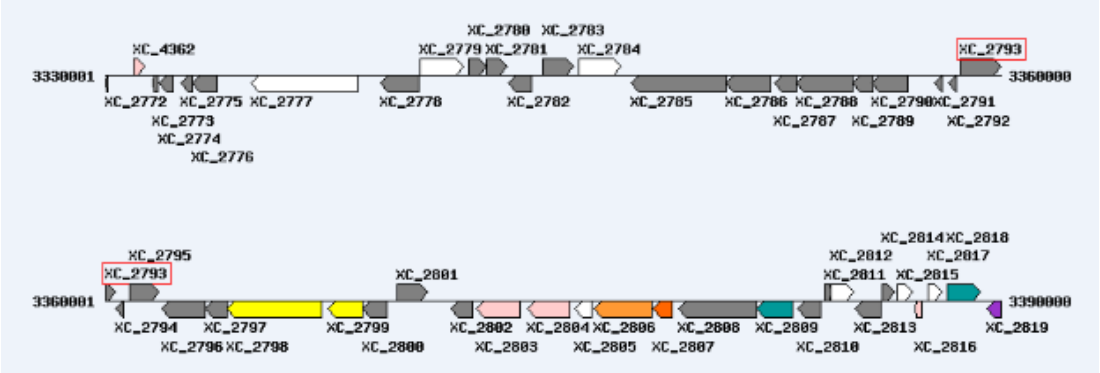

Figure 22: Genome neighbourhood of *XC2793*. The image was taken and cut from KEGG (Kanehisa and Goto, 2000; Kanehisa *et al.*, 2016).

Gene *XC2793* is followed by *XC2794*, located on the antisense strand 17 bp from *XC2793* and *XC2795,* which lies 500 bp downstream on the sense strand, suggesting that no polar effects should result from pk18mob insertion into gene *XC2793*.

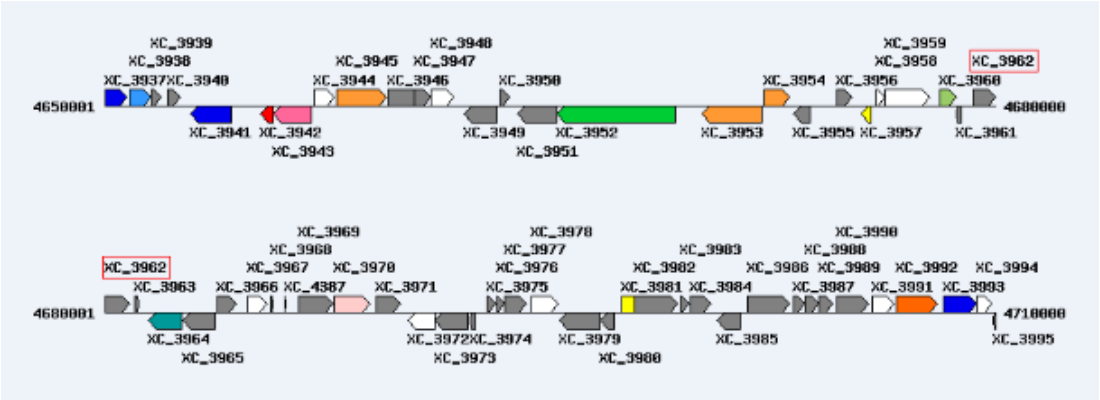

Figure 23: Genome neighbourhood of *XC3962*. The image was taken and cut from KEGG (Kanehisa and Goto, 2000; Kanehisa *et al.*, 2016).

Gene *XC3963* is located 168 bp downstream of gene *XC3962*, suggesting that both genes are probably not transcribed in one operon and therefore no polar effect should occur after the deletion of *XC3962*.

The next aim was to construct unmarked deletions to confirm that the phenotypes seen above resulted from inactivation of the gene of interest. The construction of these deletion strains is described in Section 4.2.1.10 and Appendix Figure 1. For the genes *XC0362* and *XC3962*, deletion mutants (subsequently named *ΔXC0362* and *ΔXC3962,* respectively) were designed using the suicide vector pk18mob*sacB*. Therefore, primers were used 500 bp downstream and upstream of the ORF for homologous recombination deleting the whole ORF including start and stop codon. Deletion of genes over ~1500 bp is reportedly difficult in *Xanthomonas* (Robert Ryan, personal communication). Therefore, insertion mutants (subsequently named *XC2459::pK18mob* and *XC2793::pK18mob,* respectively) were designed for genes *XC2459* (~1900 bp) and *XC2793* (~1700 bp) using the suicide vector pk18mob. The insertion of the vector was placed 280 bp after the start codon using the 500 bp upstream and downsteam of this insertion site as sequence for homologous recombination (see Appendix Figure 3). Due to time constraints, it was not possible to construct a deletion of *XC1755*, however the successful generation of the other strains was verified by PCR, the results of which are shown in Figure 20 - Figure 23. Additionally, the PCR products of the deletion mutants were sequenced to confirm that they were correct.

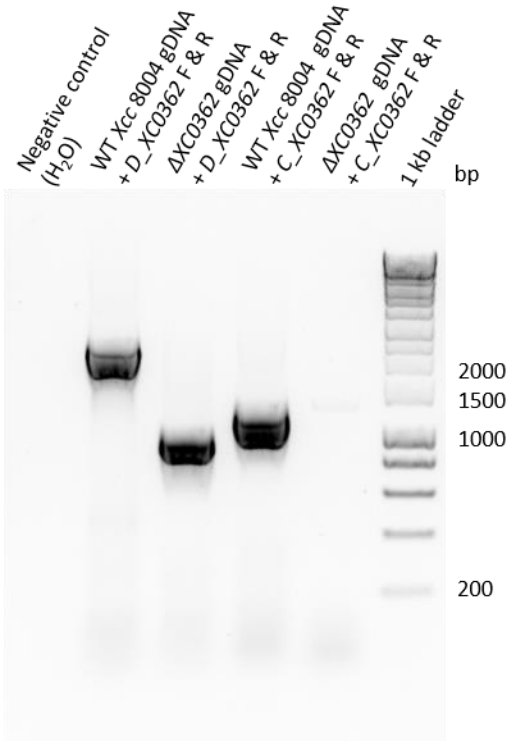

Figure 24: Agarose gel analysis of PCR products of WT *Xcc* 8004 and *ΔXC0362* gDNA to verify the presence of the *XC0362* deletion using different primer sets. Samples from left to right: Negative control (water), WT *Xcc* 8004 with D_XC0362 primer pair, *ΔXC0362* with D_XC0362 primer pair, WT *Xcc* 8004 with C_XC0362 primer pair, *ΔXC0362* with C_XC0362 primer pair. A 1.2% agarose gel was run and the HyperLadder™ 1 kb Plus (Bioline) was used for the size determination.

Figure 20 shows the results of the PCR analysis for wild type and deletion mutant *ΔXC0362* gDNA using two different primer combinations. Primer pair C_XC0362 covers the open reading frame (ORF) of the target gene and should only yield a product from wild type gDNA, and it can clearly be seen that a band at ~1000 bp is detected only from the wild type sample. Primers D_XC0362 F & R start and end 500 bp downstream or upstream of the ORF, respectively, and were used to show a size difference between the wild type and the mutant, consistent with the loss of *XC0362* in the mutant strain. Using this primer pair, a band of ~2200 bp was detected for the wild type gDNA, and ~1200 bp for *ΔXC0362* gDNA. Taken together these results confirm that the deletion of *XC0362* has been successful.

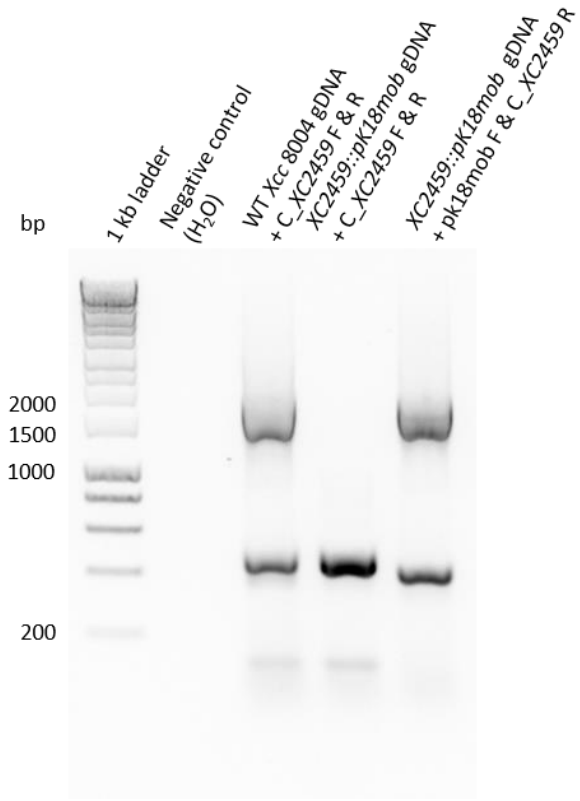

Figure 25: Agarose gel analysis of PCR products of WT *Xcc* 8004 and *XC2459::pk18mob* gDNA to verify the presence of the insertion mutation using different primer sets. Samples from left to right: Negative control (water), WT *Xcc* 8004 with C_XC2459 primer pair, *XC2459::pk18mob* with C_XC2459 primer pair, *XC2459::pk18mob* with pk18mob F and C_XC2459 R primers. A 1.2% agarose gel was run and the HyperLadder™ 1 kb Plus (Bioline) was used for the size determination.

Figure 21 shows the results of the PCR analysis for wild type and insertion mutant *XC2459::pK18mob* gDNA using different primer combinations. Primer pair C_XC2459 covers the open reading frame of the target gene and was used to show that the interrupted gene of the insertion mutant is now too large to be amplified. It can be seen that this primer pair generated a band between 1500 bp and 2000 bp from wild type gDNA whereas no band for this primer combination resulted from the gDNA of the mutant strain. The primer combination of pk18mob F and C_XC2459 R was used to verify the insertion of the suicide plasmid within the target gene, and successfully generated a band of the expected size, between 1500 bp and 2000 bp. The three lower bands visible on this gel are probably non-

specific and might appear due to mis-priming. Taken together these results confirm that the insertion of pk18mob into *XC2459* has been successful.

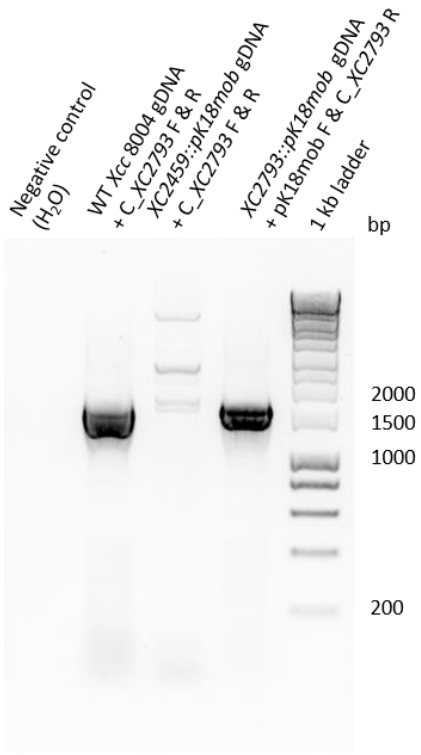

Figure 26: Agarose gel analysis of PCR products of WT *Xcc* 8004 and *XC2793::pK18mob* gDNA to verify the presence of the insertion mutation using different primer sets. Samples from left to right: Negative control (water), WT *Xcc* 8004 with C_XC2793 primer pair, *XC2793::pK18mob* with C_XC2793 primer pair, *XC2793::pK18mob* with pk18mob F and C_XC2793 R primers. A 1.2% agarose gel was run and the HyperLadder™ 1 kb Plus (Bioline) was used for the size determination.

Figure 22 shows the results of the PCR on wild type and insertion mutant *XC2793::pK18mob* gDNA using different primer combinations. Primer pair C_XC2793 covers the open reading frame of the target gene and was used to show that the interrupted gene of the insertion mutant is now too large to be amplified. This primer pair generated a band at ~1700bp from the wild type gDNA, whereas no distinct band was observed for this primer pair using the mutant gDNA. Primer combination pk18mob F and C_XC2793 R was used to verify the insertion of the plasmid within the target gene. Here, a band of ~1700 bp was generated

when *XC2793::pK18mob* gDNA was used as template. Collectively these results confirm that the insertion of pk18mob into *XC2793* has been successful.

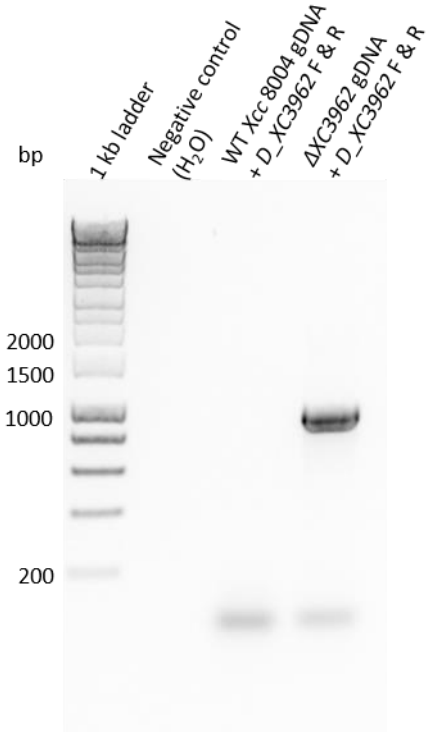

Figure 27: Agarose gel analysis of PCR products of WT *Xcc* 8004 and *ΔXC3962* gDNA to verify the presence of the *XC3962* deletion using different primer sets. Samples from left to right: Negative control (water), WT *Xcc* 8004 with D_XC3962 primer pair, *ΔXC3962* with D_XC0362 primer pair. A 1.2% agarose gel was run and the HyperLadder™ 1 kb Plus (Bioline) was used for the size determination.

Figure 23 shows the results of the PCR on wild type and deletion mutant *ΔXC3962* gDNA using the primers D_XC3962 F & R that start and end 500 bp downstream or upstream of the ORF, respectively. No band was generated when WT *Xcc* 8004 gDNA was used as template (expected size: ~2700 bp) whereas a band of the expected size of ~1000 bp was generated from the Δ*XC3962* gDNA. Unfortunately, despite using different primer combinations and gradient PCR it was not possible to amplify the gene *XC3962* (data not shown). That could also be the reason why no product was amplified using the D_XC3962 F & R primer pair as this one covers the ORF of the gene. An explanation could be a high G-C content what makes

it difficult to amplify. However, on the basis that a band of the expected size for the *XC3962* deletion was generated with primer pair primers *D_XC3962* F & R it can be concluded that *XC3962* has been successfully deleted.

It is important that any phenotypes revealed by inspection of these mutant strains are unequivocally linked to the inactivation of the selected gene by also including complementation analysis. Plasmid vector pLAFR3 was used to generate complementing constructs for strains *XC2459::pK18mob* (named *XC2459::pK18mob/pLAFR3::XC2459*) and *XC2793::pK18mob* (named *XC2793::pK18mob/pLAFR3::XC2793*) which were verified by PCR and antibiotic resistance (data not shown). Due to time constrains it was not possible to generate complementing constructs for *ΔXC0362* and *ΔXC3962* nor the wild type carrying the empty pLAFR3 vector (as a control).

5.5 Characterisation and comparison of library mutants and constructed strains for growth and phenotypes

To compare the growth of the different strains and to ensure that any phenotypic differences observed do not arise because of positive or negative growth effects, growth was measured over 24 h in 96 well plates using full NYG media. Antibiotics were added to the mediums of strains carrying a resistance. The measurements are presented in Figure 28 - Figure 32.

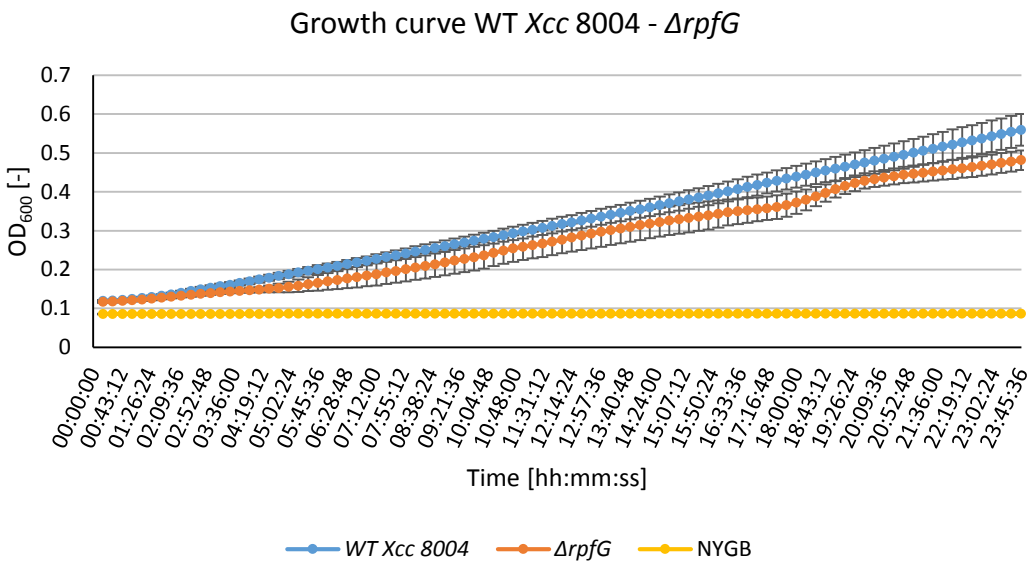

Figure 28: Growth curve of wild type *Xcc* 8004 (blue), *ΔrpfG* (orange) and NYGB (yellow). The measurement was running for 24 h in 96 well plates. No path length correction was applied. Error bars represent standard deviation. n=3x7

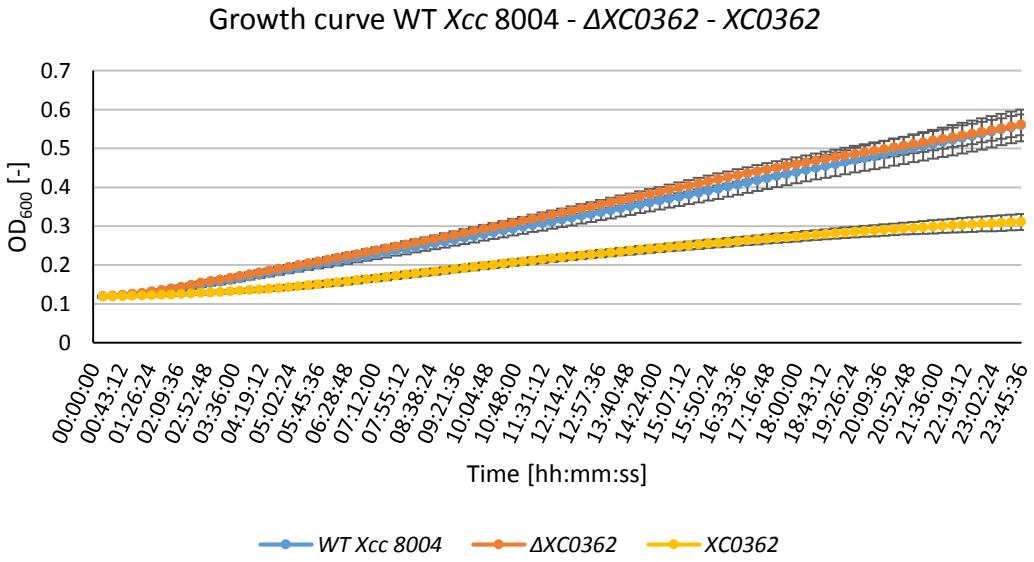

Figure 29: Growth curve of wild type *Xcc* 8004 (blue), *ΔXC0362* (orange) and *XC0362*. The measurement was running for 24 h in 96 well plates. No path length correction was applied. Error bars represent standard deviation. n=3x7

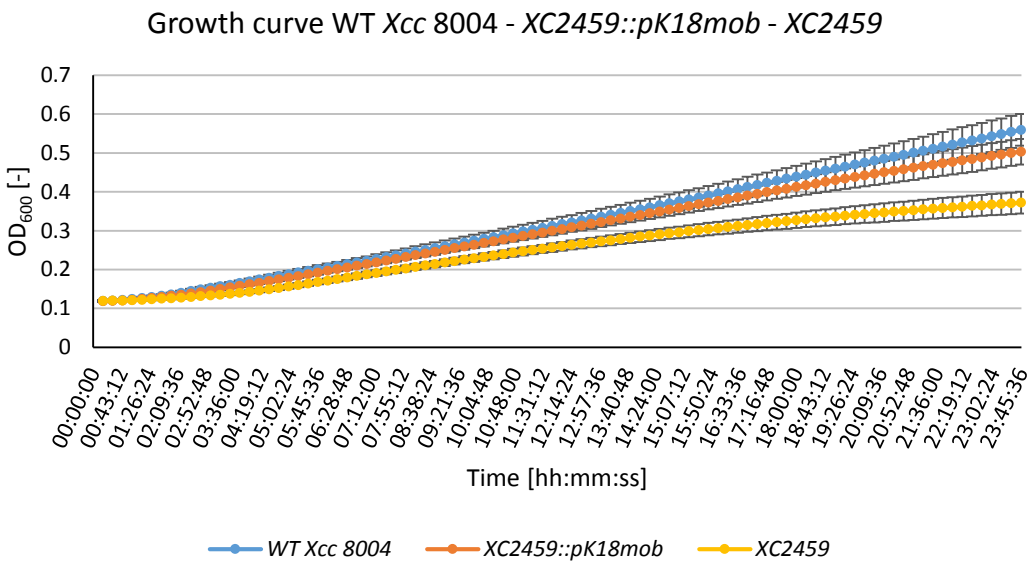

Figure 30: Growth curve of wild type *Xcc* 8004 (blue), *XC2459::pK18mob* (orange) and *XC2459* (yellow). The measurement was running for 24 h in 96 well plates. No path length correction was applied. Error bars represent standard deviation. n=3x7

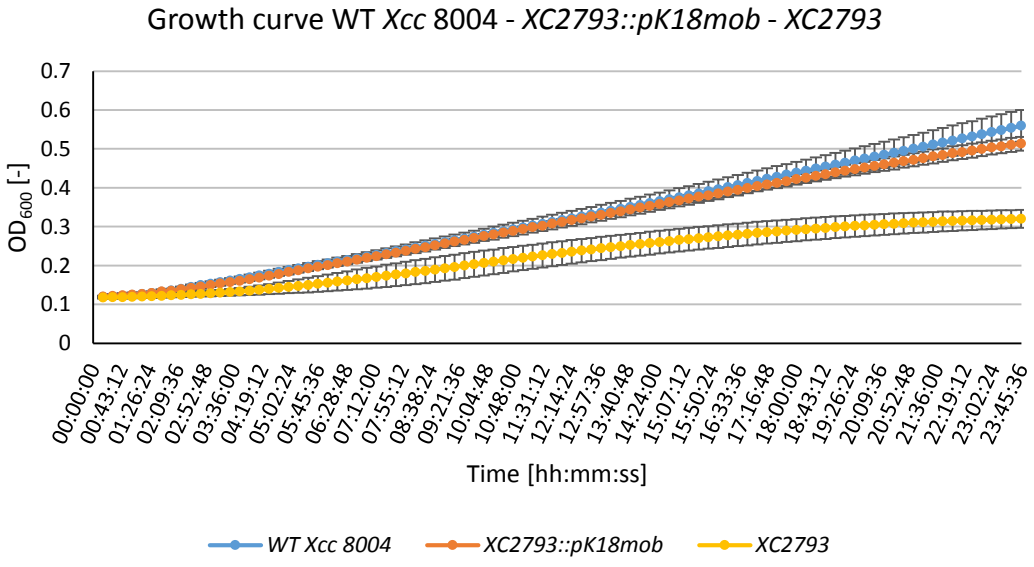

Figure 31: Growth curve of wild type *Xcc* 8004 (blue), *XC2793::pK18mob* (orange) and *XC2793* (yellow). The measurement was running for 24 h in 96 well plates. No path length correction was applied. Error bars represent standard deviation. n=3x7

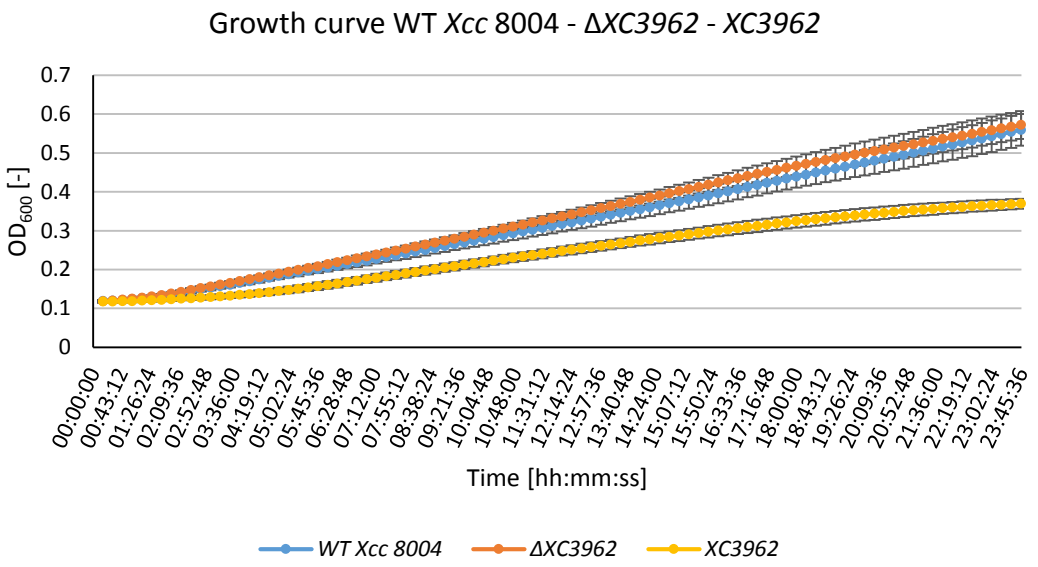

Figure 32: Growth curve of wild type *Xcc* 8004 (blue), *ΔXC3962* (orange) and *XC3962* (yellow). The measurement was running for 24 h in 96 well plates. No path length correction was applied. Error bars represent standard deviation. n=3x7

Comparing the growth of the different mutant strains to the wild type, no significant difference could be detected for the deletion mutant *ΔrpfG*, *ΔXC0362* and *ΔXC3962* as well as the pk18mob insertion mutants *XC2459::pK18mob* and *XC2793::pK18mob* under the tested conditions. However, slower growth was observed for the transposon mutants *XC0362* and *XC2459* and the pk18mob insertion mutants *XC2793* and *XC3962*. This growth disadvantage could be due to additional stress caused by the addition of Kanamycin to the medium for the transposon and pk18mob insertions (although the newly constructed insertion strains do not show this growth defect under the addition of Kanamycin) or because of other genes influenced by the insertion (either polar effects or insertion of the transposon or vector at more than one position).

To examine the phenotypes of the mutants *ΔXC0362, XC2459::pK18mob, XC2793::pK18mob* and *ΔXC3962* and to compare them to the corresponding insertion mutants from the library, phenotypic assays for motility, EPS and protease production were repeated under the same conditions as before. Furthermore, the two complemented strains *XC2459::pK18mob/pLAFR3::XC2459* and *XC2793::pK18mob/pLAFR3::XC2793* were also included to test for reversion of any observed phenotypes. The colony areas from motility and EPS assays and zone of clearing from protease assays were analysed using the software ImageJ (Schneider *et al.*, 2012), and the results presented graphically in Figure 33 - Figure 35.

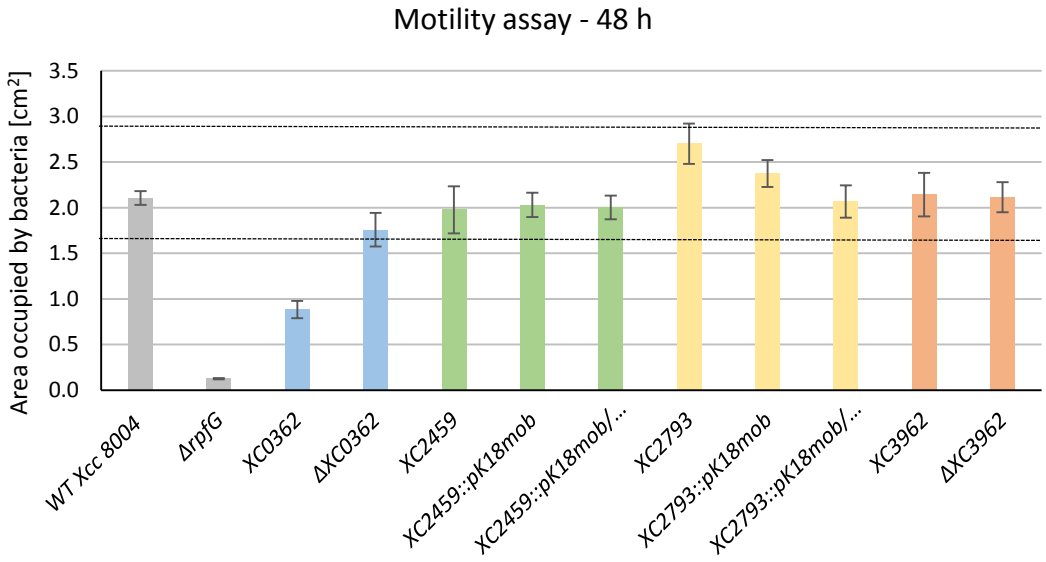

Figure 33: Quantification of motility of different *Xcc* bacterial strains after 48 h. The y-axis represents the area occupied by different *Xcc* strains in cm^2. The colours are set as follows: grey = wild type *Xcc* 8004 (n=61) and *ΔrpfG* (n=9) as controls, blue = transposon insertion mutant *XC0362* (n=8) and deletion mutant *ΔXC0362* (n=8), green = transposon insertion mutant *XC2459* (n=8), insertion mutant *XC2459::pk18mob* (n=18) and complemented strain *XC2459::pK18mob/pLAFR3::XC2459* (n=9), yellow = pk18mob insertion mutant *XC2793* (n=9), insertion mutant *XC2793::pk18mob* (n=17) and complemented strain *XC2793::pK18mob/pLAFR3::XC2793* (n=9), orange = pk18mob insertion mutant *XC3962* (n=8) and deletion mutant *ΔXC3962* (n=9). Error bars represent 95% confidence interval. The dotted lines indicate a 0.75 fold change (lower line) and 1.3 fold change (upper line) relative to the wild type value. Anything falling outside of these dotted lines was considered biologically relevant in this study.

Figure 33 shows the quantification of colony area after 48 h growth on Eiken agar plates as a measure of motility of each of the strains. The wild type showed an average area of ~2 cm^2 whereas the deletion mutant *ΔrpfG* had a strong reduction of motility with an area around ~0.2 cm^2 and a p-value of < 0.001 in a two-tailed student's t-test. The transposon insertion mutant *XC0362* also showed a significantly reduced motility ($p < 0.001$) with an area around ~0.9 cm^2, consistent with previous results (Figure 18). However, strain *ΔXC0362,* which carries a deletion in the same gene, did not phenocopy the transposon mutant strain and had a motility that was not significantly different to the wild type. Strain *XC2793* showed a statistically significant increased motility compared to the wildtype with a p-value of < 0.05. However, this difference seems not to have any biological relevance and is explainable due to the high number of replicates. All of the other strains tested (*XC2459, XC2459::pK18mob, XC2459::pK18mob/pLAFR3::XC2459, XC2793::pK18mob, XC2793::pK18mob/pLAFR3::XC2793, XC3962,* and *ΔXC3962*) did not show any significant difference in motility compared to the wild type.

The quantification of protease production by the different strains at two different time points is shown in Figure 34.

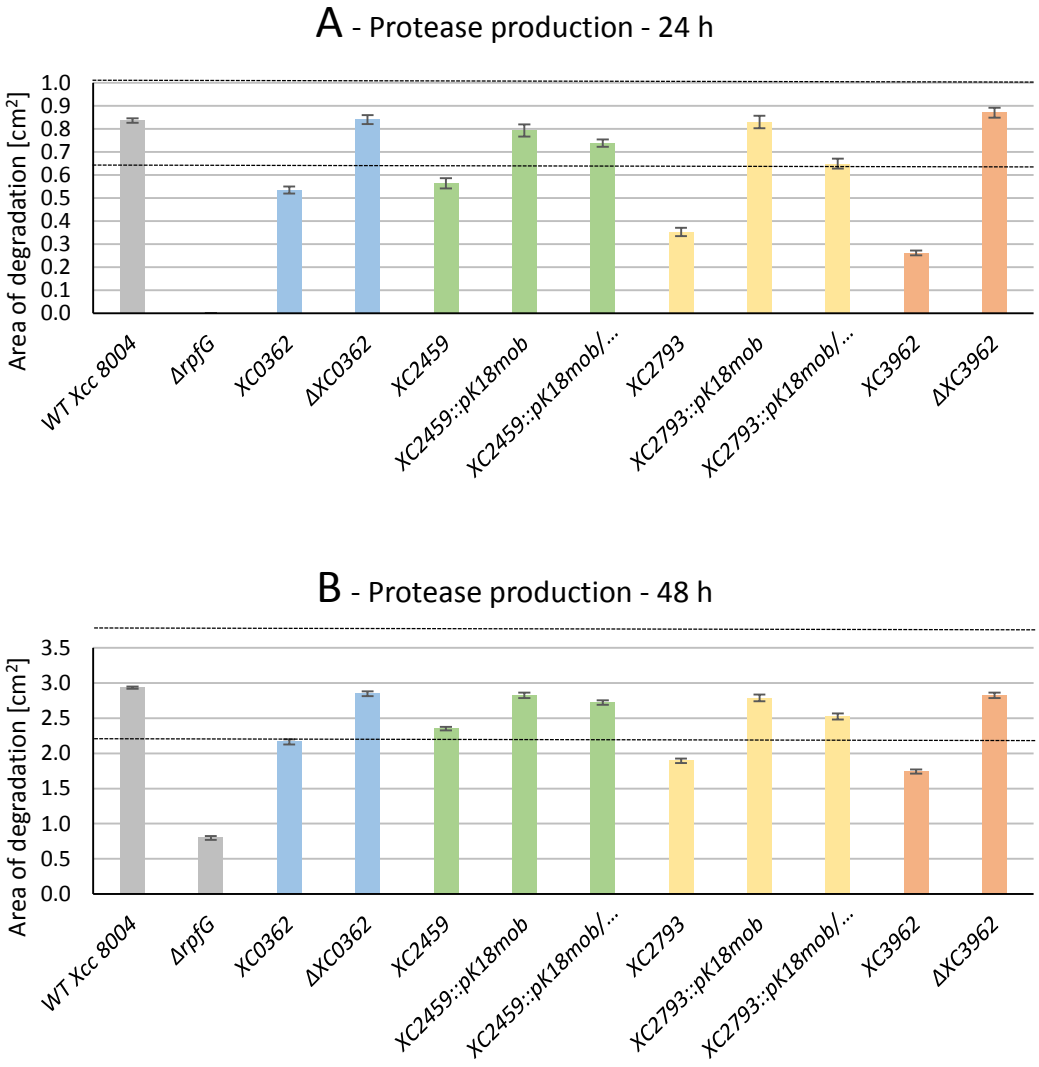

Figure 34: Quantification of protease production of different *Xcc* bacterial strains after 24 h (A) and 48 h (B). The y-axis represents the area of clearance (degraded milk) in cm^2. The colours are set as follows: grey = wild type *Xcc* 8004 (n=3x42) and *ΔrpfG* (n=3x6) as controls, blue = transposon insertion mutant *XC0362* (n=3x6) and deletion mutant *ΔXC0362* (n=3x6), green = transposon insertion mutant *XC2459* (n=3x6), insertion mutant *XC2459::pk18mob* (n=3x12) and complemented strain *XC2459::pK18mob/pLAFR3::XC2459* (n=3x6), yellow = transposon insertion mutant *XC2793* (n=3x6), insertion mutant *XC2793::pK18mob* (n=3x12) and complemented strain *XC2793::pK18mob/pLAFR3::XC2793* (n=3x6), orange = transposon insertion mutant *XC3962* (n=3x6) and deletion mutant *ΔXC3962* (n=3x6). Error bars represent 95% confidence interval. The dotted lines indicate a 0.75 fold change (lower line) and 1.3 fold change (upper line) relative to the wild type value. Anything falling outside of these dotted lines was considered biologically relevant in this study.

After 24 h, the wild type showed an area of clearing of ~0.8 cm^2 whereas no degradation of milk could be observed for the deletion mutant *ΔrpfG*. The insertion mutants *XC0362, XC2459, XC2793, XC3962, XC2459::pK18mob* and *XC2793::pK18mob* all showed a statistically significantly reduced area of clearance compared to the wild type ($p < 0.001$), but only the reduction seen for mutants *XC0362, XC2459, XC2793, XC3962* was deemed biologically relevant. Deletion mutants *ΔXC0362* and *ΔXC3962* also showed a statistically significantly reduced production with a p-value of < 0.05, but this was judged to lack biological relevance as the increase was very slight relative to the wild type level. Likewise, the two complemented strains *XC2459::pK18mob/pLAFR3::XC2459* and *XC2793::pK18mob/pLAFR3::XC2793* also showed statistically significant differences in the production of protease compared to the wild type ($p < 0.001$) that were deemed to lack biological relevance. The results after 48 h showed a similar trend except that the zone of clearance is larger (~2.9 cm^2 for the wild type), and now only the *ΔrpfG*, *XC2793* and *XC3962* mutants showed a biologically relevant reduction in protease production.

The result for the EPS assay on these strains is shown in Figure 35.

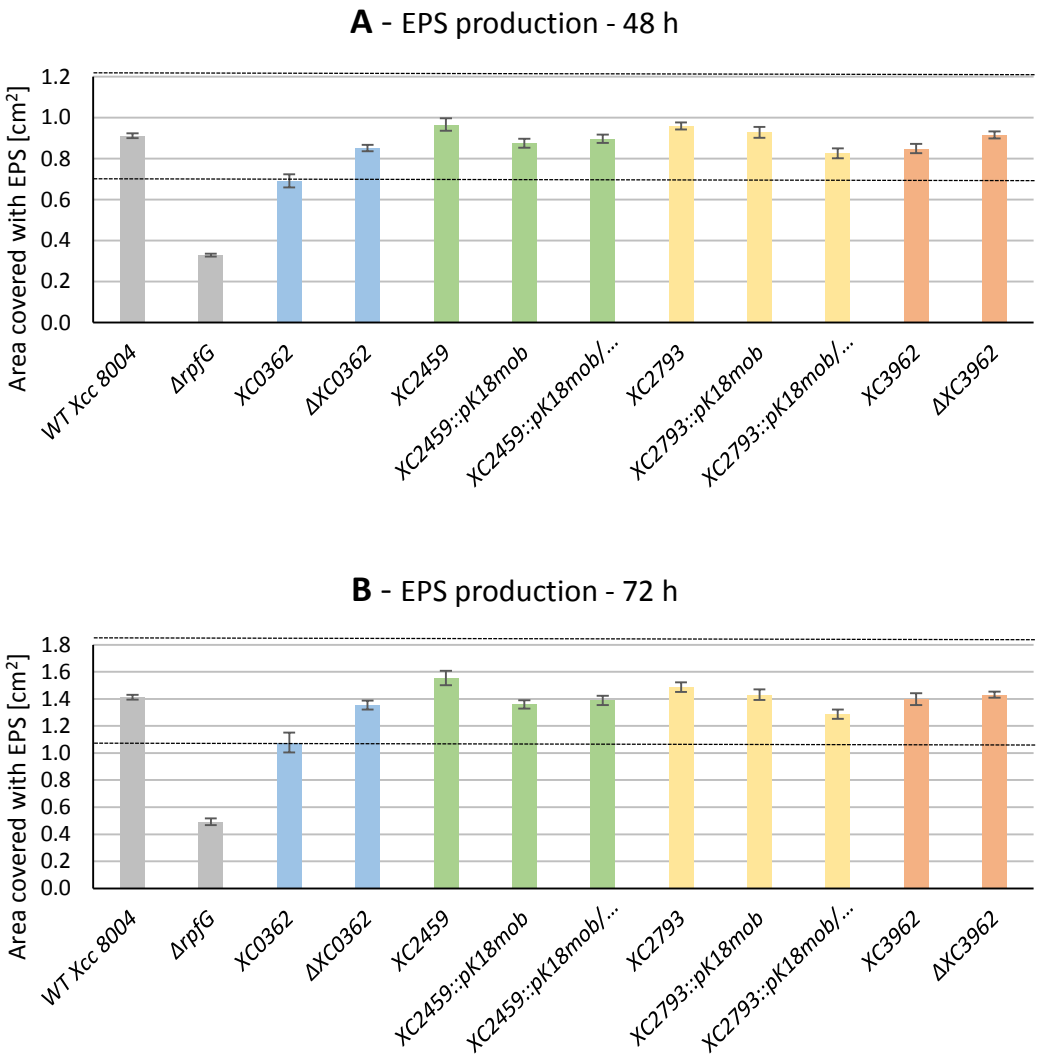

Figure 35: Quantification of EPS production of different *Xcc* bacterial strains after 24 h (A) and 48 h (B). The y-axis represents the area occupied by EPS in cm^2. The colours are set as follows: grey = wild type *Xcc* 8004 (n=3x42) and *ΔrpfG* (n=3x6) as controls, blue = transposon insertion mutant *XC0362* (n=3x6) and deletion mutant *ΔXC0362* (n=3x6), green = transposon insertion mutant *XC2459* (n=3x6), insertion mutant *XC2459::pk18mob* (n=3x12) and complemented strain *XC2459::pK18mob/pLAFR3::XC2459* (n=3x6), yellow = transposon insertion mutant *XC2793* (n=3x6), insertion mutant *XC2793::pK18mob* (n=3x12) and complemented strain *XC2793::pK18mob/pLAFR3::XC2793* (n=3x6), orange = transposon insertion mutant *XC3962* (n=3x6) and deletion mutant *ΔXC3962* (n=3x6). Error bars represent 95% confidence interval. The dotted lines indicate a 0.75 fold change (lower line) and 1.3 fold change (upper line) relative to the wild type value. Anything falling outside of these dotted lines was considered biologically relevant in this study.

The area that was covered with EPS was ~0.9 cm^2 for the wild type after 48 h, whereas the deletion mutant *ΔrpfG* showed a smaller area with ~0.3 cm^2. Insertion mutants *XC0362, XC2459, XC2793, XC3962* and *XC2459::pK18mob* as well as the complemented strain *XC2793::pK18mob/pLAFR3::XC2793* showed a statistically significantly reduced production of EPS with a p-value < 0.01 for *XC2459* and $p < 0.001$ for the rest, however all of these differences were small relative to the wild type and were deemed biologically irrelevant. A similar trend is found for the production of EPS after 72 h.

5.6 Detection and determination of c-di-GMP using mass spectrometry

To detect and determine the cellular level of c-di-GMP in the different *Xanthomonas campestris* strains, an assay using multi reaction monitoring (MRM) coupled with mass spectrometry (MS) was performed with the help of the FingerPrints Proteomics facility (School of Life Sciences, University of Dundee). Initially, c-di-GMP was isolated from the wild type bacteria grown on plates and analysed via MRM-MS. To validate the assay, the *ΔrpfG* mutant was used as a second control strain. The total ion chromatograms (TIC) for the wild type *Xcc* 8004 and the *ΔrpfG* mutant are shown in Figure 36.

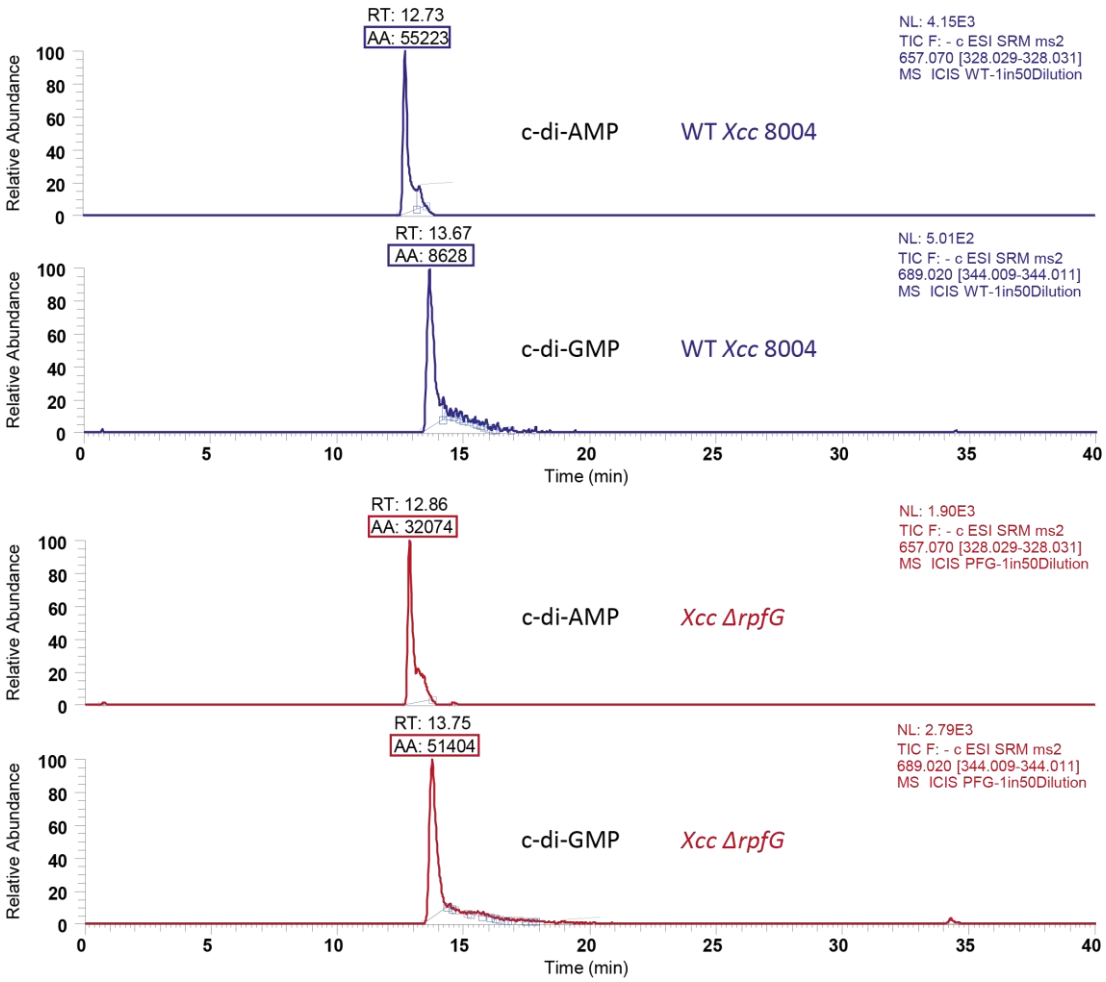

Figure 36: Total ion chromatogram of the MRM-MS analysis for the detection of c-di-GMP. The y-axis represents the relative abundance of the molecule c-di-GMP or c-di-AMP, respectively and the x-axis shows the time in minutes. Compared are the wild type sample (blue) and the mutant sample Δ*rpfG* (red), 50 pmol of c-di-AMP were used as the internal standard for each sample.

The wild type shows a retention time of 12.73 min and an area of 55223 for the internal standard cyclic di-adenosine monophosphate (c-di-AMP) and 13.67 min with an area of 8628 for c-di-GMP. In the sample for *ΔrpfG*, c-di-AMP and c-di-GMP could be detected after 12.86 min and 13.75 min, respectively. The areas represent 32074 for c-di-AMP and 51404 for c-di-GMP. The area for c-di-AMP varies between the wild type and the mutant although 50 pmol were spiked in both samples. To compare the level of c-di-GMP, the actual amount of c-di-GMP in 1 mg of wet cells was calculated based on the areas as described below.

First, the amount of c-di-GMP that was measured was calculated by the formula.

$$\frac{\mathrm{AA_{Standard}}}{50\ \mathrm{pmol}} = \frac{\mathrm{AA_{Sample}}}{x} \rightarrow \frac{\mathrm{AA_{Sample}} \times 50\ \mathrm{pmol}}{\mathrm{AA_{Standard}}} = x\ \mathrm{pmol}$$

Following, the weight of the cells that were used for the extraction had to be taken into account. Therefore, the amount of c-di-GMP was divided by the weight of the sample measured at the beginning of the extraction.

$$\frac{y}{\mathrm{Weight_{Sample}}} = z\ {}^{\mathrm{pmol}}/_{\mathrm{mg}}$$

An example of the calculation is given for the wild type.

$$\frac{55223}{50\ \mathrm{pmol}} = \frac{8628}{x} \rightarrow \frac{8628 \times 50\ \mathrm{pmol}}{55223} = 7.812\ \mathrm{pmol}$$

$$\frac{7.812\ \mathrm{pmol}}{110\ \mathrm{mg}} = 0.071\ {}^{\mathrm{pmol}}/_{\mathrm{mg}}$$

The total amount of c-di-GMP in the wild type was 0.071 pmol * mg^{-1}. The calculation for the mutant *ΔrpfG* produces an amount of 1.113 pmol * mg^{-1}, what is ~15 fold higher than for the wild type.

After the general validation of the method, it was used for another test run with one of the newly constructed mutants, *XC2459::pK18mob*. Because 50 pmol internal standard was high, only 0.5 pmol was used this time. The results for *XC2459::pK18mob* and the wild type can be found in Figure 37.

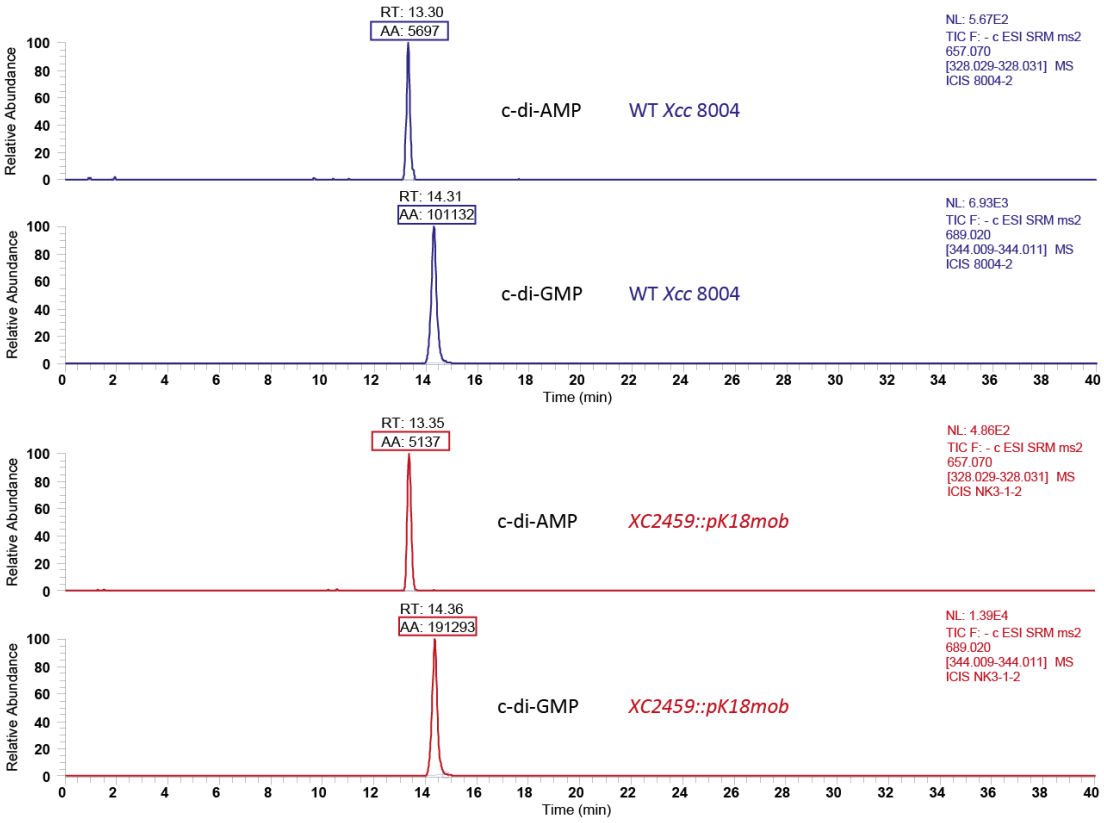

Figure 37: Total ion chromatogram of the MRM-MS analysis for the detection of c-di-GMP. The y-axis represents the relative abundance of the molecule c-di-GMP or c-di-AMP, respectively and the x-axis shows the time in minutes. Compared are the wild type sample (blue) and the mutant sample *XC2459::pk18mob* (red), 0.5 pmol of c-di-AMP were used as the internal standard for each sample.

The 0.5 pmol c-di-AMP that was used as internal standard show an area of 5967 with a retention time of 13.3 min for the wild type and an area of 5137 with a retention time of 13.35 min for the mutant. The wild type sample has a retention time of 14.31 min for c-di-GMP and the mutant *XC2459::pK18mob* 14.36 min, the areas represent 101132 and 191293, respectively. Calculating the actual amounts of c-di-GMP per mg wet cells results in 0.071 pmol * mg^{-1} for the wild type and 0.291 pmol * mg^{-1} for *XC2459::pK18mob*, which is ~4 times higher.

6 Discussion

6.1 Detection of differences in phenotypes with respect to virulence, motility, protease and EPS production of 37 *Xanthomonas campestris* strains

Recent research pointed out the importance of the second messenger cyclic di-GMP for the virulence of many different bacterial species, including *Xanthomonas campestris* pathovar *campestris* that was used for this study (Hengge, 2009; Jenal and Malone, 2006; Römling *et al.*, 2005; Wolfe and Visick, 2008). C-di-GMP is part of a multitude of different networks including regulatory systems for the production and secretion of virulence determinants like protease, exopolysaccharide and endoglucanase (Hengge, 2009; Römling *et al.*, 2013). Furthermore, c-di-GMP is known to influence the motility and biofilm formation as it is involved in the change from the motile to sessile phase of bacteria (Jenal and Malone, 2006; Römling *et al.*, 2013). Because of the important role that c-di-GMP plays in the virulence of *Xcc*, a panel of 37 mutants was used to examine effects on the virulence of *Xcc* by mutating genes possibly involved in c-di-GMP turnover identified by their domain structure (Ryan *et al.*, 2007). The results of these assays was provided by Dr Robert Ryan and was used as a basis for this study.

The analysis of the two different virulence assays, virulence by clipping and by spray assay, revealed differences between the strains and the wild type but also between the two assays. During the infection by clipping, the bacteria are directly introduced into the vascular system of the plants by leaf clipping. This assay provides a first indication of the virulence of the bacteria but it does not cover the entire infection process, which includes the movement of the bacteria towards the hydathodes and the entering of the vascular system. Therefore, the second virulence assay, infection by spraying, has also been performed. In this case the

bacteria are sprayed onto the leaves and have to go through the entire natural infection process. Twelve mutants showed a reduced virulence for the spray assay but not for the clipping assay and must therefore have a defect that suppresses the early infection stages. That could for example include reduced motility, reduced production of extracellular enzymes that help to destroy the leaf surface to mediate entry into the plant or defects in one of the secretion systems (mostly Type II and Type III) (Dow and Daniels, 2000; Dow *et al.*, 1987; Mudgett, 2005). One mutant, *XC1755*, showed an increased infection rate for the spray assay what could be the result of increased motility or overproduction of virulence determinants. For the clipping assay however, a reduced virulence was observed for this same mutant, suggesting that it is particularly virulent in the first stages of the infection but was defective during the later stages of infection. It is also conceivable that the phenotype for the spray assay is the outcome of a defective defence response of the plants resulting from molecules that might be produced by this mutant, instead of an increase in virulence.

To check whether some of these assumptions were correct, the strains were examined for motility and the production of different extracellular enzymes and polysaccharides. The deletion mutant Δ*rpfG*, which showed a reduced virulence for both assays, was used to validate the functionality of the different phenotypic assays. The phenotypes for this mutant have already been published (Ryan *et al.*, 2006) and were confirmed in this study, where a lower motility, cell aggregation and reduced production of protease, EPS and endoglucanase were observed. The mutated gene encodes an HD-GYP domain protein highly involved in the c-di-GMP turnover, thus its disruption leads to an increased c-di-GMP level and the observed phenotypes. Furthermore, RpfG contains a receiver domain that is part of a two-component system involved in the DSF signalling indicating the importance of this protein for virulence and biofilm formation in *Xanthomonas* (Barber *et al.*, 1997; Slater *et al.*, 2000).

After validating the assays, all 37 mutant strains were examined for motility, protease and EPS production. Most of the mutants showed differences in at least one of the phenotypes compared to the wild type. These results suggest that the mutated genes may have an actual impact on c-di-GMP signal transduction. Based on the results of the virulence assays and the phenotypic screens, five mutants, *XC0362, XC1755, XC2459, XC2793* and *XC3962,* were chosen for further work. The mutants *XC0362, XC2459, XC2793* and *XC3962* were selected because of their reduced virulence for the spray assay but not for the clipping assay, suggesting that the disrupted genes are important for early stages of infection. Furthermore, a reduced motility for *XC0362* as well as reduction of protease production for all four mutants was observed during the phenotypic screen. Additionally, *XC1755* was selected because of the increased virulence for the spray assay and an increased motility. However, this mutant was not followed up for the further work as the construction of a deletion mutant was not successful.

After the construction of the deletion mutants *ΔXC0362* and *ΔXC3962*, the directed pk18mob insertion mutants *XC2459::pK18mob* and *XC2793::pK18mob* and the complemented strains *XC2459::pK18mob/pLAFR3::XC2459* and *XC2793::pK18mob/pLAFR3::XC2793*, the phenotypes of these mutants were examined and compared to the corresponding mutants from the library under the same conditions as before. Furthermore, all of the strains were tested for their growth behaviour. The two complemented strains *XC2459::pK18mob/pLAFR3::XC2459* and *XC2793::pK18mob/pLAFR3::XC2793* were also included to test the reversion of any observed phenotypes. The phenotypes of the library mutants could be replicated, however, the corresponding strains that were constructed during this study did not show these phenotypes. Instead, they showed motility, EPS and protease production comparable to the wild type. The same is true for the complemented strains, as expected. The growth measurement identified a reduced growth for all insertion

strains from the library and the complemented strains but no difference for the newly constructed strains and the deletion mutant *ΔrpfG* compared to the wild type.

The most likely explanation for the phenotypic differences between the library insertion mutants and the strains constructed here lies in the pedigree of the wild type strains used in each case. The mutant library was constructed in Nanning, China using a wild type *Xcc 8004* strain that almost certainly has a different pedigree to the one that was used in this study. It is well known that even single base pair changes between strains can lead to massive phenotypic differences (Griffiths *et al.*, 2000). It is striking to note that all of the library insertion mutants showed a reduced growth rate relative to the wild type strain used here, and it is likely that this reduced growth rate arises from the parental strain rather than being a unique property of each of the mutants. This could be tested in future by obtaining the wild type strain used by the group in Nanning for comparative analysis.

Another, less likely, explanation for the differences seen between the library insertion mutants and the strains constructed here is potential polar effects of the insertions. Polar effects can occur if the mutation not only disrupts the specific gene of interest but also genes located downstream, for example if those genes are transcribed as an operon. Furthermore, insertion of genes could potentially have an effect on overlapping genes located on the antisense or sense strand, respectively. Therefore, the genomic regions downstream of the genes of interest were analysed. All four genes *XC0362, XC2459, XC2793* and *XC3962* are separated by at least 168 bp of predicted non-coding sequence from the next downstream located gene on the same strand, suggesting that these genes are not transcribed in an operon. In case of *XC2459* and *XC2793*, the closest genes are located 81 bp and 17 bp, respectively, from the gene of interest on the complementary strand. It is rather unlikely that an insertion would have an effect on these genes, and moreover, two insertion mutants (in

exactly the same two genes but with insertions at defined positions that differed from the library mutations) were constructed in this study, therefore making polarity or antisense effects an unlikely explanation, at least for these two particular genes. It should, however, be noted that the Tn5 and pk18mob insertions from the library were constructed in a non-directed way, and there may be more than one insertion within the genome. This could be determined by whole genome sequencing of the mutant strains.

Having a closer look at the genes of interest and their encoded proteins, a domain analysis was performed. Each of the strains carries a mutation in a gene predicted to be involved in the c-di-GMP signalling pathway. Hence, the encoded protein XC0362 contains an HD-GYP domain, XC2459 and XC3962 each contain an EAL domain and XC2793 a GGDEF domain. Furthermore, each protein additionally contain sensory and signalling domains, suggesting that their activities might be responsive to the environment.

GGDEF domain proteins are known to be involved in c-di-GMP synthesis (Ryan *et al.*, 2012). That means disruption of gene *XC2793* would be predicted to result in a reduced c-di-GMP level and therefore an increased motility and virulence but reduced biofilm formation. However, these phenotypes were not observed, instead the mutant from the library showed a reduced production of protease but no differences in motility or EPS production. The observed phenotype could potentially be explained if other genes are affected, for example by polarity or because more than one copy of pK18mob has inserted into the genome. Furthermore, some of the encoded DGCs and PDEs in several bacteria have already been shown to be inactive (Ryan *et al.*, 2012), and therefore it could be that XC2793 is not active and thus a mutation would not directly affect c-di-GMP synthesis. The observed reduction of protease production could then be caused by the noticeable growth defect of the strain instead of resulting from an increased or decreased c-di-GMP level.

It has also been shown that PDEs can directly interact with DGCs what could in this case lead to a missing interaction between XC2793 and a potential PDE resulting in the observed phenotype (Andrade *et al.*, 2006). However, XC2793 also contains two further protein domains, a GAF and a CHASE3 domain. GAF domains are ubiquitous motifs present in cyclic GMP (cGMP)-regulated cyclic nucleotide phosphodiesterases, certain adenylyl cyclases and hundreds of other signalling and sensory proteins in bacteria, archaea and eukaryotes (Ho *et al.*, 2000). The folded structure is similar to the PAS domain, another ubiquitous signalling and sensory transducer (Ho *et al.*, 2000). Both domains, GAF and PAS, are common domain architectures involving GGDEF, EAL and HD-GYP domains (Römling *et al.*, 2013). CHASE3 is an extracellular sensory domain that is found in at least four classes of transmembrane receptors, including histidine kinases, adenylate cyclases, predicted diguanylate cyclases, and methyl-accepting chemotaxis proteins. The variety of signalling pathways using the CHASE-type domains suggest that these domains can sense some important extracellular signals (Zhulin *et al.*, 2003). Both additional domains indicate that the protein might be involved in several signalling pathways by sensing and responding to environmental signals, apart from the c-di-GMP signalling network.

HD-GYP and EAL domain proteins are predicted to be part of the c-di-GMP degradation in a two-step process (Christen *et al.*, 2005; Paul *et al.*, 2004; Ryan, 2013). Hence, mutations of *XC0362, XC2459* and *XC3962* are expected to result in an increased c-di-GMP level and therefore a reduced motility and virulence (Jenal and Malone, 2006; Römling *et al.*, 2013). One reason why these phenotypes could not be observed for the newly constructed strains could again be because the enzymes are inactive or the effects are too small to be detected in the performed assays (potentially due to redundancy). The reduced growth rate of the library strains could be an explanation for the reduced production of protease for these mutants. The additional domains present in these proteins could also have an impact on their

function. XC0362 contains a DUF3391 domain in addition to the HD-GYP domain, whose function is still unknown (Mckee *et al.*, 2014). However, DUF3391 is associated with PF01966, the HD domain, linked to phosphohydrolase activity (http://pfam.xfam.org/family/DUF3391 (Finn *et al.*, 2016)). These enzymes appear to be involved in nucleic acid metabolism and signal transduction (Aravind and Koonin, 1999). The HD-GYP domain itself is a variant of the widespread HD-type phosphohydrolase containing an additional C-terminal subdomain (GYP) (Galperin, 2005). These findings go along with the prediction of XC0362 being a phosphodiesterase.

The EAL domain protein XC2459 contains an additional GAF domain that has already been discussed previously as part of GGDEF, EAL and HD-GYP domain proteins. The second EAL domain protein XC3962 includes a CSS motif. CSS sequence motifs are often found at the N-terminal of EAL domain proteins in many c-di-GMP phosphodiesterases and are therefore considered to be specific for c-di-GMP signalling (http://pfam.xfam.org/family/CSS-motif (Finn *et al.*, 2016)). Five of these EAL phosphodiesterases with a membrane-integrated sensory CSS domain were found in *E. coli,* which are all expressed but inactive due to disulphide bond formation. Reduction of the CSS domain or mutations that eliminate the relevant cysteine residues result in activated PDE activity (Hengge *et al.*, 2016). However, the CSS-motif has not been well characterised so far (Cruz *et al.*, 2012). These findings could imply that the CSS-motif of XC3962 represses the activity of the protein as phosphodiesterase so that the expected phenotype cannot be observed. Other explanations that have already been discussed for the previous proteins can also be considered here. In either case, it is important to bear in mind that the c-di-GMP network is very complex, thus the disruption of genes involved in the c-di-GMP regulation could interfere with other pathways resulting in the observed phenotypes.

6.2 Adaptation of c-di-GMP detection method via MRM-MS results in different levels of the second messenger in mutants compared to the wild type

To demonstrate that the mutations of the selected genes have an actual impact on the c-di-GMP level, the amount of this second messenger in cells was measured via MRM-MS. This method was used to determine the concentration of a particular molecule with a known composition in a sample. This targeted mass spectrometry has a high specificity, sensitivity and precision. MRM-MS can enhance the lower detection limit for peptides by up to 100 fold (as compared to full scan MS/MS analysis) by allowing rapid and continuous monitoring of the specific ions of interest (Keshishian *et al.*, 2007). One advantage over other methods like High Performance Liquid Chromatography (HPLC) is the fact that the result will only give precise information about the molecule of interest rather than about all molecules that are present in the sample. For this study, the c-di-GMP amount present in *Xanthomonas* wild type cells was first compared to the *ΔrpfG* mutant. There was a ~15 fold increase in c-di-GMP amount in the *ΔrpfG* mutant compared to the wild type with 1.113 pmol*mg^{-1} and 0.071 pmol*mg^{-1}, respectively. This result was expected as RpfG is a highly active PDE and is in accord with the phenotypes describes previously (Römling *et al.*, 2013). The method was also applied to detect differences in the production of c-di-GMP for the wild type compared to the insertion mutant *XC2459::pK18mob*. The result shows a c-di-GMP amount of 0.071 pmol*mg^{-1} for the wild type and 0.291 pmol*mg^{-1} for *XC2459::pK18mob*, which is ~4 times higher than wild type. The result supports the hypothesis that the mutation of *XC2459* has an actual impact on the c-di-GMP level. The increase of c-di-GMP amount was expected, assuming that XC2459 is a functional phosphodiesterase and hence the disruption would lead to an increased c-di-GMP level.

The aim of this assay was to identify differences in the c-di-GMP level between mutant strain and the wild type rather than to determine the accurate amount of c-di-GMP in the cells. However, comparing the result with the literature, it seems that the calculated amount is relatively low. No information could be found for *Xanthomonas* species but in *Pseudomonas aeruginosa*, the concentration of c-di-GMP in planktonically grown cells was 30 pmol*mg^{-1}, and for biofilm-grown cells 101 pmol*mg^{-1} on average (Barraud *et al.*, 2009). It could be that the concentration of c-di-GMP in *Pseudomonas* in general is higher than in *Xanthomonas* making it difficult to compare both species. It might also be possible that c-di-GMP get lost during the extraction process resulting in a lower quantification by mass spectrometry. This should be examined by adding a known amount of isotopically labelled molecule to the sample at the beginning of the extraction to verify how much of the molecule could still be detected after the measurement. Additionally, more replicates are necessary to confirm the results presented here as only one replicate per mutant has been used so far because this study was a first trial to test and improve the method.

Another aspect is the internal standard c-di-AMP that was used because of its similarity to c-di-GMP. The standard was added to the sample after the c-di-GMP extraction with a known concentration, so that the area of the measurement should roughly be the same for the two samples measured in one preparation. Yet, the areas of c-di-AMP for the wild type and the deletion mutant *ΔrpfG* are very different, 55223 and 32074, respectively. Therefore, consultation with the FingerPrints facility, who performed the actual measurement, should be held to optimise this step and ensure comparable results.

7 Conclusion and future work

The role of c-di-GMP in the virulence of *Xanthomonas campestris* pathovar *campestris* has been reported many times. A domain search of the predicted proteome revealed 37 genes encoding proteins with a c-di-GMP associated domain. Analysis of a panel of mutants was performed after which five genes were selected for a more detailed analysis based on motility, virulence and production of virulence determinants. After the successful construction of the deletion mutants *ΔXC0362* and *ΔXC3962* and the insertion mutants *XC2459::pK18mob* and *XC2793::pK18mob*, differences in growth and phenotypes between these mutants and the panel mutants were observed so that no clear conclusion about the influence of the mutations could be made. The primary difference results from the pedigree of the wild type strains used in this work. It would be imperative to compare the Nanning and Dundee *Xcc 8004* strains, for example looking at growth rate (as all of the mutants in the Nanning strain background grew more slowly than the strains constructed in this study). Ideally, whole genome sequencing could be used to look for SNPs between the two strains that might account for growth rate and other phenotypic differences.

Proteases and exopolysaccharides are not the only known virulence determinants. No observed differences in these assays therefore does not mean that these mutants do not differ from the wild type. Further phenotypic assays could be performed to identify differences between the wild type and the mutants, for example by looking at the mannanase production that also has been shown to be involved in virulence (Lu *et al.*, 2012). Also, the cell aggregation assay and endoglucanase production assay that has been performed for *ΔrpfG* should be performed for the selected mutants to identify any potential differences.

Furthermore, a domain analysis was performed and identified additional domains for the proteins of interest. To get a more detailed idea whether the proteins are active or not, an *in vitro* assay could be performed. Thereby, DGC or PDE activities could be identified by using c-di-GMP as substrate for predicted PDEs and GTP as substrate for DGCs. The level of c-di-GMP could then be measured after certain time points.

To measure the level of c-di-GMP, a method using MRM-MS has already been established. The results presented here should be further verified using more replicates and the c-di-GMP level should be compared for all selected mutants. It should be considered if isotope labelled c-di-GMP should be used for the further measurements instead of c-di-AMP to gain 100% conformity between the standard and molecule of interest.

All assays performed during this study were carried out under laboratory conditions. Future experiments should thus also be carried out under natural conditions, in case of *Xcc* in the plant environment. Differences between the wild type and the mutants could then become more noticeable. Regarding c-di-GMP analysis for example, the bacteria could be harvested directly from the leaves of the plants for the analysis.

In conclusion, it could be confirmed that c-di-GMP plays an important role in the virulence of *Xanthomonas campestris* analysing different virulence assays and phenotypic screens. However, there are still a lot of outstanding question about the actual role of predicted DGCs and PDEs regarding plant infection and the colonisation of *Xcc*.

8 Bibliography

Altschul, S. F., Gish, W., Miller, W., Myers, E. W. and Lipman, D. J. 1990. Basic local alignment search tool. *J Mol Biol,* 215**,** 403-410.

Alvarez, A. M. 2000. Black rot of crucifers. *In:* Slusarenko, A. J., Fraser, R. S. and Van Loon, L. C. (eds.) Mechanisms of Resistance of Plant Diseases. 1 ed.: Springer Netherlands.

Amikam, D. and Benziman, M. 1989. Cyclic diguanylic acid and cellulose synthesis in *Agrobacterium tumefaciens*. *J Bacteriol,* 171**,** 6649-6655.

Andrade, M. O., Alegria, M. C., Guzzo, C. R., Docena, C., Rosa, M. C., Ramos, C. H. and Farah, C. S. 2006. The HD-GYP domain of RpfG mediates a direct linkage between the Rpf quorum-sensing pathway and a subset of diguanylate cyclase proteins in the phytopathogen *Xanthomonas axonopodis* pv citri. *Mol Microbiol,* 62**,** 537-551.

Aravind, L. and Koonin, E. V. 1999. The HD domain defines a new superfamily of metal-dependent phosphohydrolases. *Trends in Biochemical Sciences,* 23**,** 469-472.

Aslam, S. N., Newman, M. A., Erbs, G., Morrissey, K. L., Chinchilla, D., Boller, T., Jensen, T. T., De Castro, C., Ierano, T., Molinaro, A., Jackson, R. W., Knight, M. R. and Cooper, R. M. 2008. Bacterial polysaccharides suppress induced innate immunity by calcium chelation. *Curr Biol,* 18**,** 1078-1083.

Averre, C. W. 1914. Black Rot of cabbage and Related Crops. *Plant Pathology Extension*.

Barber, C. E., Tang, J. L., Feng, J. X., Pan, M. Q., Wilson, T. J. G., Slater, H., Dow, J. M., Williams, P. and Daniels, M. J. 1997. A novel regulatory system required for pathogenicity of *Xanthomonas campestris* is mediated by a small diffusible signal molecule. *Mol Microbiol,* 24**,** 555-566.

Barraud, N., Schleheck, D., Klebensberger, J., Webb, J. S., Hassett, D. J., Rice, S. A. and Kjelleberg, S. 2009. Nitric oxide signaling in Pseudomonas aeruginosa biofilms mediates phosphodiesterase activity, decreased cyclic di-GMP levels, and enhanced dispersal. *J Bacteriol,* 191**,** 7333-7342.

Becker, A., Katzen, F., Puhler, A. and Ielpi, L. 1998. Xanthan gum biosynthesis and application: a biochemical/genetic perspective. *Appl Microbiol Biotechnol.,* 50**,** 145-152.

Bonas, U., Schulte, R., Fenselau, S., Minsavage, G. V., Staskawicz, B. J. and Stall, R. E. 1991. Isolation of a gene cluster from *Xanthomonas campestris* pv. *vesicatoria* that determines pathogenicity and the hypersensitive response on pepper and tomato. *Molecular Plant-Microbe Interactions,* 4**,** 81-88.

Cerca, N., Jefferson, K. K., Oliveira, R., Pier, G. B. and Azeredo, J. 2006. Comparative antibody-mediated phagocytosis of *Staphylococcus* epidermidis cells grown in a biofilm or in the planktonic state. *Infect Immun,* 74**,** 4849-4855.

Chan, J. W. Y. F. and Goodwin, P. H. 1999. The molecular genetics of virulence of *Xanthomonas campestris*. *Biotechnology Advances,* 17**,** 489-508.

Chou, F. L., Chou, H. C., Lin, Y. S., Yang, B. Y., Lin, N. T., Weng, S. F. and Tseng, Y. H. 1997. The *Xanthomonas campestris gumD* Gene Required for Synthesis of Xanthan Gum Is Involved in Normal Pigmentation and Virulence in Causing Black Rot. *Biochemical and Biophysical Research Communications,* 233**,** 265-269.

Christen, M., Christen, B., Folcher, M., Schauerte, A. and Jenal, U. 2005. Identification and characterization of a cyclic di-GMP-specific phosphodiesterase and its allosteric control by GTP. *J Biol Chem,* 280**,** 30829-30837.

Colvin, K. M., Irie, Y., Tart, C. S., Urbano, R., Whitney, J. C., Ryder, C., Howell, P. L., Wozniak, D. J. and Parsek, M. R. 2012. The Pel and Psl polysaccharides provide Pseudomonas aeruginosa structural redundancy within the biofilm matrix. *Environ Microbiol,* 14**,** 1913-1928.

Costerton, J. W., Stewart, P. S. and Greenberg, E. P. 1999. Bacterial Biofilms: A common cause of Persistent Infections. *Science,* 284**,** 1318-1322.

Cruz, D. P., Huertas, M. G., Lozano, M., Zárate, L. and Zambrano, M. M. 2012. Comparative analysis of diguanylate cyclase and phosphodiesterase genes in *Klebsiella pneumoniae*. *BMC Microbiol,* 12.

Darouiche, R. O., Mansouri, M. D., Gawande, P. V. and Madhyastha, S. 2009. Antimicrobial and antibiofilm efficacy of triclosan and DispersinB combination. *J Antimicrob Chemother,* 64**,** 88-93.

Delmer, D. P. 1999. Cellulose biosynthesis: exciting times for a difficult field of study. *Annu Rev Plant Physiol. Plant Mol. Biol.,* 50**,** 245-276.

Denny, T. P. 1995. Involvement of Bacterial Polysaccharides in Plant Pathogenesis. *Annu Rev Phytopathol,* 33**,** 173-197.

Department of Agriculture Forestry and Fisheries, S. A.: Directorate Agricultural Information Services. Available: http://www.nda.agric.za/docs/Brochures/ProdGuideCabbage.pdf [Accessed 3 May 2016].

Dharmapuri, S. and Sonti, R. V. 1999. A transposon insertion in the *gumG* homologue of *Xanthomonas oryzae* pv. *oryzae* causes loss of extracellular polysaccharide production and virulence. *FEMS Microbiology Letters,* 179**,** 53-59.

Dow, J. M., Crossman, L., Findlay, K., He, Y. Q., Feng, J. X. and Tang, J. L. 2003. Biofilm dispersal in *Xanthomonas campestris* is controlled by cell-cell signaling and is required for full virulence to plants. *Proc Natl Acad Sci U S A,* 100**,** 10995-11000.

Dow, J. M. and Daniels, M. J. 2000. *Xylella* genomics and bacterial pathogenicity to plants. *Yeast,* 17**,** 263-271.

Dow, J. M., Scofield, G., Trafford, K., Turner, P. C. and Daniels, M. J. 1987. A gene cluster in *Xanthomonas campestris* pv. *campestris* required for pathogenicity controls the excretion of polygalacturonate lyase and other enzymes. *Physiological and Molecular Plant Pathology,* 31**,** 261-271.

Dums, F., Dow, J. M. and Daniels, M. J. 1991. Structural characterization of protein secretion genes of the bacterial phytopathogen *Xanthomonas campestris* pathovar *campestris*: relatedness to secretion systems of other gram-negative bacteria. *Mol Gen Genet,* 229**,** 357-364.

Elder, M. J., Stapleton, F., Evans, E. and Dart, J. K. G. 1995. Biofilm-related infections in ophthalmology. *Eye,* 9**,** 102-109.

Elias, S. and Banin, E. 2012. Multi-species biofilms: living with friendly neighbors. *FEMS Microbiol Rev,* 36**,** 990-1004.

Fargier, E. and Manceau, C. 2007. Pathogenicity assays restrict the species *Xanthomonas campestris* into three pathovars and reveal nine races within *X. campestris* pv. *campestris*. *Plant Pathology,* 56**,** 805-818.

Finn, R. D., Coggill, P., Eberhardt, R. Y., Eddy, S. R., Mistry, J., Mitchell, A. L., Potter, S. C., Punta, M., Qureshi, M., Sangrador-Vegas, A., Salazar, G. A., Tate, J. and Bateman, A. 2016. The Pfam protein families database: towards a more sustainable future. *Nucleic Acids Res,* 44**,** D279-285.

Food and Agriculture Organization of the United Nations. 2013. Available: http://faostat3.fao.org/browse/Q/QC/E [Accessed 3 May 2016].

Fujishige, N. A., Kapadia, N. N. and Hirsch, A. M. 2006. A feeling for the micro-organism: structure on a small scale. Biofilms on plant roots. *Botanical Journal of the Linnean Society,* 150**,** 79-88.

Fux, C. A., Costerton, J. W., Stewart, P. S. and Stoodley, P. 2005. Survival strategies of infectious biofilms. *Trends Microbiol,* 13**,** 34-40.

Galperin, M. Y. 2005. A census of membrane-bound and intracellular signal transduction proteins in bacteria: bacterial IQ, extroverts and introverts. *BMC Microbiol,* 5**,** 35.

Galperin, M. Y., Natale, D. A., Aravind, L. and Koonin, E. V. 1999. A specialized version of the HD hydrolase domain implicated in signal transduction. *J. Mol. Microbiol. Biotechnol.,* 1**,** 303-305.

Galperin, M. Y., Nikolskaya, A. N. and Koonin, E. V. 2001. Novel domains of the prokaryotic two-component signal transduction systems. *FEMS Microbiology Letters,* 203**,** 11-21.

Griffiths, A. J. F., Miller, J. H., Suzuki, D. T., Lewontin, R. C. and Gelbart, W. M. 2000. An Introduction to Genetic Analysis, New York: W. H. Freeman.

Hall-Stoodley, L. and Stoodley, P. 2009. Evolving concepts in biofilm infections. *Cell Microbiol,* 11**,** 1034-1043.

Hanahan, D. 1985. Heritable formation of pancreatic beta-cell tumours in transgenic mice expressing recombinant insulin/simian virus 40 oncogenes. *Nature,* 315**,** 115-122.

Hansen, S. K., Haagensen, J. A., Gjermansen, M., Jorgensen, T. M., Tolker-Nielsen, T. and Molin, S. 2007. Characterization of a *Pseudomonas putida* rough variant evolved in a mixed-species biofilm with *Acinetobacter* sp. strain C6. *J Bacteriol,* 189**,** 4932-4943.

Hassett, D. J., Cuppoletti, J., Trapnell, B., Lymar, S. V., Rowe, J. J., Yoon, S. S., Hilliard, G. M., Parvatiyar, K., Kamani, M. C., Wozniak, D. J., Hwang, S., Mcdermott, T. R. and Ochsner, U. A. 2002. A naerobic metabolism and quorum sensing by *Pseudomonas aeruginosa* biofilms in chronically infected cystic fibrosis airways: rethinking antibiotic treatment strategies and drug targets. *Advanced Drug Delivery Reviews,* 54**,** 1425–1443.

He, Y. W., Boon, C., Zhou, L. and Zhang, L. H. 2009. Co-regulation of *Xanthomonas campestris* virulence by quorum sensing and a novel two-component regulatory system RavS/RavR. *Mol Microbiol,* 71**,** 1464-1476.

He, Y. W., Ng, A. Y., Xu, M., Lin, K., Wang, L. H., Dong, Y. H. and Zhang, L. H. 2007. *Xanthomonas campestris* cell-cell communication involves a putative nucleotide receptor protein Clp and a hierarchical signalling network. *Mol Microbiol,* 64**,** 281-292.

Hengge, R. 2009. Principles of c-di-GMP signalling in bacteria. *Nat Rev Microbiol,* 7**,** 263-273.

Hengge, R., Grundling, A., Jenal, U., Ryan, R. and Yildiz, F. 2016. Bacterial Signal Transduction by Cyclic Di-GMP and Other Nucleotide Second Messengers. *J Bacteriol,* 198**,** 15-26.

Hickman, J. W. and Harwood, C. S. 2008. Identification of FleQ from Pseudomonas aeruginosa as a c-di-GMP-responsive transcription factor. *Mol Microbiol,* 69**,** 376-389.

Ho, Y. S. J., Burden, L. M. and Hurley, J. H. 2000. Structure of the GAF domain, a ubiquitous signaling motif and a new class of cyclic GMP receptor. *19,* 20.

Høiby, N., Bjarnsholt, T., Givskov, M., Molin, S. and Ciofu, O. 2010. Antibiotic resistance of bacterial biofilms. *Int J Antimicrob Agents,* 35**,** 322-332.

Huang, J. 1986. Ultrastructure of bacterial penetration in plants. *Phytopathology,* 24**,** 141-157.

Itoh, Y., Wang, X., Hinnebusch, B. J., Preston, J. F., 3rd and Romeo, T. 2005. Depolymerization of beta-1,6-*N*-acetyl-D-glucosamine disrupts the integrity of diverse bacterial biofilms. *J Bacteriol,* 187**,** 382-387.

Izano, E. A., Amarante, M. A., Kher, W. B. and Kaplan, J. B. 2008a. Differential roles of poly-*N*-acetylglucosamine surface polysaccharide and extracellular DNA in *Staphylococcus aureus* and *Staphylococcus epidermidis* biofilms. *Appl Environ Microbiol,* 74**,** 470-476.

Izano, E. A., Sadovskaya, I., Wang, H., Vinogradov, E., Ragunath, C., Ramasubbu, N., Jabbouri, S., Perry, M. B. and Kaplan, J. B. 2008b. Poly-N-acetylglucosamine

mediates biofilm formation and detergent resistance in *Aggregatibacter actinomycetemcomitans*. *Microb Pathog,* 44**,** 52-60.

Jahangir, M., Kim, H. K., Choi, Y. H. and Verpoorte, R. 2009. Health-Affecting Compounds in *Brassicaceae*. *Comprehensive Reviews in Food Science and Food Safety,* 8**,** 31-43.

Jansson, P. E., Kenne, L. and Lindberg, B. 1975. Structure of the extracellular polysaccharide from *Xanthomonas campestris*. *Carbohydrate Research,* 45**,** 275-282.

Jenal, U. and Malone, J. 2006. Mechanisms of cyclic-di-GMP signaling in bacteria. *Annu Rev Genet,* 40**,** 385-407.

Jesaitis, A. J., Franklin, M. J., Berglund, D., Sasaki, M., Lord, C. I., Bleazard, J. B., Duffy, J. E., Beyenal, H. and Lewandowski, Z. 2003. Compromised Host Defense on *Pseudomonas aeruginosa* Biofilms: Characterization of Neutrophil and Biofilm Interactions. *The Journal of Immunology,* 171**,** 4329-4339.

Kanehisa, M. and Goto, S. 2000. KEGG: Kyoto Encyclopedia of Genes and Genomes *Nucleic Acids Research,* 28**,** 27-30.

Kanehisa, M., Sato, Y., Kawashima, M., Furumichi, M. and Tanabe, M. 2016. KEGG as a reference resource for gene and protein annotation. *Nucleic Acids Res,* 44**,** D457-462.

Kaplan, J. B., Ragunath, C., Velliyagounder, K., Fine, D. H. and Ramasubbu, N. 2004. Enzymatic detachment of *Staphylococcus epidermidis* biofilms. *Antimicrob Agents Chemother,* 48**,** 2633-2636.

Katzen, F., Ferreiro, D. U., Oddo, C. G., Ielmini, M. V., Becker, A., Pühler, A. and Ielpi, L. 1998. *Xanthomonas campestris* pv. campestris *gum* Mutants: Effects on Xanthan Biosynthesis and Plant Virulence. *J Bacteriol,* 180**,** 1607-1617.

Keshishian, H., Addona, T., Burgess, M., Kuhn, E. and Carr, S. A. 2007. Quantitative, Multiplexed Assays for Low Abundance Proteins in Plasma by Targeted Mass Spectrometry and Stable Isotope Dilution. *Mol Cell Proteomics,* 6**,** 2212-2229.

Koebnik, R., Krüger, A., Thieme, F., Urban, A. and Bonas, U. 2006. Specific binding of the *Xanthomonas campestris* pv. vesicatoria AraC-type transcriptional activator HrpX to plant-inducible promoter boxes. *J Bacteriol,* 188**,** 7652-7660.

Lee, H. M., Wang, K. C., Liu, Y. L., Yew, H. Y., Chen, L. Y., Leu, W. M., Chen, D. C. and Hu, N. T. 2000. Association of the Cytoplasmic Membrane Protein XpsN with the Outer Membrane Protein XpsD in the Type II Protein Secretion Apparatus of *Xanthomonas campestris* pv. Campestris. *J Bacteriol,* 182**,** 1549-1557.

Leong, S. A., Ditta, G. S. and Helinski, D. R. 1982. Heme biosynthesis in *Rhizobium*. Identification of a cloned gene coding for delta-aminolevulinic acid synthetase from *Rhizobium meliloti. Journal of Biological Chemistry,* 257**,** 8724-8730.

Letunic, I., Doerks, T. and Bork, P. 2015. SMART: recent updates, new developments and status in 2015. *Nucleic Acids Res,* 43**,** D257-260.

Leyns, F., De Cleene, M., Swings, J. G. and De Ley, J. 1984. The host range of the genus *Xanthomonas*. *The botanic Review,* 50**,** 308-356.

Lu, H., Patil, P., Van Sluys, M. A., White, F. F., Ryan, R. P., Dow, J. M., Rabinowicz, P., Salzberg, S. L., Leach, J. E., Sonti, R., Brendel, V. and Bogdanove, A. J. 2008. Acquisition and evolution of plant pathogenesis-associated gene clusters and candidate determinants of tissue-specificity in xanthomonas. *PLoS One,* 3**,** e3828.

Lu, T. K. and Collins, J. J. 2007. Dispersing biofilms with engineered enzymatic bacteriophage. *Proc Natl Acad Sci U S A,* 104**,** 11197-11202.

Lu, X. H., An, S. Q., Tang, D. J., Mccarthy, Y., Tang, J. L., Dow, J. M. and Ryan, R. P. 2012. RsmA regulates biofilm formation in *Xanthomonas campestris* through a regulatory network involving cyclic di-GMP and the Clp transcription factor. *PLoS One,* 7**,** e52646.

Mann, E. E. and Wozniak, D. J. 2012. *Pseudomonas* biofilm matrix composition and niche biology. *FEMS Microbiol Rev,* 36**,** 893-916.

Mansfield, J., Genin, S., Magori, S., Citovsky, V., Sriariyanum, M., Ronald, P., Dow, M., Verdier, V., Beer, S. V., Machado, M. A., Toth, I., Salmond, G. and Foster, G. D. 2012. Top 10 plant pathogenic bacteria in molecular plant pathology. *Mol Plant Pathol,* 13**,** 614-629.

Mcdowell, J. M., Cuzick, A., Can, C., Beyon, J., Dangl, J. L. and Holub, E. B. 2000. Downy mildew (*Perenospora parasitica*) resistance genes in Arabidopsis vary in functional requirements for *NDR1, EDS1, NPR1* and salicylic acid accumulation. *The Plant Journal,* 22**,** 523-529.

Mckee, R. W., Kariisa, A., Mudrak, B., Whitaker, C. and Tamayo, R. 2014. A systematic analysis of the *in vitro* and *in vivo* functions of the HD-GYP domain proteins of *Vibrio cholerae*. *BMC Microbiol,* 14.

Mole, B. M., Baltrus, D. A., Dangl, J. L. and Grant, S. R. 2007. Global virulence regulation networks in phytopathogenic bacteria. *Trends Microbiol,* 15**,** 363-371.

Mudgett, M. B. 2005. New insights to the function of phytopathogenic bacterial type III effectors in plants. *Annu. Rev. Plant Biol.,* 56**,** 509-531.

Nielsen, A. T., Tolker-Nielsen, T., Barken, K. B. and Molin, S. 2000. Role of commensal relationships on the spatial structure of a surface-attached microbial consortium. *Environ Microbiol,* 2**,** 59-68.

Noël, L., Thieme, F., Nennstiel, D. and Bonas, U. 2001. cDNA-AFLP analysis unravels a genome-wide *hrpG*-regulon in the plant pathogen *Xanthomonas campestris* pv. *vesicatoria*. *Mol Microbiol,* 41**,** 1271-1281.

Noël, L., Thieme, F., Nennstiel, D. and Bonas, U. 2002. Two Novel Type III-Secreted Proteins of *Xanthomonas campestris* pv. vesicatoria Are Encoded within the *hrp* Pathogenicity Island. *J Bacteriol,* 184**,** 1340-1348.

Paul, R., Weiser, S., Amiot, N. C., Chan, C., Schirmer, T., Giese, B. and Jenal, U. 2004. Cell cycle-dependent dynamic localization of a bacterial response regulator with a novel di-guanylate cyclase output domain. *GENES & DEVELOPMENT,* 18**,** 715-727.

Pfeilmeier, S., Saur, I. M., Rathjen, J. P., Zipfel, C. and Malone, J. G. 2016. High levels of cyclic-di-GMP in plant-associated Pseudomonas correlate with evasion of plant immunity. *Mol Plant Pathol,* 17**,** 521-531.

Ploetz, R. C. 2006. Fusarium Wilt of Banana Is Caused by Several Pathogens Referred to as *Fusarium oxysporum* f. sp. *cubense*. *Phytopathology,* 96**,** 653-656.

Potnis, N., Timilsina, S., Strayer, A., Shantharaj, D., Barak, J. D., Paret, M. L., Vallad, G. E. and Jones, J. B. 2015. Bacterial spot of tomato and pepper: diverse *Xanthomonas* species with a wide variety of virulence factors posing a worldwide challenge. *Mol Plant Pathol,* 16**,** 907-920.

Qian, W., Han, Z. J. and He, C. 2008a. Two-Component Signal Transduction Systems of *Xanthomonas spp*.: A Lesson from Genomics. *Molecular Plant-Microbe Interactions,* 21**,** 151-161.

Qian, W., Han, Z. J., Tao, J. and He, C. 2008b. Genome-Scale Mutagenesis and Phenotypic Characterization of Two-Component Signal Transduction Systems in *Xanthomonas campestris* pv. *campestris* ATCC 33913. *Molecular Plant-Microbe Interactions,* 21**,** 1128-1138.

Qian, W., Jia, Y., Ren, S. X., He, Y. Q., Feng, J. X., Lu, L. F., Sun, Q., Ying, G., Tang, D. J., Tang, H., Wu, W., Hao, P., Wang, L., Jiang, B. L., Zeng, S., Gu, W. Y., Lu, G., Rong, L., Tian, Y., Yao, Z., Fu, G., Chen, B., Fang, R., Qiang, B., Chen, Z., Zhao, G. P., Tang, J. L. and He, C. 2005. Comparative and functional genomic analyses of the pathogenicity of phytopathogen *Xanthomonas campestris* pv. *campestris*. *Genome Res,* 15**,** 757-767.

Rajagopal, L., Sundari, C. S., Balasubramanian, D. and Sonti, R. V. 1997. The bacterial pigment xanthomonadin offers protection against photodamage. *FEBS Letters,* 415**,** 125-128.

Rickard, A. H., Palmer, R. J., Jr., Blehert, D. S., Campagna, S. R., Semmelhack, M. F., Egland, P. G., Bassler, B. L. and Kolenbrander, P. E. 2006. Autoinducer 2: a concentration-dependent signal for mutualistic bacterial biofilm growth. *Mol Microbiol,* 60**,** 1446-1456.

Römling, U., Galperin, M. Y. and Gomelsky, M. 2013. Cyclic di-GMP: the first 25 years of a universal bacterial second messenger. *Microbiol Mol Biol Rev,* 77**,** 1-52.

Römling, U., Gomelsky, M. and Galperin, M. Y. 2005. C-di-GMP: the dawning of a novel bacterial signalling system. *Mol Microbiol,* 57**,** 629-639.

Ross, P., Weinhouse, H., Aloni, Y., Michaeli, D., Weinberger-Ohana, P., Mayer, R., Braun, S., De Vroom, E., Van Der Marel, G. A., Van Boom, J. H. and Benziman, M. 1987. Regulation of cellulose synthesis in *Acetobacter xylinum* by cyclic diguanylic acid. *Nature,* 325**,** 279-281.

Rubatzky, V. E. and Yamaguchi, M. 1997. World Vegetables: Principles, production and nutritive values, Springer US.

Ryan, R. P. 2013. Cyclic di-GMP signalling and the regulation of bacterial virulence. *Microbiology,* 159**,** 1286-1297.

Ryan, R. P. and Dow, J. M. 2010. Intermolecular interactions between HD-GYP and GGDEF domain proteins mediate virulence-related signal transduction in *Xanthomonas campestris*. *Virulence,* 1**,** 404-408.

Ryan, R. P. and Dow, J. M. 2011. Communication with a growing family: diffusible signal factor (DSF) signaling in bacteria. *Trends Microbiol,* 19**,** 145-152.

Ryan, R. P., Fouhy, Y., Lucey, J. F., Crossman, L. C., Spiro, S., He, Y. W., Zhang, L. H., Heeb, S., Camara, M., Williams, P. and Dow, J. M. 2006. Cell-cell signaling in *Xanthomonas campestris* involves an HD-GYP domain protein that functions in cyclic di-GMP turnover. *Proc Natl Acad Sci U S A,* 103**,** 6712-6717.

Ryan, R. P., Fouhy, Y., Lucey, J. F., Jiang, B. L., He, Y. Q., Feng, J. X., Tang, J. L. and Dow, J. M. 2007. Cyclic di-GMP signalling in the virulence and environmental adaptation of *Xanthomonas campestris*. *Mol Microbiol,* 63**,** 429-442.

Ryan, R. P., Tolker-Nielsen, T. and Dow, J. M. 2012. When the PilZ don't work: effectors for cyclic di-GMP action in bacteria. *Trends Microbiol,* 20**,** 235-242.

Ryan, R. P., Vorhölter, F. J., Potnis, N., Jones, J. B., Van Sluys, M. A., Bogdanove, A. J. and Dow, J. M. 2011. Pathogenomics of *Xanthomonas*: understanding bacterium-plant interactions. *Nat Rev Microbiol,* 9**,** 344-355.

Sauer, K., Camper, A. K., Ehrlich, G. D., Costerton, J. W. and Davies, D. G. 2002. *Pseudomonas aeruginosa* Displays Multiple Phenotypes during Development as a Biofilm. *J Bacteriol,* 184**,** 1140-1154.

Schaad, N. W., Jones, J. B. and Chun, W. 2001. Laboratory Guide for Identification of Plant Pathogenic Bacteria, Third Edition, American Phytopathological Society (APS Press), St. Paul.

Schäfer, A., Tauch, A., Jäger, W., Kalinowski, J., Thierbach, G. and Pühler, A. 1994. Small mobilizable multi-purpose cloning vectors derived from the Escherichia coli plasmids pK18 and pK19: selection of defined deletions in the chromosome of *Corynebacterium glutamicum*. *Gene,* 145**,** 69-73.

Schneider, C. A., Rasband, W. S. and Eliceiri, K. W. 2012. NIH Image to ImageJ: 25 years of image analysis. *Nature Methods,* 9**,** 671-675.

Schulte, R. and Bonas, U. 1992. Expression of the *Xanthomonas campestris* pv. vesicatoria *hrp* Gene Cluster, Which Determines Pathogenicity and Hypersensitivity on Pepper and Tomato, Is Plant Inducible. *J Bacteriol,* 174**,** 815-823.

Schultz, J., Milpetz, F., Bork, P. and Ponting, C. P. 1998. SMART, a simple modular architecture research tool: Identification of signaling domains. *Proc Natl Acad Sci U S A,* 95**,** 5857-5864.

Serrania, J., Vorhölter, F. J., Niehaus, K., Pühler, A. and Becker, A. 2008. Identification of *Xanthomonas campestris* pv. campestris galactose utilization genes from transcriptome data. *J Biotechnol,* 135**,** 309-317.

Slater, H., Alvarez-Morales, A., Barber, C. E., Daniels, M. J. and Dow, J. M. 2000. A two-component system involving an HD-GYP domain protein links cell±cell signalling to pathogenicity gene expression in *Xanthomonas campestris*. *Mol Microbiol,* 2000**,** 5.

Staskawicz, B., Dahlbeck, D., Keen, N. and Napoli, C. 1987. Molecular Characterization of Cloned Avirulence Genes from Race 0 and Race 1 of *Pseudomonas syringae* pv. *glycinea*. *J Bacteriol,* 169.

Tal, R., Wong, H. C., Calhoon, R., Gelfand, D., Fear, A. L., Volman, G., Mayer, R., Ross, P., Amikam, D., Weinhouse, H., Cohen, A., Sapir, S., Ohana, P. and Benziman, M. 1998. Three *cdg* Operons Control Cellular Turnover of Cyclic Di-GMP in *Acetobacter xylinum*: Genetic Organization and Occurrence of Conserved Domains in Isoenzymes. *J Bacteriol,* 180**,** 4416-4425.

Tao, F., He, Y. W., Wu, D. H., Swarup, S. and Zhang, L. H. 2010. The cyclic nucleotide monophosphate domain of *Xanthomonas campestris* global regulator Clp defines a new class of cyclic di-GMP effectors. *J Bacteriol,* 192**,** 1020-1029.

Thermofisher Scientific. Available: https://www.thermofisher.com/uk/en/home/life-science/cloning/competent-cells-for-transformation/competent-cells-resources/genotypes-of-competent-cells.html [Accessed 7 June 2016].

Thieme, F., Koebnik, R., Bekel, T., Berger, C., Boch, J., Buttner, D., Caldana, C., Gaigalat, L., Goesmann, A., Kay, S., Kirchner, O., Lanz, C., Linke, B., Mchardy, A. C., Meyer, F., Mittenhuber, G., Nies, D. H., Niesbach-Klösgen, U., Patschkowski, T., Rückert, C., Rupp, O., Schneiker, S., Schuster, S. C., Vorhölter, F. J., Weber, E., Pühler, A., Bonas, U., Bartels, D. and Kaiser, O. 2005. Insights into genome plasticity and pathogenicity of the plant pathogenic bacterium *Xanthomonas campestris* pv. vesicatoria revealed by the complete genome sequence. *J Bacteriol,* 187**,** 7254-7266.

Tolker-Nielsen, T., Brinch, U. C., Ragas, P. C., Andersen, J. B., Jacobsen, C. S. and Molin, S. 2000. Development and Dynamics of *Pseudomonas* sp. Biofilms. *J Bacteriol,* 182**,** 6482–6489.

Torres, P. S., Malamud, F., Rigano, L. A., Russo, D. M., Marano, M. R., Castagnaro, A. P., Zorreguieta, A., Bouarab, K., Dow, J. M. and Vojnov, A. A. 2007. Controlled synthesis of the DSF cell-cell signal is required for biofilm formation and virulence in *Xanthomonas campestris*. *Environ Microbiol,* 9**,** 2101-2109.

Turner, P., Barber, C. and Daniels, M. 1984. Behaviour of the transposons Tn5 and Tn7 in *Xanthomonas campestris* pv. *campestris*. *Molecular and General Genetics,* 195**,** 101-107.

Vasudevan, R. 2014. Biofilms: Microbial Cities of Scientific Significance. *Journal of Microbiology & Experimentation,* 1.

Venketaraman, V., Lin, A. K., Le, A., Kachlany, S. C., Connell, N. D. and Kaplan, J. B. 2008. Both leukotoxin and poly-*N*-acetylglucosamine surface polysaccharide protect *Aggregatibacter actinomycetemcomitans* cells from macrophage killing. *Microb Pathog,* 45**,** 173-180.

Von Bodman, S. B., Bauer, W. D. and Coplin, D. L. 2003. Quorum sensing in plant-pathogenic bacteria. *Annu Rev Phytopathol,* 41**,** 455-482.

Vorhölter, F. J., Schneiker, S., Goesmann, A., Krause, L., Bekel, T., Kaiser, O., Linke, B., Patschkowski, T., Rückert, C., Schmid, J., Sidhu, V. K., Sieber, V., Tauch, A., Watt, S. A., Weisshaar, B., Becker, A., Niehaus, K. and Pühler, A. 2008. The genome of *Xanthomonas campestris* pv. campestris B100 and its use for the reconstruction of metabolic pathways involved in xanthan biosynthesis. *J Biotechnol,* 134**,** 33-45.

Wengelnik, K. and Bonas, U. 1996. HrpXv, an AraC-type regulator, activates expression of five of the six loci in the *hrp* cluster of *Xanthomonas campestris* pv. vesicatoria. *J Bacteriol,* 178**,** 3462-3469.

Wolfe, A. J. and Visick, K. L. 2008. Get the message out: cyclic-Di-GMP regulates multiple levels of flagellum-based motility. *J Bacteriol,* 190**,** 463-475.

Yu, X., Liang, X., Liu, K., Dong, W., Wang, J. and Zhou, M. G. 2015. The *thiG* Gene Is Required for Full Virulence of *Xanthomonas oryzae* pv. *oryzae* by Preventing Cell Aggregation. *PLoS One,* 10**,** e0134237.

Yuan, Z., Wang, L., Sun, S., Wu, Y. and Qian, W. 2013. Genetic and proteomic analyses of a *Xanthomonas campestris* pv. *campestris purC* mutant deficient in purine biosynthesis and virulence. *J Genet Genomics,* 40**,** 473-487.

Yun, M. H., Torres, P. S., El Oirdi, M., Rigano, L. A., Gonzalez-Lamothe, R., Marano, M. R., Castagnaro, A. P., Dankert, M. A., Bouarab, K. and Vojnov, A. A. 2006. Xanthan induces plant susceptibility by suppressing callose deposition. *Plant Physiol,* 141**,** 178-187.

Zhulin, I. B., Nikolskaya, A. N. and Galperin, M. Y. 2003. Common Extracellular Sensory Domains in Transmembrane Receptors for Diverse Signal Transduction Pathways in Bacteria and Archaea. *J Bacteriol,* 185**,** 285-294.

9 List of Figures

10 List of Tables

11 Appendix

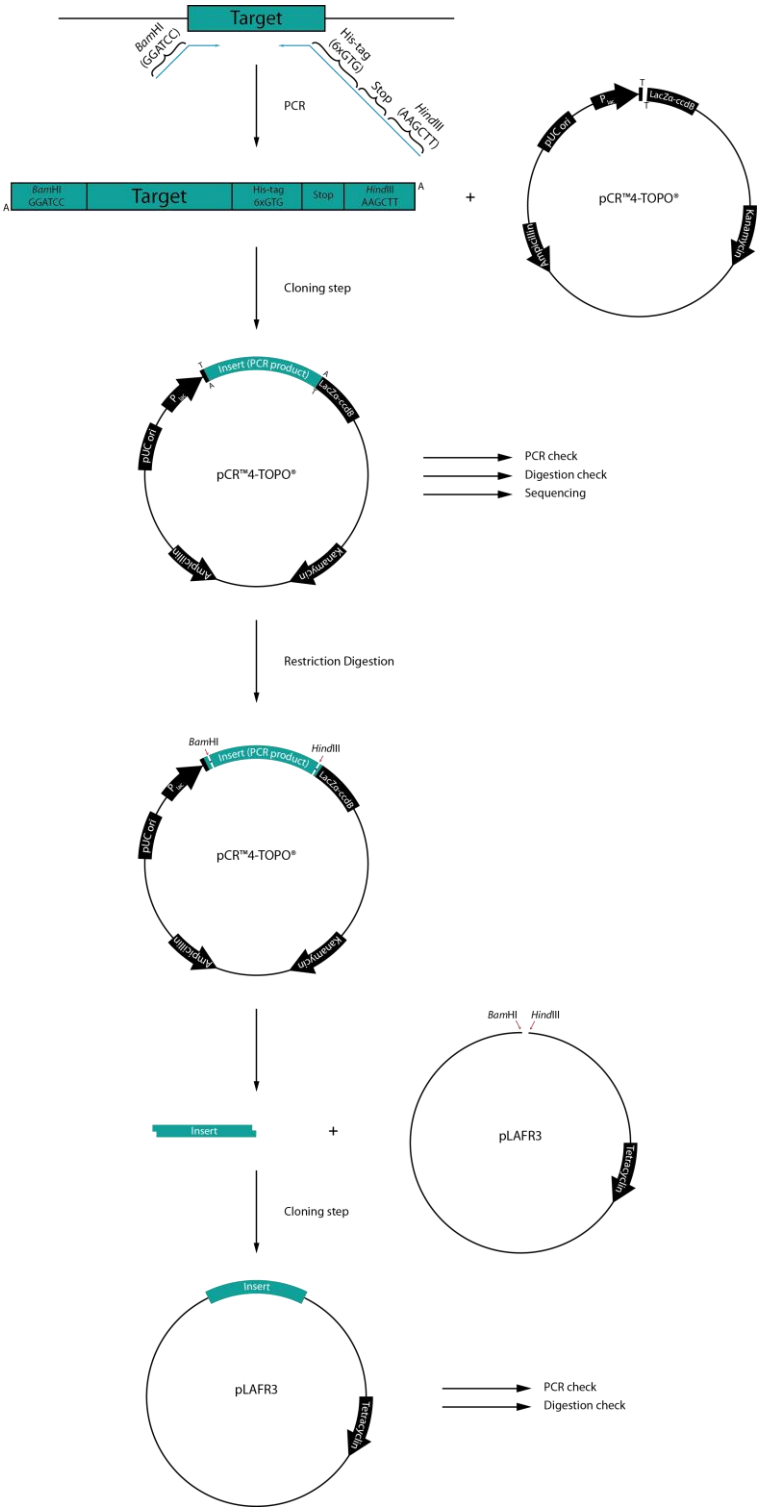

Appendix Figure 1: Schematic representation of the construction of complementation.

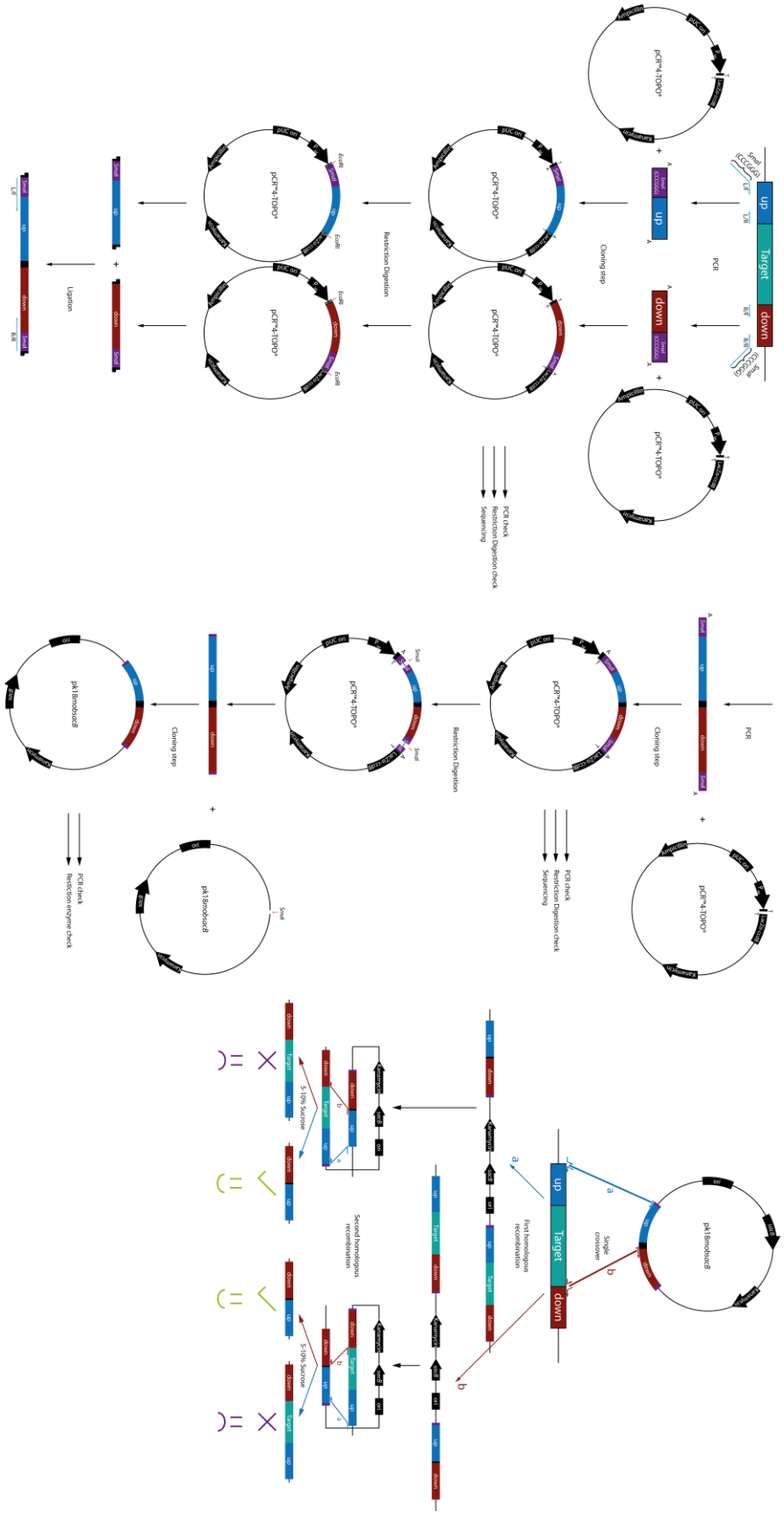

Appendix Figure 2: Schematic representation of the construction of deletion mutants.

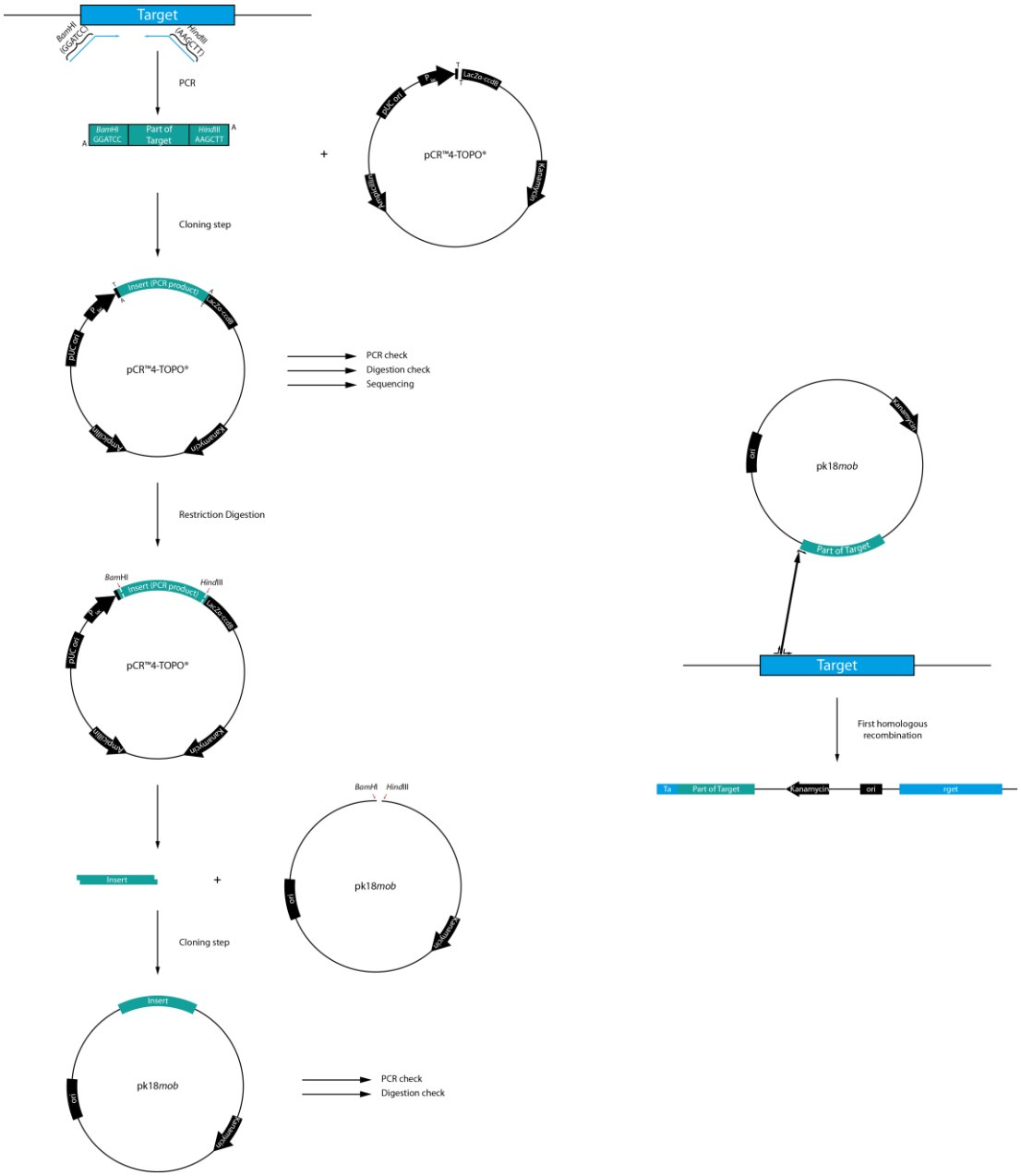

Appendix Figure 3: Schematic representation of the construction of insertion mutants.

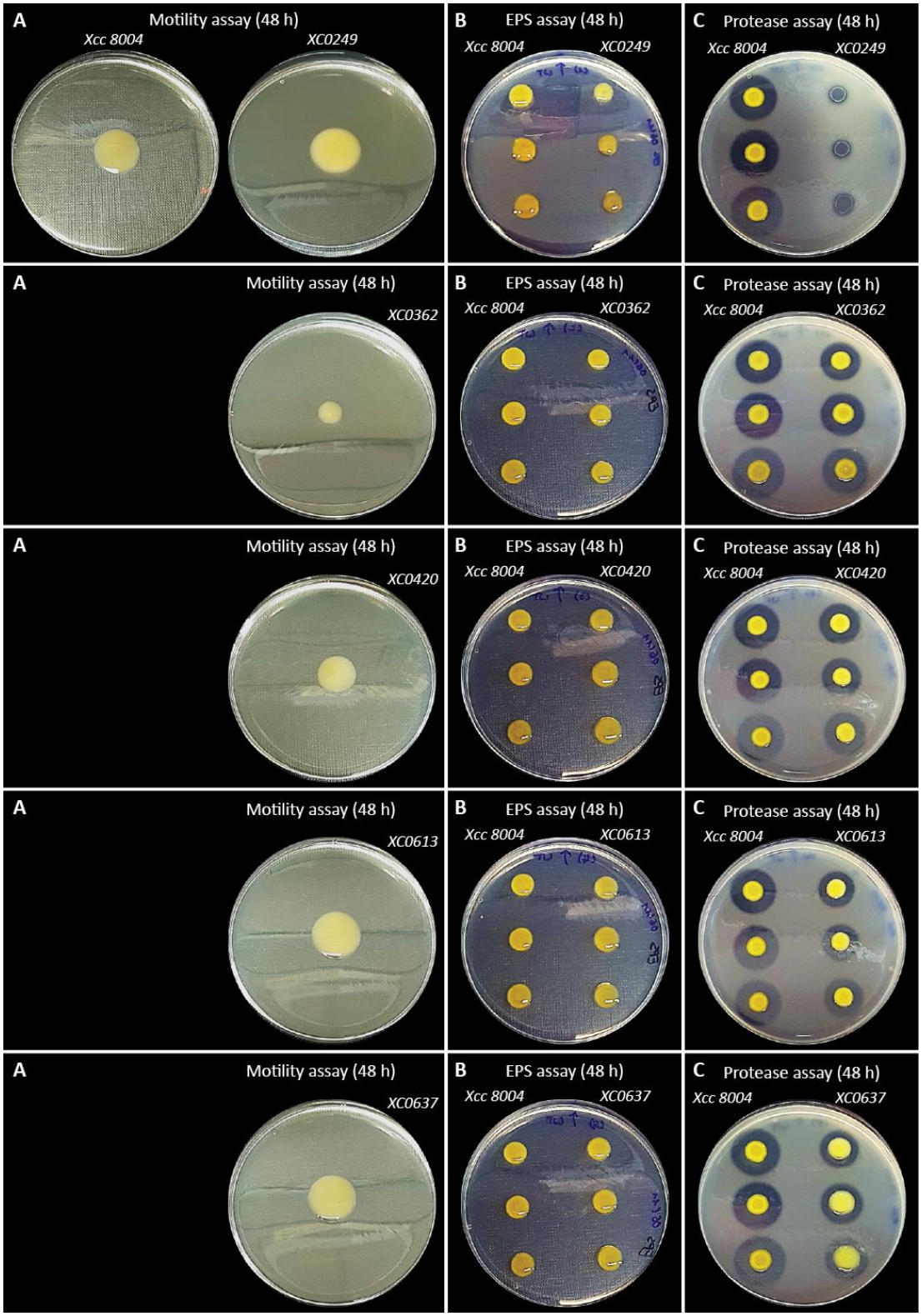
A
Motility assay (48 h)
Xcc 8004
XC0249
B
EPS assay (48 h)
Xcc 8004
XC0249
C
Protease assay (48 h)
Xcc 8004
XC0249
A
Motility assay (48 h)
XC0362
B
EPS assay (48 h)
Xcc 8004
XC0362
C
Protease assay (48 h)
Xcc 8004
XC0362
A
Motility assay (48 h)
XC0420
B
EPS assay (48 h)
Xcc 8004
XC0420
C
Protease assay (48 h)
Xcc 8004
XC0420
A
Motility assay (48 h)
XC0613
B
EPS assay (48 h)
Xcc 8004
XC0613
C
Protease assay (48 h)
Xcc 8004
XC0613
A
Motility assay (48 h)
XC0637
B
EPS assay (48 h)
Xcc 8004
XC0637
C
Protease assay (48 h)
Xcc 8004
XC0637

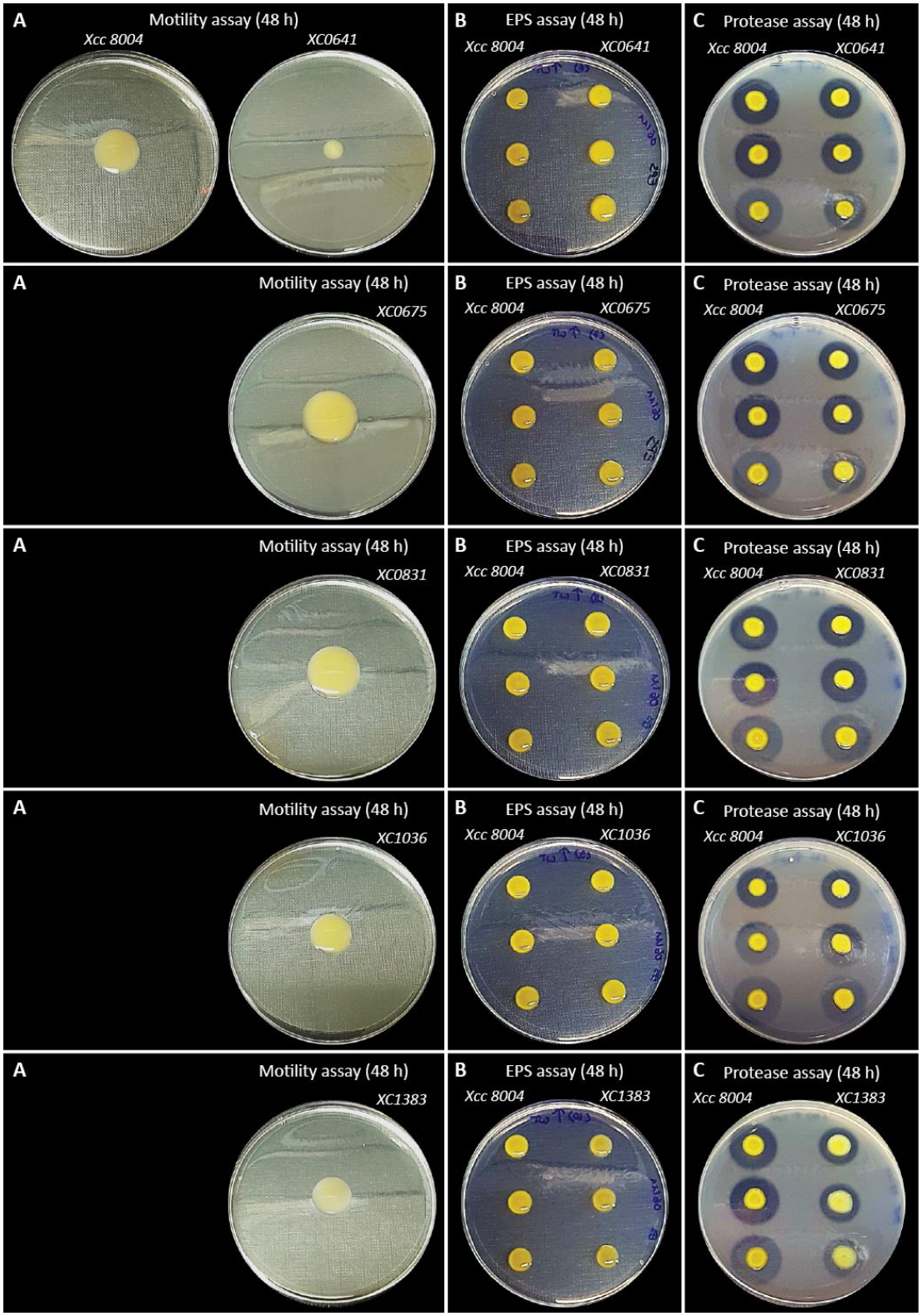
A
Motility assay (48 h)
Xcc 8004
XC0641
B
EPS assay (48 h)
Xcc 8004
XC0641
C
Protease assay (48 h)
Xcc 8004
XC0641
A
Motility assay (48 h)
XC0675
B
EPS assay (48 h)
Xcc 8004
XC0675
C
Protease assay (48 h)
Xcc 8004
XC0675
A
Motility assay (48 h)
XC0831
B
EPS assay (48 h)
Xcc 8004
XC0831
C
Protease assay (48 h)
Xcc 8004
XC0831
A
Motility assay (48 h)
XC1036
B
EPS assay (48 h)
Xcc 8004
XC1036
C
Protease assay (48 h)
Xcc 8004
XC1036
A
Motility assay (48 h)
XC1383
B
EPS assay (48 h)
Xcc 8004
XC1383
C
Protease assay (48 h)
Xcc 8004
XC1383

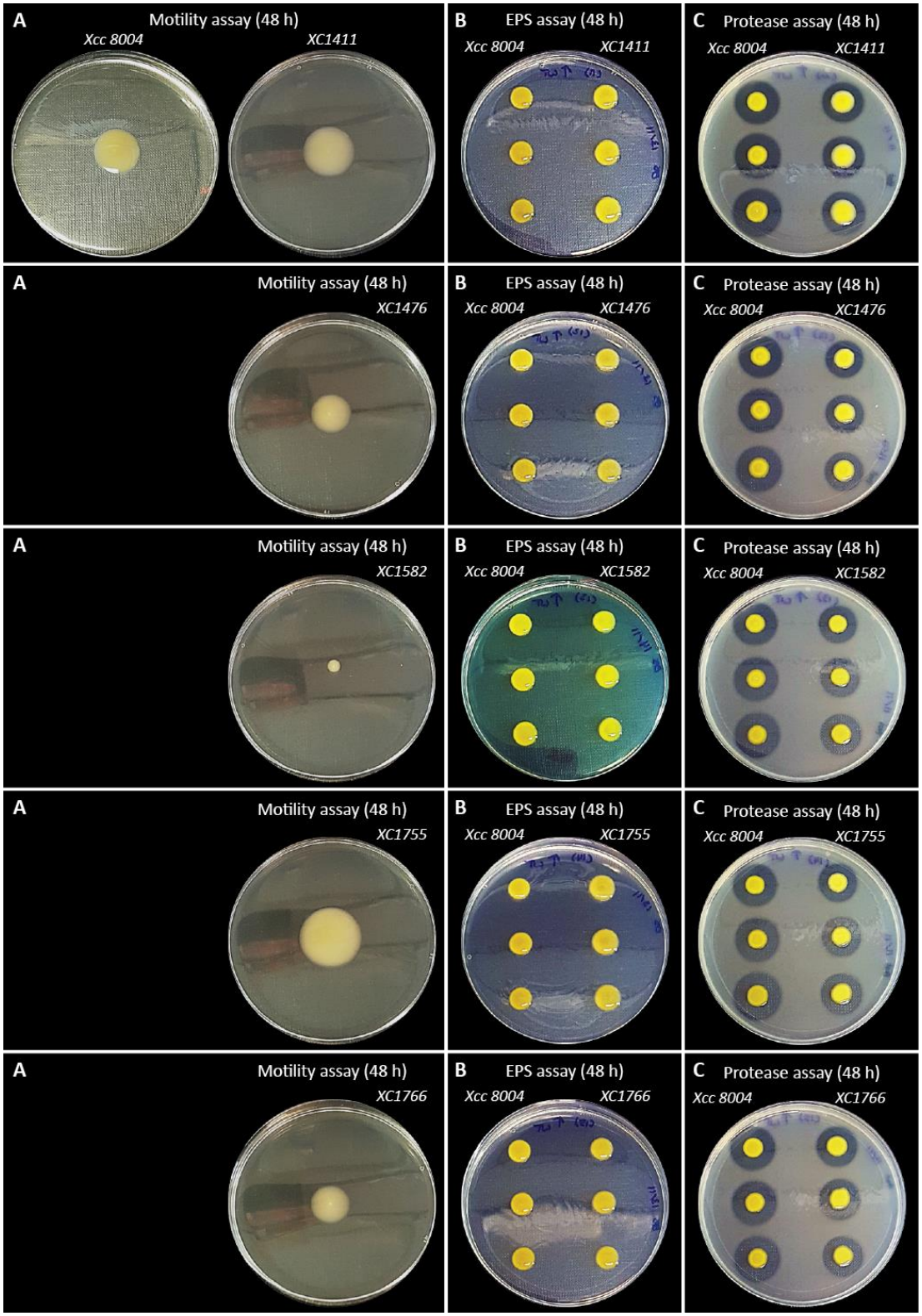
A
Motility assay (48 h)
Xcc 8004
XC1411
B
EPS assay (48 h)
Xcc 8004
XC1411
C
Protease assay (48 h)
Xcc 8004
XC1411
A
Motility assay (48 h)
XC1476
B
EPS assay (48 h)
Xcc 8004
XC1476
C
Protease assay (48 h)
Xcc 8004
XC1476
A
Motility assay (48 h)
XC1582
B
EPS assay (48 h)
Xcc 8004
XC1582
C
Protease assay (48 h)
Xcc 8004
XC1582
A
Motility assay (48 h)
XC1755
B
EPS assay (48 h)
Xcc 8004
XC1755
C
Protease assay (48 h)
Xcc 8004
XC1755
A
Motility assay (48 h)
XC1766
B
EPS assay (48 h)
Xcc 8004
XC1766
C
Protease assay (48 h)
Xcc 8004
XC1766

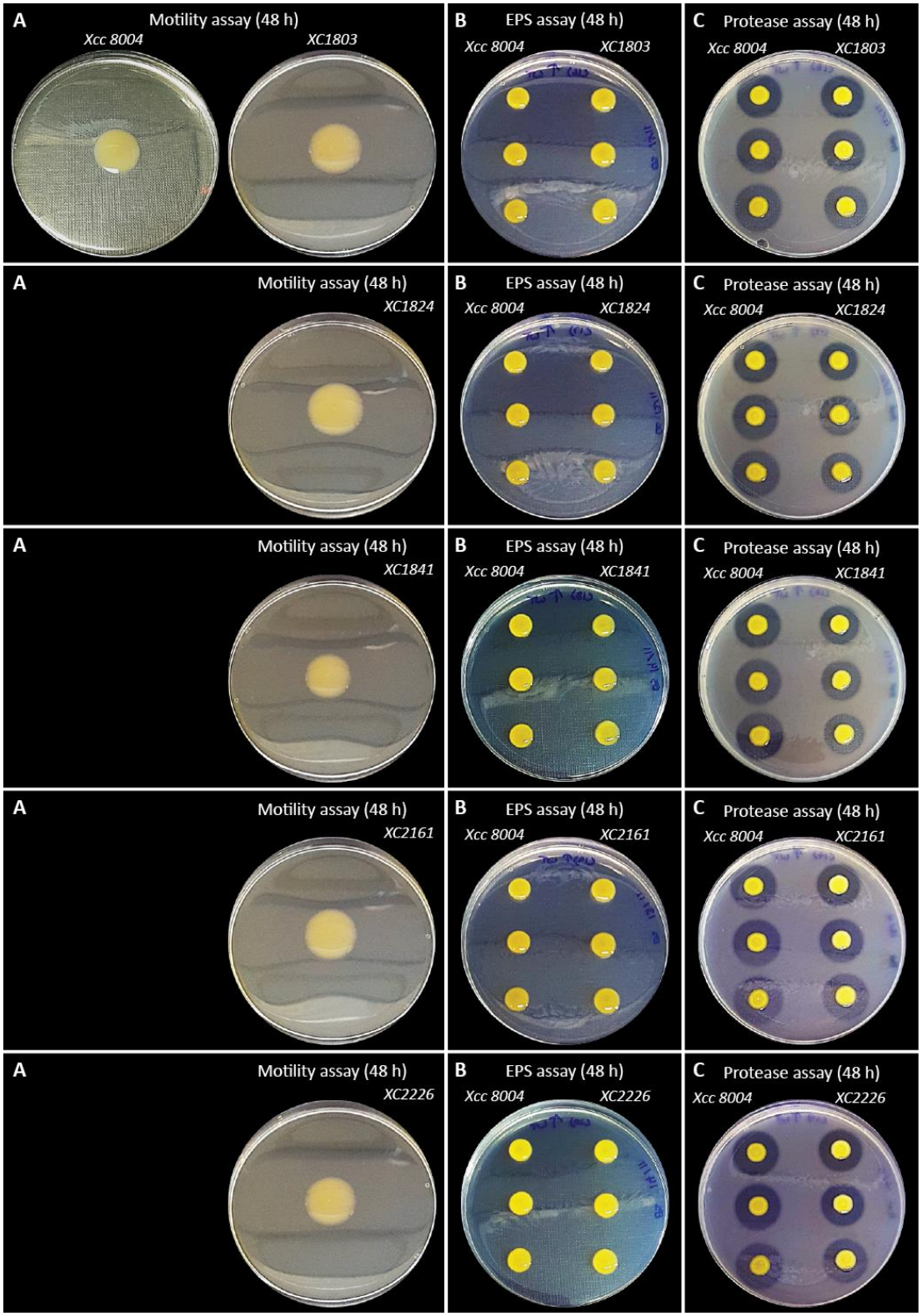
A
Motility assay (48 h)
Xcc 8004
XC1803
B
EPS assay (48 h)
Xcc 8004
XC1803
C
Protease assay (48 h)
Xcc 8004
XC1803
A
Motility assay (48 h)
XC1824
B
EPS assay (48 h)
Xcc 8004
XC1824
C
Protease assay (48 h)
Xcc 8004
XC1824
A
Motility assay (48 h)
XC1841
B
EPS assay (48 h)
Xcc 8004
XC1841
C
Protease assay (48 h)
Xcc 8004
XC1841
A
Motility assay (48 h)
XC2161
B
EPS assay (48 h)
Xcc 8004
XC2161
C
Protease assay (48 h)
Xcc 8004
XC2161
A
Motility assay (48 h)
XC2226
B
EPS assay (48 h)
Xcc 8004
XC2226
C
Protease assay (48 h)
Xcc 8004
XC2226

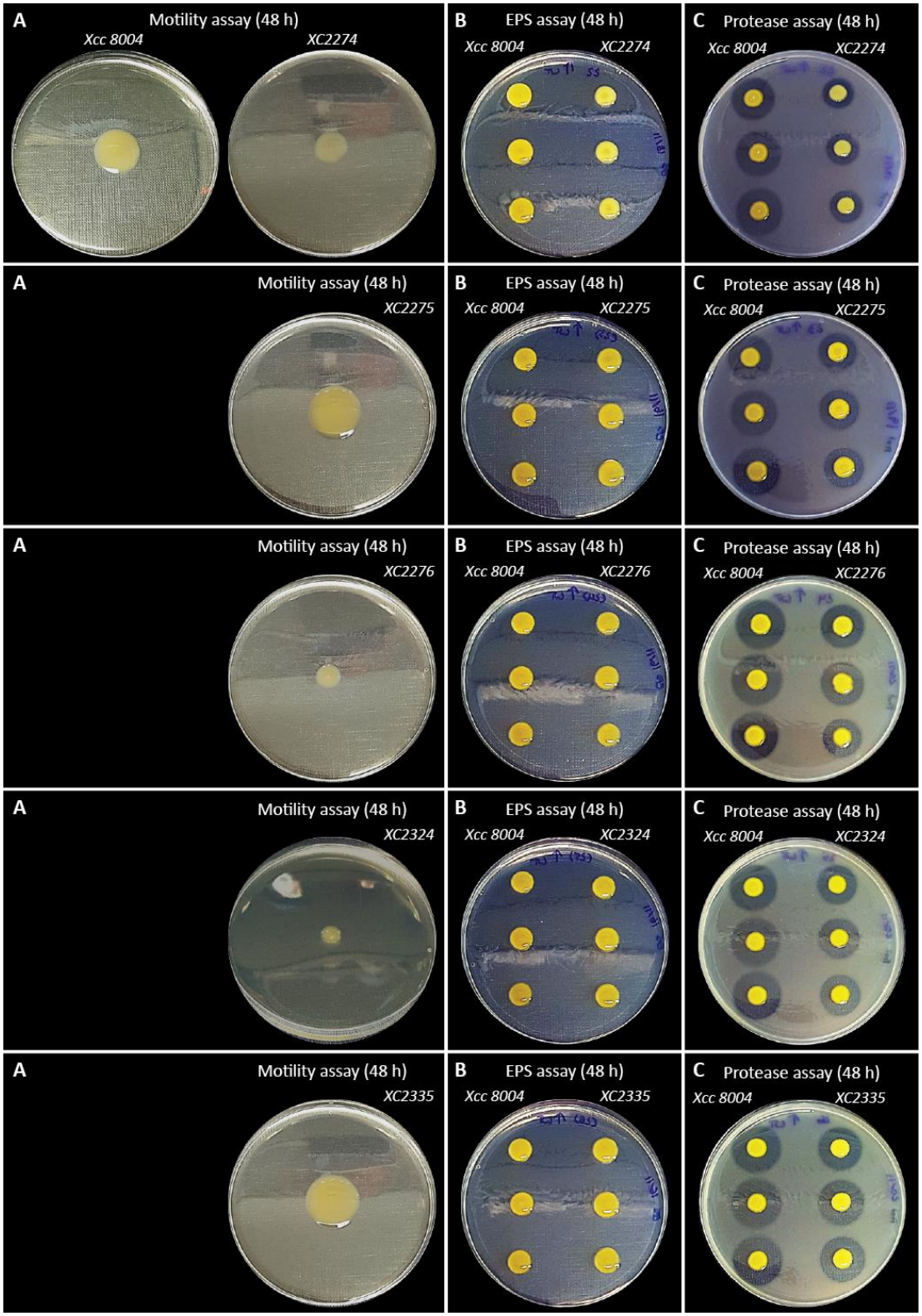
A
Motility assay (48 h)
Xcc 8004
XC2274
B
EPS assay (48 h)
Xcc 8004
XC2274
C
Protease assay (48 h)
Xcc 8004
XC2274
A
Motility assay (48 h)
XC2275
B
EPS assay (48 h)
Xcc 8004
XC2275
C
Protease assay (48 h)
Xcc 8004
XC2275
A
Motility assay (48 h)
XC2276
B
EPS assay (48 h)
Xcc 8004
XC2276
C
Protease assay (48 h)
Xcc 8004
XC2276
A
Motility assay (48 h)
XC2324
B
EPS assay (48 h)
Xcc 8004
XC2324
C
Protease assay (48 h)
Xcc 8004
XC2324
A
Motility assay (48 h)
XC2335
B
EPS assay (48 h)
Xcc 8004
XC2335
C
Protease assay (48 h)
Xcc 8004
XC2335

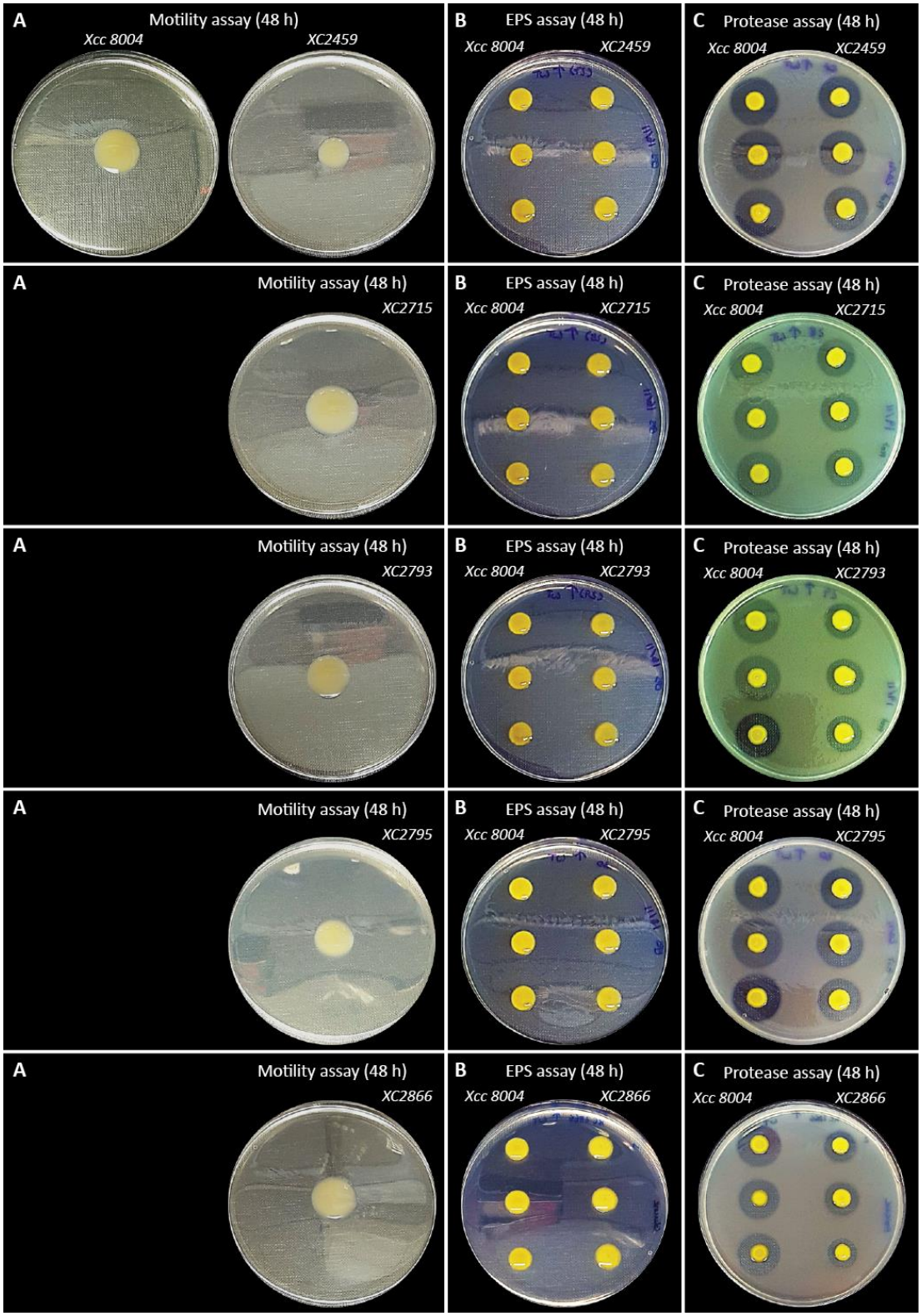
A
Motility assay (48 h)
Xcc 8004
XC2459
B
EPS assay (48 h)
Xcc 8004
XC2459
C
Protease assay (48 h)
Xcc 8004
XC2459
A
Motility assay (48 h)
XC2715
B
EPS assay (48 h)
Xcc 8004
XC2715
C
Protease assay (48 h)
Xcc 8004
XC2715
A
Motility assay (48 h)
XC2793
B
EPS assay (48 h)
Xcc 8004
XC2793
C
Protease assay (48 h)
Xcc 8004
XC2793
A
Motility assay (48 h)
XC2795
B
EPS assay (48 h)
Xcc 8004
XC2795
C
Protease assay (48 h)
Xcc 8004
XC2795
A
Motility assay (48 h)
XC2866
B
EPS assay (48 h)
Xcc 8004
XC2866
C
Protease assay (48 h)
Xcc 8004
XC2866

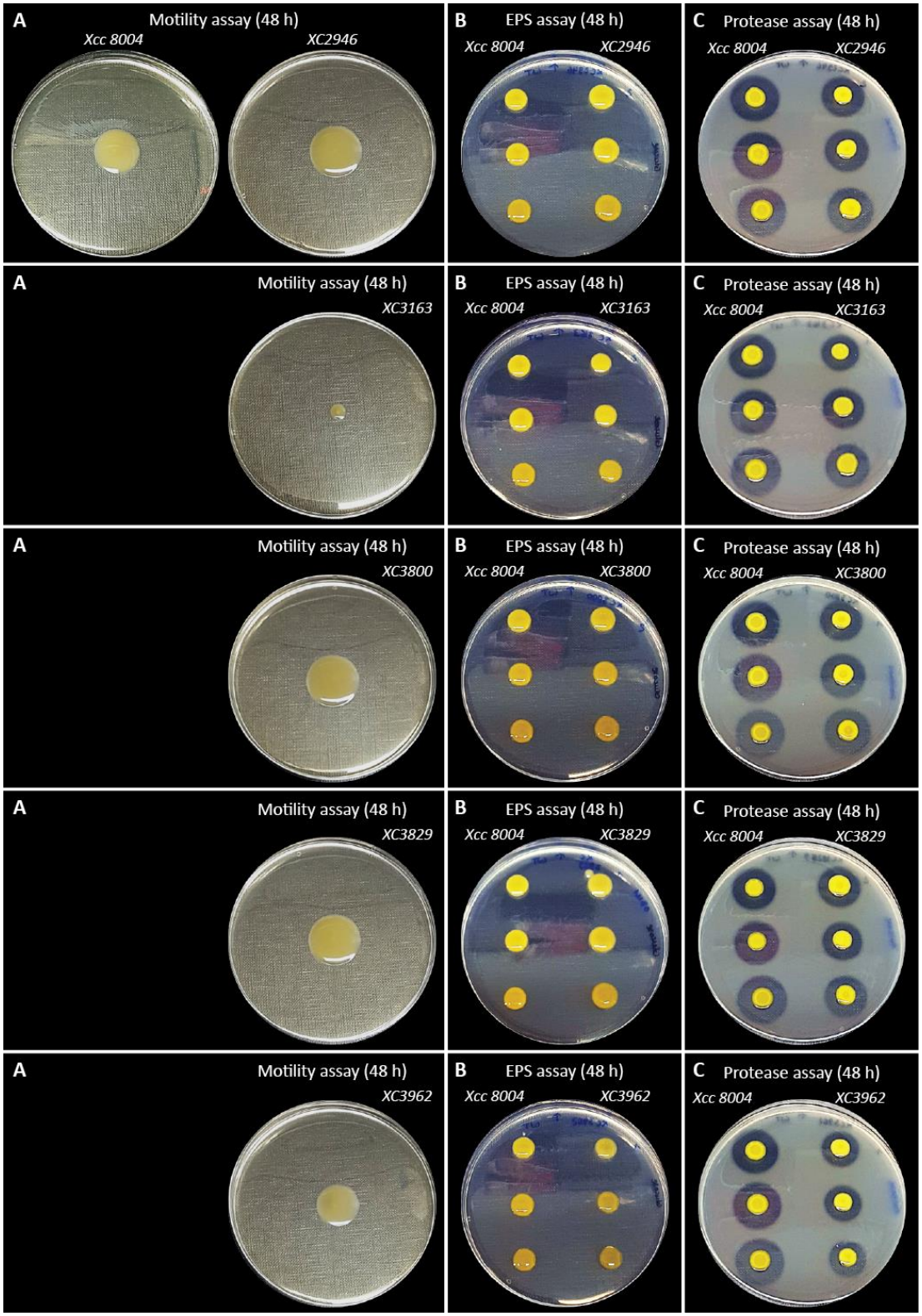
A
Motility assay (48 h)
Xcc 8004
XC2946
B
EPS assay (48 h)
Xcc 8004
XC2946
C
Protease assay (48 h)
Xcc 8004
XC2946
A
Motility assay (48 h)
XC3163
B
EPS assay (48 h)
Xcc 8004
XC3163
C
Protease assay (48 h)
Xcc 8004
XC3163
A
Motility assay (48 h)
XC3800
B
EPS assay (48 h)
Xcc 8004
XC3800
C
Protease assay (48 h)
Xcc 8004
XC3800
A
Motility assay (48 h)
XC3829
B
EPS assay (48 h)
Xcc 8004
XC3829
C
Protease assay (48 h)
Xcc 8004
XC3829
A
Motility assay (48 h)
XC3962
B
EPS assay (48 h)
Xcc 8004
XC3962
C
Protease assay (48 h)
Xcc 8004
XC3962

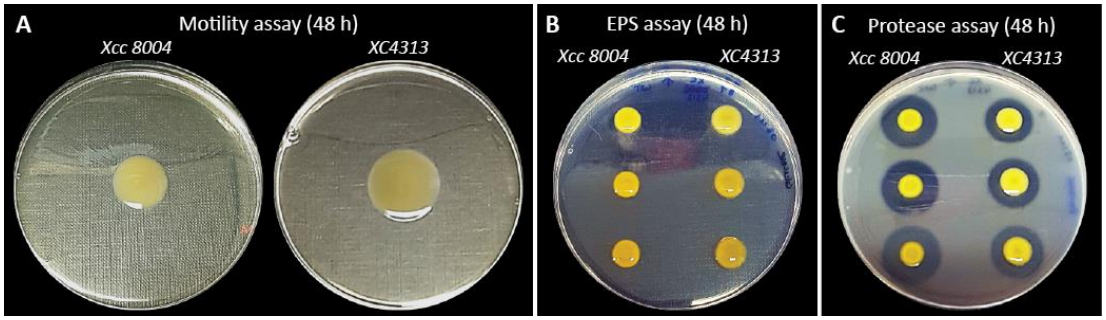

Appendix Figure 4: Representative images of phenotypic analysis of panel of mutants using motility, EPS and protease assay compared to the WT *Xcc* 8004 (the same representative WT taken for all images). A) Motility assay after 48 h. **B)** EPS assay after 48 h. **C)** Protease assay after 24 h and 48 h.